Dissertation for the degree of Doctor of Natural Sciences

Single cell analysis uncovers clonal heterogeneity in the adult exocrine pancreas

by

Damian Wollny

2016

Single cell analysis uncovers clonal heterogeneity in the adult exocrine pancreas

Dissertation submitted to the Combined Faculties for the Natural Sciences and for Mathematics of the Ruperto-Carola University of Heidelberg, Germany for the degree of

Doctor of Natural Sciences

presented by

Dipl. Biol. Damian Wollny

born in Salzkotten, Germany

Oral Examination: 22.09.2016

Single cell analysis uncovers clonal heterogeneity in the adult exocrine pancreas

Referees:

Prof. Dr. Ana Martin-Villalba

Prof. Dr. Jan Lohmann

Abstract

The pancreas is a dual organ, performing endocrine and exocrine functions. The exocrine pancreas harbours duct, centroacinar and acinar cells in charge of production, secretion, and transport of digestive enzymes. Acinar cells are producing large amounts of proteins and account for the majority of all cells in the pancreas. The acinar cell pool is believed to be a population of equipotent cells, which are equal in form and function. However, by examining acinar cells on the single cell level, we find that acinar cells represent a heterogeneous pool of morphologically, functionally and molecularly distinct cells.

Long-term, multicolour lineage tracing reveals the existence of previously neglected progenitor-like acinar cells with the ability to persistently generate acinar cells for at least one year. In a complementary *in vitro* approach, we find that only a subpopulation of acinar cells is able to form organoids, if in direct contact with a supporting acinar cell. We demonstrate that binuclear acinar cells are proliferation deficient and uncover their existence in the human pancreas. Chemically induced pancreatitis transiently activates a population of acinar cells, distinct from the proliferating acinar cells that maintain homeostasis. Furthermore, single cell mRNA sequencing of acinar cells confirms their functional heterogeneity on the molecular level. Altogether, our study transforms our understanding of the acinar cell compartment as a pool of equipotent secretory cells and provides a framework to further disentangle the cellular complexity within the exocrine pancreas in the future.

Zusammenfassung

Die Bauchspeicheldrüse ist ein Organ, welches endokrine und exokrine Funktionen erfüllt. Die exokrine Bauchspeicheldrüse besteht aus Duktzellen, zentroazinären Zellen und Azinuszellen, welche zusammen verantwortlich sind für die Produktion, Sekretion und den Transport von Verdauungsenzymen. Azinuszellen produzieren große Mengen an Proteinen und repräsentieren die Mehrzahl aller Zellen in der Bauchspeicheldrüse. Die Azinuszellen gelten als eine Population von einheitlichen Zellen, die in Form und Funktion identisch sind. In dieser Studie von Azinuszellen auf Einzelzellebene zeigen wir jedoch, dass Azinuszellen eine heterogene Zellpopulation darstellen, welche sich morphologisch, funktionell und molekular unterscheiden.

Langzeituntersuchungen von Azinuszellen mittels *multicolour lineage tracing* offenbart die Existenz von bisher nicht bekannten, vorläuferzell-ähnlichen Azinuszellen. Diese Azinuszellen besitzen die Fähigkeit über lange Zeitspannen kontinuierlich neue Azinuszellen zu bilden. In einer komplementären *in vitro* Untersuchung fanden wir, dass nur eine Subpopulation von Azinuszellen in der Lage ist Organoide zu bilden, wenn direkter Zell-Zell Kontakt mit unterstützenden Azinuszellen besteht. Wir zeigen, dass zweikernige Azinuszellen ein Proliferationsdefizit aufweisen und demonstrieren erstmals ihre Existenz in der menschlichen Bauchspeicheldrüse. Chemisch induzierte Pankreatitis aktiviert vorübergehend eine Subpopulation von Azinuszellen, die sich von den Azinuszellen unterscheiden, welche in der intakten Bauchspeicheldrüse kontinuierlich proliferieren. Ferner bestätigt eine Einzelzell-Sequenzierungsanalyse von mRNA aus Azinuszellen die funktionelle Heterogenität dieser Zellen auf molekularer Ebene. Zusammenfassend verändert diese Studie unser Verständnis von Azinuszellen als einheitliche Population bestehend aus identischen, sekretorischen Zellen. Des weiteren liefert diese Arbeit ein Grundgerüst, anhand dessen zukünftig die volle, zelluläre Komplexität der exokrinen Bauchspeicheldrüse entschlüsselt werden kann.

Contents

3 Results

4 Discussion

5 References

Appendix

1 Introduction

1.1 The diversity of cell types

Life on earth evolved in form of single celled organisms (Alberts et al., 2014). In the course of time the unicellular organisms evolved into multicellular organisms – so-called metazoans (Fig. 1a,b) (Alberts et al., 2014). Although multicellularity is usually considered to be a eukaryotic feature, prokaryotes like cyanobacteria or myxobacteria formed cellular aggregates consisting of multiple cell types (Knoll, 2011). Genomic analysis suggests that the unicellular choanoflagellates are most closely related to metazoans (Carr et al., 2008). Choanoflagellates were shown to have tyrosine kinases and the closely related Minestera harbour components related to cell adhesion such as integrin-beta and cadherin (Manning et al., 2008; Shalchian-Tabrizi et al., 2008). The evolution of molecular prerequisites for metazoan development at the unicellular stage opened the path to the development of multicellular organisms. This raises the question for the trigger of metazoan evolution. One hypothesis is that cellular aggregation is protecting the organism from phagotrophic prey (King, 2004). Evidence for this hypothesis was provided by a prey-predator experiment involving the unicellular alga Chlorella vulgaris (Boraas et al., 1998). Co-culturing the algae with phagotrophic predators selected for formation of a multicellular Chlorella vulgaris population (Boraas et al., 1998). Another possible explanation for the evolution of multicellularity is given by the example of flagellation constraint (King, 2004). The microtubule organizing centre (MTOC) represents the cellular machinery for both, cellular/flagellar motility as well as mitosis (King, 2004). As a result the two functions are mutually exclusive and no flagellated or ciliated animal cell seems to be able to divide (Buss, 1987). Thus, it was proposed that multicellular organisms might have a selective advantage by dividing these two functions into distinct cell types within the same organism (Buss, 1983).

This example of "division of labour" illustrates the evolutionary benefit of multicellularity and the increase in cell type diversity among metazoans. In addition to this segregation of function to sister cells, the divergence of function has been proposed to be another driver of multicellularity (Arendt, 2008). In this model both sister cells retain the function, but in a modified form. A prime example for this divergence is the evolution of rods and cones. Both cell types retained the ability to sense light, however at different wavelengths (Arendt, 2008). A third mechanism that was proposed to drive the diversity of cell types was the acquisition

of new function through a mechanism called gene co-option (Arendt, 2008). This mechanism is exemplified by the evolution of drosophila wings. The drosophila common ancestor wings were unspotted and the drosophila wing epithelial cells gained pigmentation (Prud'homme et al., 2006).

The cellular diversity is at the heart of every multicellular organism. Yet, the definition of a cell type - although representing the basic building block of multicellular life - is surprisingly ill defined up to this day (Trapnell, 2015). Historically, most novel cell types have been defined on the basis of morphological differences. In the late 19th century the Spanish anatomist Santiago Ramon y Cajal improved a silver staining called "Golgi´s method" to decipher the complexity of the central nervous system (CNS) (Cajal et al., 1899). Investigations using this method revealed the morphological complexity of cells within the nervous system and subsequently led to the notion that the CNS was composed of individual, anatomically and functionally distinct cells (Fig. 1c) (Cajal et al., 1899). The concept that built on this idea became known as the neuron doctrine (Bullock et al., 2005). Another classic example for using morphological features to unravel new cell types was the discovery of dendritic cells by Steinman and Cohn (Steinman and Cohn, 1973). Upon isolation of cells from murine peripheral lymphoid organs a large, adherent cell population was noticed (Fig. 1d) (Steinman and Cohn, 1973). The cytoplasm was arranged in pseudopods containing phase-dense granules and a large, contorted nucleus, which was clearly distinct from other cell types isolated from lymphoid organs such as phagocytes, granulocytes, and lymphocytes (Steinman and Cohn, 1973). In a series of follow-up studies detailed sub-cellular characteristics, functional properties *in vitro* and *in vivo*, surface markers and tissue distribution were carefully characterized (Steinman and Cohn, 1974; Steinman et al., 1975; 1979; 1974). The discovery of dendritic cells as antigen-presenting cells opened the door to understand basic mechanisms of adaptive immunity. Previous to this work it remained a mystery how lymphocytes are activated upon antigen presence given that the addition of the sole antigen was not enough to stimulate proliferation of lymphocytes (Katsnelson, 2006). The example of dendritic cell discovery illustrates the use of morphological features to distinguish new cell types. However, functionally distinct cells might be hidden within morphologically similar cellular populations. The discovery of stem cells in the adult mouse provides a paradigm example of how new cell types can be identified by function.

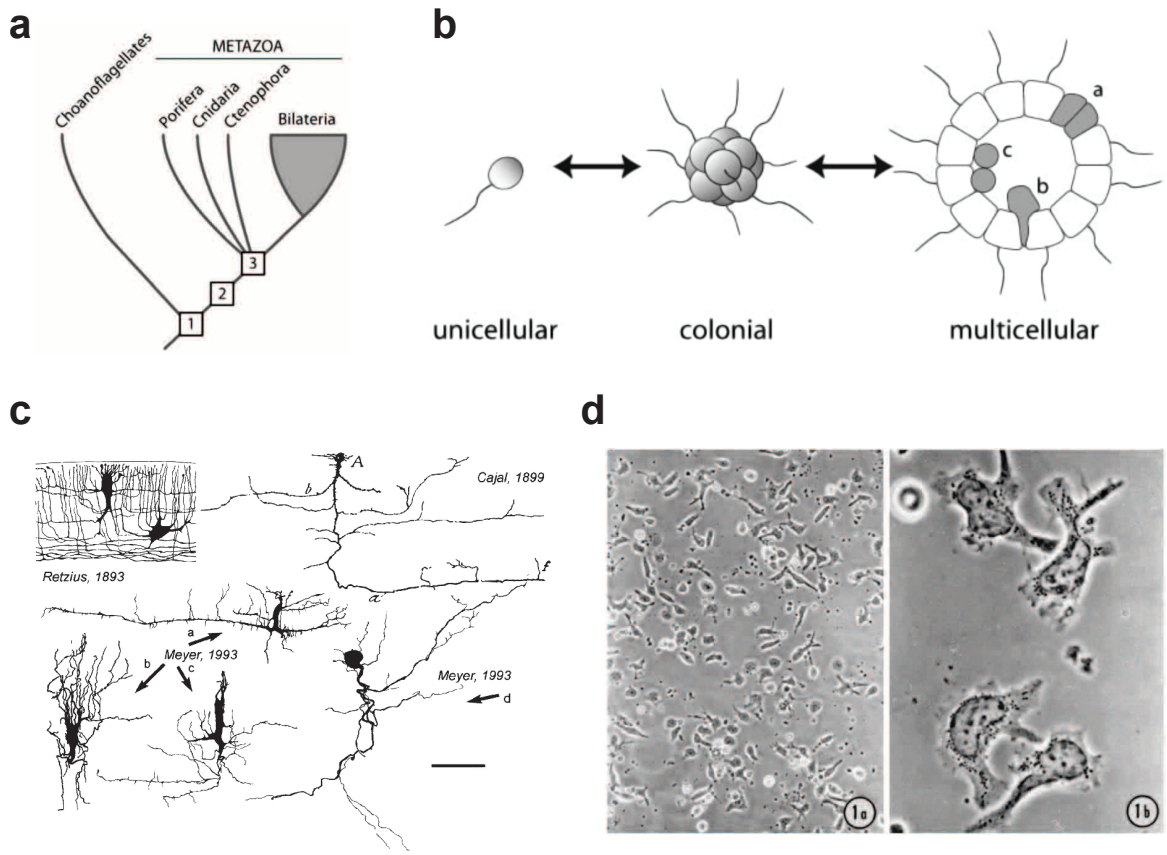

Figure 1. Evolution of cell type diversity. (**a**) From (King, 2004). Choanoflagellates represent the last common ancestor between metazoa and unicellular organisms. (**b**) From (King, 2004). Evolution of unicellular flagellates towards multicellularity (**c**) From (Meyer et al., 1999). Drawings of neuronal subtypes by Retzius, Cajal and Meyer. (**d**) From (Steinman and Cohn, 1974). Phase contrast images of isolated dendritic cells.

1.2 Discovery of somatic stem cells

More complex multicellular organisms compartmentalize different cell types into organs. During the lifetime of an organism cells have to be replaced as a result of injury or due to day-to-day deterioration (Alberts et al., 2014). The replacement of lost cells is accomplished by somatic stem cells. Stem cells are defined by functional features such as their ability to self-renew and their ability to differentiate into multiple lineages (multipotency) in place of morphological characteristics (Fig. 2a) (Weissman, 2000).

In an initial attempt to study the radiation sensitivity of bone marrow cells the physicist James Till together with the haematologist Ernest McCulloch demonstrated, for the first time, the existence of multipotent stem cells in adult mice (BECKER et al., 1963). It was noted that transplantation of hematopoietic cells from the bone marrow into sub-lethally radiated mice was linearly related to the appearance of nodules on the spleen consisting of erythrocytes, granulocytes and megakaryocytes (Till and McCulloch, 1961). The authors subsequently

demonstrated that a single cell is capable of forming nodules on the spleen of recipient mice containing several cell types by taking advantage of radiation induced chromosomal abnormalities which "barcode" the cellular progeny (BECKER et al., 1963). The study therefore provided the first experimental evidence for multipotency of single, adult, murine cells. The cells derived from spleen colonies were shown to be colony-forming themselves demonstrating that in addition to multipotency these cells were also capable of self-renewal (Siminovitch and McCULLOCH, 1963). In the following years the hematopoietic stem cell (HSC) system became the most thoroughly studied somatic stem cell system in higher organisms (Wilson et al., 2009). Technical advances related to the development of monoclonal antibodies and flow cytometry based cell-sorting approaches enabled the purification and characterization of hematopoietic stem cells based on surface markers (Spangrude et al., 1988). Once able to isolate these cells, transplantation assays were established, leading to numerous discoveries including the identification of phenotypically distinct HSC populations with long-term repopulating capacity (Morrison and Weissman, 1994). Subsequent studies unravelled the lineage hierarchy of HSCs from long-term over short-term HSC, all the way towards the mature cell types within the blood (Weissman, 2000).

Decades of research have consequently led to the discovery of stem cells in many organs of the mammalian body by taking advantage of numerous methodical advances (Fig. 2b) (Snippert and Clevers, 2011). The technique that remained the gold standard in mammals for many years was stem cell transplantation into recipient mice because it directly tested the self-renewal and multipotency of the transplanted cells (Snippert et al., 2013). Besides the above-mentioned example of HSC discovery, transplantation into fat pads of recipient mice led to the identification of mammary gland stem cells (Shackleton et al., 2006; Stingl et al., 2006). These studies demonstrated for the first time that a single epithelial stem cell was able to reconstitute the entire mammary tree upon transplantation (Shackleton et al., 2006; Stingl et al., 2006). An important feature of the mammary stem cells was their high proliferative activity (Stingl et al., 2006). Interestingly however, high mitotic activity is not a feature of stem cells *per se*. Stem cells in the skin were identified by their slow-cycling properties as demonstrated by label-retention assays (Cotsarelis et al., 1990; Tumbar et al., 2004). Upon transplantation these cells were able to give rise to all lineages of the hair follicle sebaceous gland and interfollicular epidermis (Morris et al., 2004).

A major disadvantage of transplantation assays is that the stem cells are removed from their natural, cellular environment. In contrast, genetic lineage tracing enables researchers to

permanently label cells in their native environment. This label will be stably inherited by each daughter cell (Kretzschmar and Watt, 2012). The most common way to genetically label specific cell types in mammals in by the use of the Cre-loxP system (Sauer and Henderson, 1988). In this system the Cre recombinase is expressed under a cell- or tissue-specific promotor and removes a transcriptional roadblock enabling the permanent expression of a reporter enzyme or fluorophore (Kretzschmar and Watt, 2012). With this tool at hand, stemness features like multipotency and self-renewal can be tested directly in situ. The power of lineage tracing is exemplified by the discovery of stem cells in the small intestine (Barker et al., 2007). Wnt signalling has been demonstrated to be indispensable for stem cells maintenance of the adult small intestine (Korinek et al., 1998). Barker and colleagues thus hypothesized that a Wnt target gene, like *Lgr5*, would provide a faithful marker for intestinal stem cells (Barker et al., 2007). By using an inducible Cre recombinase under the promoter of Lgr5 it was demonstrated that $Lgr5^+$ cells are self-renewing, multipotent stem cells in the intestine and colon (Barker et al., 2007).

A refined way of using lineage tracing has been developed by tracking cells on the clonal level. By carefully titrating down the amount of labelled cells one can trace the clonal expansion of single cells. One of the first study that took advantage of this approach traced single progenitors of the murine epidermis over time (Clayton et al., 2007). Analysis of the clone-size distribution over time suggested that all epidermal progenitors are equally capable of generating progeny and whether these cells do so or not was stochastically determined (Clayton et al., 2007). This finding laid the basis for a new model of homeostasis maintenance in which stem cells and committed progenitors are not hierarchically organized (Fig. 2c). Rather than that, homeostasis was maintained by a single type of equipotent progenitors which are stochastically activated (Klein and Simons, 2011b). A similar mechanism of tissue maintenance was proposed for other tissues (Doupé et al., 2012; 2010; Klein et al., 2010). Another elegant way to perform lineage tracing of single cells was enabled by the introduction of multicolour reporters (Kretzschmar and Watt, 2012). This system barcodes single cells with different colours upon Cre recombination (Livet et al., 2007). Thus, in contrast to conventional lineage tracing in which the fate of a cell population can be traced, multicolour lineage tracing enables the discrimination between single cells among the population of interest. The potential of this approach was demonstrated in studies of the small intestine. As described above lineage tracing revealed that the $Lgr5^+$ population represents the stem cells of the small intestine (Barker et al., 2007). However, it was not known whether all $Lgr5^+$ cells were multipotent, self-renewing stem cells and whether all $Lgr5^+$ cells contributed

equally to homeostasis. By taking advantage of a multicolour system it was possible to label each $Lgr5^+$ stem cells randomly with one of four colours as a result of Cre recombination (Snippert et al., 2010). Tracing single $Lgr5^+$ cells confirmed multipotency and self-renewing capability on the clonal level (Snippert et al., 2010). Surprisingly, multicolour lineage tracing of revealed that competition dynamics among $Lgr5^+$ stem cells leading to monoclonality of intestinal crypts though a mechanisms called "neutral drift dynamics" (Snippert et al., 2010). Thus, lineage tracing is not only a powerful tool to discover stem cells in a non-manipulated system, it further permits the tracing of single (stem) cells within a population.

An alternative method for probing stem cell features is provided by *in vitro* culture. *In vitro* assays are conducted in an artificial environment and thus possibly lack crucial signals provided by the *in vivo* setting. Yet, cell culture assays have remained an important technological asset to stem cell studies for many years (Snippert et al., 2013). Besides obvious advantages such as cost-effectiveness, *in vitro* assays are less labour intensive and allow rapid and direct manipulation of the cell type of interest. Furthermore, many *in vitro* studies facilitated the identification of stem cells in certain tissues and instigated our current understanding of stem cell properties. This is exemplified by the hallmark study by Barrandon & Green (Barrandon and Green, 1987). Based on the proliferative capacity of keratinocytes *in vitro* three clonal cell types were defined (Barrandon and Green, 1987). Among these cell types so called "holoclones" displayed the greatest proliferative potential and were proposed to be the stem cells (Barrandon and Green, 1987). Subsequently, these cells were molecularly characterized and isolated from human tissue based on the expression of β_1 integrins which opened the door for more detailed studies of human epidermal stem cells (Jones and Watt, 1993).

Despite the success of *in vitro* expansion and characterization of epidermal stem cells, no long-term culture system was available for many other stem cell systems (Sato and Clevers, 2013). Recently, a three-dimensional cell culture system was developed in which stem cells can be cultured in matrigel, a laminin-rich basement membrane composition isolated from mouse sarcoma (Hughes et al.). Using this system single $Lgr5^+$ stem cells isolated from the small intestine where shown to grow into three-dimensional structures, referred to as "organoids", which resemble the crypt-like organization found *in vivo* (Sato et al., 2009). Interestingly, of all cells isolated from the small intestine, only stem cells were able to form organoids (Sato et al., 2009). Thus, the ability to form organoids seems to be stem cell-specific trait, which has been confirmed in several murine and human tissues (Sasai, 2013). In a follow-up study Sato and colleagues demonstrated that direct contact of $Lgr5^+$ stem cells

with the secretory paneth cells drastically facilitated organoid formation (Sato et al., 2010). This finding is explained by secretion of essential niche factors by paneth cells which was confirmed *in vivo* (Sato et al., 2010). Thus, the organoid formation assay does not only serve as a means to identify stem cells from various organs but also define the respective stem cell niche.

Despite all above-mentioned technical advances for stem cell identification, it remains controversial whether all adult organs harbour stem-/progenitor cells (Wagers and Weissman, 2004). One organ for which the existence of adult stem cells was extensively debated is the pancreas (Kong et al., 2011; Stanger and Hebrok, 2013; Ziv et al., 2013).

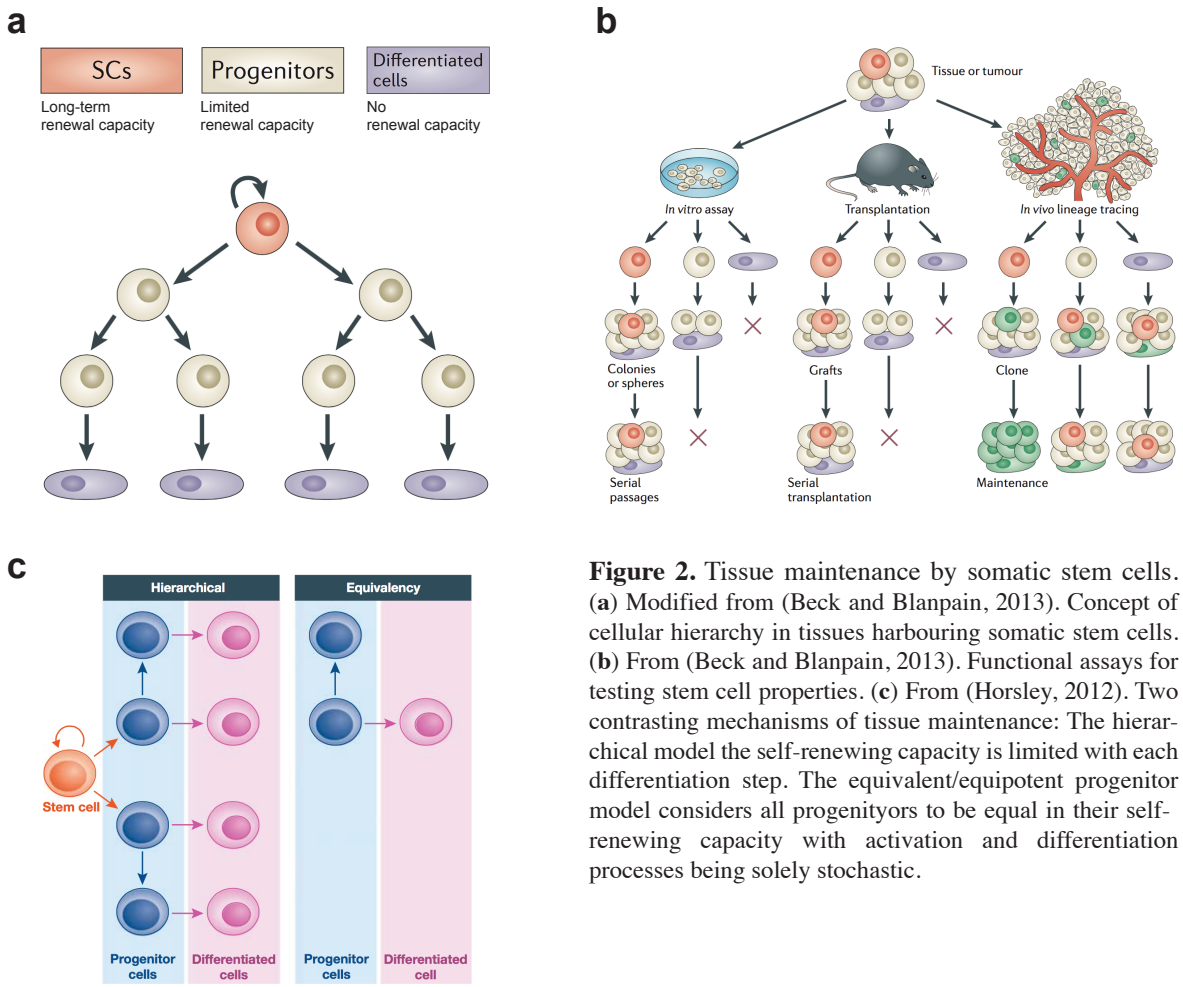

Figure 2. Tissue maintenance by somatic stem cells. (**a**) Modified from (Beck and Blanpain, 2013). Concept of cellular hierarchy in tissues harbouring somatic stem cells. (**b**) From (Beck and Blanpain, 2013). Functional assays for testing stem cell properties. (**c**) From (Horsley, 2012). Two contrasting mechanisms of tissue maintenance: The hierarchical model the self-renewing capacity is limited with each differentiation step. The equivalent/equipotent progenitor model considers all progenityors to be equal in their self-renewing capacity with activation and differentiation processes being solely stochastic.

1.3 Pancreatic cell types and their specification

The murine pancreas starts to develop at embryonic day E8.5 (Zaret and Grompe, 2008). A particularity of pancreatic development is that the organ initiates from two distinct positions

of the endoderm (Puri and Hebrok, 2010). Cells from the dorsal and ventral part of the definitive endoderm start budding into the surrounding mesenchyme (Fig. 3a) (Zaret and Grompe, 2008). At E11.5 rotation of the gut leads to the fusion of the ventral and dorsal pancreas and the organ further expands as a whole into the mesenchyme until all adult cell types are specified at E15.5 (Puri and Hebrok, 2010).

During embryonic development multipotent progenitors have been shown to drive pancreatic organogenesis (Gu et al., 2002; Zhou et al., 2007). Pancreatic cells expressing the transcription factor Pdx-1 were shown to harbour multipotent progenitors which give rise to all pancreatic cell types (Gu et al., 2002). As the developing pancreas starts to branch and become morphologically more complex, *Cpa-1*-expressing multipotent progenitors are localized at the distal tip of the branching pancreas (Fig. 3a) (Zhou et al., 2007). From E12.5 on, these pancreatic progenitors lose their multipotency and become lineage restricted (Gu et al., 2002). The specification of the pancreatic cell types during development requires a large number of spatially and temporally controlled signalling pathway such as FGF-, Notch- and Hh signalling and have extensively reviewed elsewhere (Puri and Hebrok, 2010).

The adult pancreas can be functionally divided in two main units: The endocrine pancreas, that is, the Islets of Langerhans, regulating hormonal homeostasis in the animal and the exocrine pancreas, which is responsible for secreting digestive enzymes into the intestinal tract (Fig. 3b). The cell types defining the exocrine compartment are the digestive enzyme-producing acinar cells that are structurally connected to duct cells, which line the secretory channel for the enzymes (Fig. 3b). The centroacinar cells represent the third exocrine cell type, their function, however, remains the most enigmatic of all exocrine cells (Cleveland et al., 2012). Endocrine cells of the pancreas comprise α, β and δ cells, which produce and secrete hormones such as glucagon, insulin and somatostatin (Fig. 3b).

Arguably the best-studied cell type of the adult pancreas is the endocrine β cell. β cells express and secrete insulin upon food intake in order to reduce the blood glucose concentration (Alberts et al., 2014). In a pathological condition called Type 1 Diabetes, β cells get attacked by the host´s immune system and lost over time (Alberts et al., 2014). Thus, the endocrine research community has put extensive effort in finding ways to replace the lost β cells. The idea that endogenous, adult stem cells, once activated, might replace the lost β cells has efforts to find multipotent stem cells in the adult pancreas. The first evidence for the potential existence of pancreatic stem cells was provided by the isolation and *in vitro* culture of clonogenic cells from the adult pancreas (Rovira et al., 2010; Seaberg et al., 2004; Smukler et al., 2011). Nestin-expressing cells in pancreatic islets and ducts were shown to be

multipotent *in vitro* (Seaberg et al., 2004; Zulewski et al., 2001). Similarly, ALDH1-expressing centroacinar cells were able to differentiate into exocrine and endocrine cells arguing for multipotent capacity *in vitro* (Rovira et al., 2010). More recently, organoid formation assays demonstrated the ability of duct cells to form endocrine and acinar organoids (Jin et al., 2013). In a similar study, $Lgr5^+$ duct cells were shown to generate organoids with unlimited *in vitro* expansion capacity and the ability to give rise to duct and endocrine cells (Huch et al., 2013a). These results indicated that adult pancreatic cells possess the capacity to give rise to multiple cell types, albeit only *in vitro*. Whether some adult pancreatic cells are truly multipotent in their natural environment had to be demonstrated by lineage tracing experiments. Given the large interest from the diabetes research field, the laboratory of Douglas Melton tried to settle the debate by rigorously testing whether β cells would be generated by a multipotent, undifferentiated stem cell (Dor et al., 2004). In this study, the researcher genetically labelled β cells of young mice and chased the islet turnover over the course of one year (Dor et al., 2004). If the majority of newly generated β cells would be generated by undifferentiated stem cells (which does not express insulin) then the genetic label of the islets should dilute out over time. The authors demonstrated that the proportion of labelled β cells stayed constant over time, indicating that the majority of β cells are generated by pre-existing β cells (Dor et al., 2004). Similarly, it was also demonstrated that in the adult pancreas, acinar cells only give rise to acinar cells and thus, are unlikely to harbour multipotent cells (Desai et al., 2007). Further, *Sox9*-expressing duct cells only give rise to duct cells in the adult animal (Kopp et al., 2011). Collectively, these studies led to the prevalent perception that multipotency is lost during development and that the adult pancreas does not contain multipotent stem cells as classically defined and found in other adult organs (McCulloch and Till, 2005). Despite this notion, a few lineage-tracing studies seemed to detect multipotent subpopulations in the adult organ leading to controversy in the field (Kong et al., 2011; Stanger and Hebrok, 2013; Ziv et al., 2013). One example was given by tracing of $Sox9^+$ cells in the liver, intestine and pancreas. The authors found that, in contrast to another study published shortly after, Sox9 expressing pancreatic duct cells give rise to acinar cells (Furuyama et al., 2011; Kopp et al., 2011).

Regardless of the controversy about multipotency under homeostatic conditions, there is a large body of evidence for the loss of lineage restriction under non-homeostatic conditions (Puri and Hebrok, 2010; Puri et al., 2015). Similar to other tissues, relatively little genetic manipulation of pancreatic cells types leads to cell type conversion. For instance elevated Hedgehog signalling as a result of expressing an active form of the transcription factor GLI2

leads to β cell dedifferentiation assessed by expression of markers expressed in the developing pancreas (Landsman et al., 2011). Similarly, loss of the E3 ubiquitin ligase substrate recognition component Fbw7 leads to transdifferentiation of duct cells into α, β and δ cells (Sancho et al., 2014). By now it has been demonstrated that genetic reprogramming takes little genetic manipulations for cells from most tissues (Xu et al., 2016).

The pancreas however, seems to display a remarkable degree of cellular plasticity in several injury paradigms even in the absence of genetic manipulations (Puri and Hebrok, 2010; Puri et al., 2015). Acinar cells transiently convert into duct-like cells, a process termed acinar-to-ductal metaplasia, as demonstrated for several different injury models (Jensen et al., 2005; Morris et al., 2010; Puri et al., 2015). Upon injury acinar cells start to express embryonic markers indicating a dedifferentiation upon injury (Pan et al., 2013). It has been speculated that this dedifferentiation step might be prerequisite for regeneration of the pancreas (Jensen et al., 2005). Building on this concept, it was proposed that the adult pancreas might harbour so-called facultative stem cells (Kong et al., 2011; Yanger and Stanger, 2011). The term facultative stem cells describes cells which act as terminally differentiated somatic cells under homeostatic conditions while transforming into stem cells under conditions such as injury (Yanger and Stanger, 2011). However, the lack of solid data supporting this hypothesis leads to scepticism in the field as to whether this concept applies to the adult pancreas (Kopp et al., 2016). Besides acinar-to-ductal metaplasia, acinar cells have also been shown to give rise to β-like cells after transient treatment with the cytokines EGF and CNTF (Baeyens et al., 2013). Researchers are currently trying to exploit the plasticity of adult acinar cells for acinar-to-β cell reprogramming efforts as an attempt to cure type I diabetes (Li et al., 2014; Zhou et al., 2008).

Aside from the cumulative evidence for acinar plasticity, the endocrine cells of the pancreas also display marked disengagement from lineage restriction. Under conditions of extreme β cell loss α and δ cells convert into insulin producing β cells (Chera et al., 2014; Thorel et al., 2010). Further, in multiple diabetes mouse models β cells were shown to be lost as a result of dedifferentiation as opposed to cell death as previously believed (Talchai et al., 2012). Thus, the interconversion among endocrine cells indicates that marked plasticity during injury might be a general feature of cells from the adult pancreas.

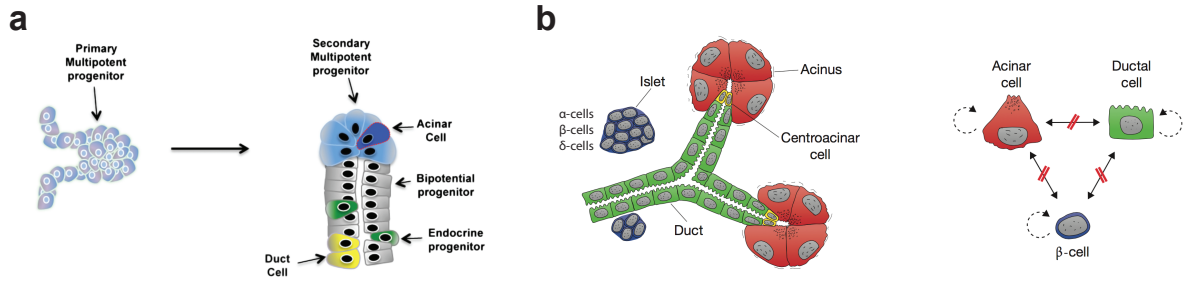

Figure 3. Cell types of the developing and adult pancreas. (**a**) From (Puri et al., 2015). Specification of cell types in the developing pancreas. (**b**) Modified from (Kopp et al., 2016). Left panel: Cell types of the adult pancreas. Right panel: No lineage plasticity among acinar, duct and β-cells in the adult pancreas under homeostatic conditions.

1.4 Pancreatic cancer

Recent year´s research has established a link between cellular plasticity and susceptibility to tumour formation for many types of cancer (Roy and Hebrok, 2015). The above-described evidence for plasticity among cell types of the adult pancreas thus potentially renders endocrine and exocrine cells highly susceptible for development of pancreatic cancer. Pancreatic tumours can arise from endocrine or exocrine cells. Pancreatic endocrine tumours represent a rare form of pancreatic malignancies and can be further classified depending on which endocrine cell type it arises from (Babu et al., 2013). The most common type of pancreatic cancer, pancreatic ductal adenocarcinoma (PDAC), originates from the exocrine pancreas (Roy and Hebrok, 2015). One hallmark of PDAC is it´s poor prognosis for patients diagnosed with this disease, with an overall 5-year survival rate of under 5% (Hidalgo, 2010). It has been extensively investigated which cell type within the exocrine pancreas is the cell type of origin for PDAC. The ductal morphology and marker expression of the tumour cells, hence the name ductal adenocarcinoma, suggested that the cell of origin of PDAC is a duct cell (Roy and Hebrok, 2015). The most commonly found mutation in PDAC patients, a K-*Ras* point mutation, was subsequently introduced in murine duct cells hoping to create a mouse model for PDAC (Brembeck et al., 2003). Surprisingly, this model did not efficiently induce PDAC (Brembeck et al., 2003). In contrast, many groups found that introducing a K-*Ras* mutation in acinar cells led to very efficient development of tumour precursor lesion called pancreatic intraepithelial neoplasia (PanIN) and PDAC (Carrière et al., 2007; Guerra et al., 2011; 2007; Habbe et al., 2008; La O et al., 2008). A recent study aimed to directly compare the tumour initiating capacity of acinar and duct cells by introducing the oncogenic K-*Ras* mutation in the respective cell types (Kopp et al., 2012). This study demonstrated that, acinar

cells are clearly more susceptible to oncogenic transformation while duct and centroacinar cells are surprisingly refractory (Kopp et al., 2012). Thus, according to the data accumulated from mouse model studies, acinar cells likely represent the cell of origin for PDAC (Fig 4a). The degree of susceptibility however, seems to depend on state of the acinar cell. It was shown that oncogenic K-*Ras* mutations in embryonic or early postnatal acinar cells render these cells more prone to tumour formation as compared to adult introduction of the same mutation in adult acinar cells (Guerra et al., 2007). Additionally, it was demonstrated that inflammation increases the susceptibility of adult acinar cells to oncogenic transformation (Carrière et al., 2011; Guerra et al., 2007).

Another interesting observation made by Guerra and colleagues was that although the authors introduced the K-*Ras* mutation in a large number of acinar cells, many cells seem to be resistant to oncogenic transformation and appeared unaffected (Guerra et al., 2007). This notion led to the hypothesis that the adult pancreas might harbour subpopulation of cells which might be more or less susceptible to tumour initiation (Fig. 4b) (Roy and Hebrok, 2015). In fact mouse models for many different types of cancer demonstrated that in order to efficiently generate tumours the oncogenic mutation needs to be introduced in the stem-/progenitor cells of the respective tissues (Visvader, 2011). Whether acinar cells represent a heterogeneous pool of cells that contains stem-/progenitor-like cells is currently not known.

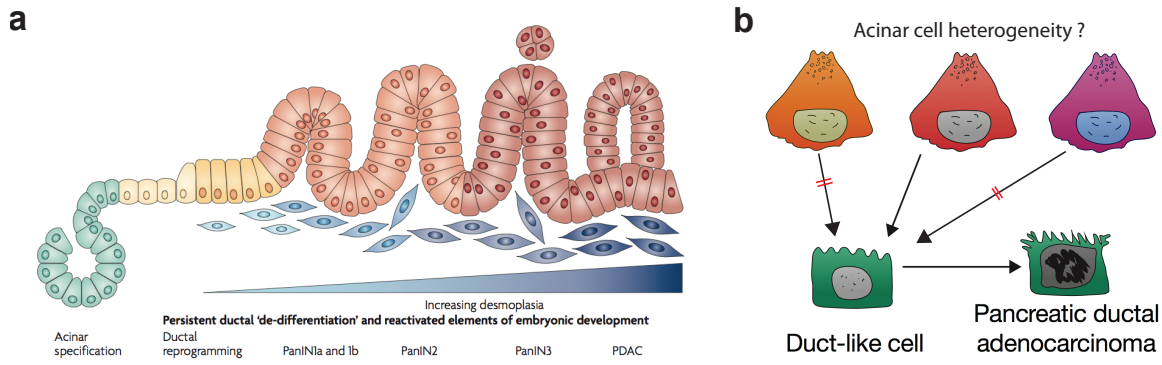

Figure 4. Acinar cells represent the cell of origin for pancreatic ductal adenocarcinoma (PDAC). (**a**) Modified from (Morris et al., 2010). Acinar-to-ductal metaplasia during pancreatic tumour initiation. (**b**) Modified from (Kopp et al., 2016). Potential acinar heterogeneity underlying varying susceptibility of acinar cells to tumour initiation.

2 Materials & Methods

2.1 Materials

2.1.1 Chemicals & Reagents

Reagent	Manufacturer
2-mercaptoethanol	Sigma-Aldrich
Acetone	Sigma-Aldrich
Agencourt Ampure XP beads	Beckman Coulter
B27 Serum-Free Supplement	Gibco
Betaine (BioUltra ≥99.0%)	Sigma-Aldrich
Bovine serum albumin (BSA)	Sigma-Aldrich
Cerulein	Sigma-Aldrich
Dithiothreitol (DTT)	Invitrogen
DNA-OFF	Takara Bio
Eosin solution	Merck
Ethanol	Sigma-Aldrich
Fluoromount G	eBioscience
Guanidine-HCl	Sigma-Aldrich
Hoechst 33342	Biotrend
Hydrochloric acid (HCl)	VWR
Matrigel	BD Biosciences
Magnesium chloride (MgCl2; anhydrous)	Sigma-Aldrich
Mayer's hemalum	Merck
N-2 Supplement	Gibco
OCT compound	Sakura
Paraformaldehyd (Roti®-Histofix)	Carl Roth
Penicillin-Streptomycin	Gibco
RNaseZap	Ambion
Sucrose	Sigma-Aldrich
Tamoxifen	Sigma-Aldrich
Triton-X 100	Sigma-Aldrich
Tween-20	Sigma-Aldrich
Xylene	Sigma-Aldrich

2.1.2 Buffers & Media

Buffer / Medium	Composition
Acinar cell isolation buffers	
C solution	4% BSA in PBS
D solution	1mg/ml collagenase, 0.25% BSA in PBS
I solution	0.1% BSA in PBS
R solution	1% BSA in PBS
Acinar cell medium	1:1 Dulbecco's Modified Eagle's Medium - high glucose & Ham's F-12 Nutrient Mix – GlutaMAX, 2% (vol/vol) B27 Serum-Free Supplement, 1% (vol/vol) N-2 Supplement, 20ng/ml rHu EGF, 20ng/mL human FGF-2,

	1% Penicillin-Streptomycin (100 units/ml)
Acinar Lysis Buffer for single cell RNA-seq	6M Guanidine-HCl and 0.1% (vol/vol) Triton X-100
Dehydration Buffer	PBS containing 30% Sucrose
FACS Buffer	PBS containing 10% FCS
Hank's Balanced Salt Solution (HBSS)	Purchased from Life Technologies
PBS	160 g/l NaCl, 23 g/l Na2HPO4, 28.84 g/l NaH2PO4, 4 g/l KCl, 4 g/l KH2PO4 in H2O. Adjust pH to 7.4 with HCl
Wash/Block Buffer	5% Horse Serum, 0.5% BSA, 0.2% Tween-20 in PBS

2.1.3 Kits

Kit	Manufacturer
Agilent high-sensitivity DNA kit	Agilent Technologies
DeadEnd™ Fluorometric TUNEL System	Promega
EdU click-iT kit	Life Technologies
KAPA HiFi HotStart ReadyMix	KAPA Biosystems
Nextera XT 24-index kit	Illumina
Nextera XT DNA sample preparation kit	Illumina
Power SYBR® Green PCR Master Mix	Life Technologies
Superscript III First Strand Synthesis SuperMix	Invitrogen
TruSeq dual-index sequencing primer kit for single-read runs	Illumina

2.1.4 Recombinant Proteins

Proteins / Enzymes	Manufacturer
Collagenase Type CLS IV	Biochrom
rHu EGF	Promokine
human FGF-2	ReliaTech
Superscript II reverse transcriptase	Invitrogen
Recombinant RNase inhibitor	Clontech

2.1.5 Antibodies

Antibody	Dilution	Clone / Manufacturer
Rabbit anti-α-Amylase	1:200	#A8273 / Sigma-Aldrich
Rat anti-Cytokeratin 19	1:100	Troma III, Hybridoma Bank, Iowa University
Rat anti-E-cadherin	1:1000	#13-1900 / Invitrogen
Mouse anti-Insulin	1:200	#I2018 / Sigma-Aldrich
Mouse anti-Ki67	1:100	#556003 / BD Bioscience
Rabbit anti-phospho-Histone	1:500	#06-570 / Millipore

H3		
Mouse anti-OP18 (A-4) – STMN1	1:200	#sc-48362 / Santa Cruz Biotechnology
Chicken anti-GFP	1:1000	#1020 / Aves

2.1.6 Oligonucleotides

Oligonucleotide	Sequence	Manufacturer
Amy2a_fw (Amylase)	5´-TGCAGGTCTCTCCACCCAATGAAA-3´,	Eurofins MWG Operon
Amy2a_rev (Amylase)	5´-TGCACCTTGTCACCATGTCTCTGA-3´	Eurofins MWG Operon
Bhlha15_fw (Mist1)	5´-AATAAGGAGGGTGAGTGGTTGGCA-3´	Eurofins MWG Operon
Bhlha15_rev (Mist1)	5´-AAGGAAGAGGCCAAGGACAAGTGA-3´	Eurofins MWG Operon
Cela1_fw (Elastase)	5´-AATGTCATTGCCTCCAACTGAGCG-3´	Eurofins MWG Operon
Cela1_fw (Elastase)	5´-ATTAGACAAGTGCTCGGCCACTGA-3´	Eurofins MWG Operon
ERCC Spike-In RNAs	See manufacturers instructions	Ambion
Hnf1b_fw	5´-ACAATCCCAGCAATCTCAGAA-3´	Eurofins MWG Operon
Hnf1b_rev	5´-GCTGCTAGCCACACTGTTAATGA-3’	Eurofins MWG Operon
ISPCR oligo	5’-AAGCAGTGGTATCAACGCAGAGT-3’	Eurofins MWG Operon
Krt19_fw (Cytokeratin 19)	5´-TCCCAGCTCAGCATGAAAGCT-3´	Eurofins MWG Operon
Krt19_rev (Cytokeratin 19)	5´-AAAACCGCTGATCAGCTCTG-3’	Eurofins MWG Operon
Oligo-dT30VN	5’–AAGCAGTGGTATCAACGC AGAGTACT30VN-3’	Eurofins MWG Operon
Ptf1a_fw	5´-TGCGCTTGGCCATAGGCTACATTA-3’	Eurofins MWG Operon
Ptf1a_rev	5´-AGATGATAACCTTCTGGGCCTGGT-3’	Eurofins MWG Operon
Sox9_fw	5´-CAAGACTCTGGGCAAGCTCTG-3´	Eurofins MWG Operon
Sox9_rev	5´-TCCGCTTGTCCGTTCTTCAC-3´	Eurofins MWG Operon
Template Switching Oligo (TSO)	5’-AAGCAGTGGTATCAA CGCAGAGTACATrGrG+G-3’ rG = riboguanosines, +G = LNA-modified guanosine	Eurogentec

2.1.7 Laboratory Equipment

Equipment / Software	Manufacturer
ABO 7500 Fast Real-Time PCR System Cycler	Applied- Biosystem
Adobe Illustrator CS V15.0.0	Adobe
Adobe Photoshop CS5 Extended V12.0	Adobe
Agilent 2100 Bioanalyzer	Agilent
Cell strainer (70μm)	BD Bioscience
FACSCanto II Flow Cytometer	BD Bioscience
Fiji	doi:10.1038/nmeth.2019
Flaming/Brown Micropipette Puller P-87	Sutter Instrument Co.
Illumina HiSeq2000 sequencer	Illumina
Integrative Genome Viewer	Broad Institute
Lab-Tek chamber slides	IBDI
Leica CM 1950 Cryomicrotome	Leica
R studio	RStudio, Inc.
TCS SP5 confocal microscope	Leica
Zeiss Cell Observer	Zeiss

2.1.8 Mouse Strains

Mouse Strain	Origin
C57BL/6N	Charles River Laboratories
B6(D2)-Tg(CAG-Brainbow1.0)2Eggn/J	kindly provided by Dr. Kevin Eggan
B6.Cg-Tg(Nes-cre/Esr1)GSc	kindly provided by Dr. Günther Schütz
B6-Gt(ROSA)26Sortm3Sia	kindly provided by Dr. Jan Ellenberg

2.2 Methods

2.2.1 Tissue Preparation for Rainbow2 Imaging

In order to induce rainbow2 colours adult rainbow2 mice were intraperitonally injected with 100μl of 10mg/ml Tamoxifen (Sigma-Aldrich) twice daily for 5 consecutive days. At given time points the mice were perfused with HBSS (room temperature) following 4% ice cold PFA. The pancreas was extracted, adipose tissue carefully removed, and the pancreas was post-fixed for 15 min in 4% PFA on ice. Afterwards the pancreas was transferred to 30% sucrose in PBS and incubated at 4°C until the tissue settled on the bottom of the vessel. The pancreas was embedded in OCT compound (Sakura) and stored at -20 overnight. Tissue sectioning was performed using a Leica CM 1950 Cryomicrotome (Leica) with the cryochamber and specimen head at -20°C. Section thickness for time points 1, 7 28, 84 dpi was 20μm and for time point 365 dpi 50μm. Four consecutive sections were collected on each glass slides, mounted with Fluoromount G (eBioscience) and directly imaged at a Leica TCS SP5 confocal microscope (Leica).

2.2.2 Confocal Analysis of Rainbow2 Pancreas Sections

Images were acquired as XYZ stacks at a 1024 x 1024 pixel resolution. Z planes of images were quantified separately. For representation maximum projection of z planes was used. For fluorophore excitation the following settings were used: dTomato (helium–neon laser 561nm; 1mW, emitted photons collected between 572nm and 686nm), Cerulean (argon multiline laser 458nm, 100mW, emitted photons collected between 464nm and 504nm), eYFP (argon multiline laser 514nm, 100mW, emitted photons collected between 522nm and 576nm). Tunable spectral PMTs were used as detectors. Clones were discriminated by colour composition and clone size was determined by counting of nuclei within a clone.

2.2.3 Acinar Cell Isolation and Culture

Mice were perfused with 20ml HBSS (Gibco), the pancreas was extracted and adipose tissue removed. Four solutions were prepared, including D solution: 1mg/ml Collagenase Type CLS IV supplemented with 0.25% BSA (Sigma-Aldrich), R solution: 1% BSA dissolved in PBS, C

solution: 4% BSA in PBS and I solution: 0.1% BSA in PBS. The tissue was chopped into small pieces and incubated in 10ml of D solution at 37°C for 30 minutes. The digestion product was filtered through a 70µm cell strainer (Islets of Langerhans were thereby removed). 10ml of R solution was pipetted on the cell strainer. A quarter of the filtered cell suspension was gently transferred on top of 6ml C solution to achieve layer separation of the liquids. Acini were spun down at 50g for 2 minutes and washed with C solution and I solution successively. Purified acini were treated with 2ml Accutase (Sigma-Aldrich) for 5min to acquire acinar cell suspension containing single cells and clusters of acinar cells.

Single acinar cells or acinar doublets isolated from H2B-mcherry mice were handpicked using a heat pulled glass capillaries (bevelled at 30°C with an inner diameter of appr. 75-100 µm) and transferred to 20μl of Matrigel, which was kept unpolymerized on ice. Cell viability and correct cell number were assessed immediately afterwards by fluorescence microscopy.

For 500 acinar cell experiments the mixture was pipetted as drops in selected cell culture plates or dishes and incubated at 37°C for 20 minutes before the addition of culture medium. The cells were cultured 11 days and imaged on day 0-4 as well as on day 6 and 11.

The medium used to culture pancreatic cells was composed of a 1:1 mixture of Dulbecco's Modified Eagle's Medium - high glucose (Sigma-Aldrich) and Ham's F-12 Nutrient Mix - GlutaMAX (Gibco), with the supplementary of 2% (vol/vol) B27 Serum-Free Supplement (Gibco), 1% (vol/vol) N-2 Supplement (Gibco), 20ng/ml rHu EGF (Promokine), 20ng/mL human FGF-2 (ReliaTech) and 1% Penicillin-Streptomycin (100 units/ml, Gibco). Cells were cultured at 37 °C and the medium was refreshed every third day. Organoid imaging was conducted using a Zeiss Cell Observer (Zeiss).

2.2.4 Flow Cytometry

For flow cytometry analysis the cells were isolated as described above and resuspended in 2ml pancreatic cell medium. The cells were fixed with 1% PFA for 10min at room temperature and permeabilized with 0.1% Triton-X 100 in PBS. After a single washing step with ice cold FACS Buffer (PBS containing 10% FCS (Biochrom) primary antibodies were diluted in ice cold FACS Buffer and incubated for 1 hour at 4°C. After the incubation cells were washed twice. Secondary antibodies were diluted in ice cold FACS Buffer and cells were incubated for 30min at 4°C. Next cells were washed twice and resuspended in the FACS Buffer for flow cytometry analysis using a FACSCanto II Flow Cytometer (BD Bioscience).

Following antibodies were used: Amylase (Rabbit anti-α-Amylase, 1:200, Sigma-Aldrich #A8273), CK19 (Rat anti-Cytokeratin 19, 1:100, Troma III, Hybridoma Bank, Iowa University).

2.2.5 Immunoflourescence Stainings

For immunohistochemical analysis the mice were perfused with HBSS and 4% PFA pancreatic tissue was post-fixed for 2 hours at 4°C. Afterwards the pancreas was transferred to 30% sucrose in PBS and incubated at 4°C until the tissue settled on the bottom of the vessel. The tissue was embedded in OCT compound (Sakura) and cut into 20μm sections. For stainings of organoids the acinar cells were cultured in Matrigel on Lab-Tek chamber slides (IBDI) and at given timepoints fixed with 1% PFA at 4°C for 10min in the chambers. After a single washing step with PBS the cells were stained as described for tissue sections.
The sections were incubated in PBS at room temperature until OCT surrounding the sections was washed away. The tissue was incubated with 0.1% Triton-X 100 (Sigma-Aldrich) in PBS for 30min. For blocking the sections were incubated with Wash/Block Buffer containing 5% Serum (Biochrom), 0.5% BSA, 0.2% Tween-20 (Sigma-Aldrich) in PBS. The primary antibodies were diluted in Wash/Block Buffer and incubated over night at 4°C. On the next day the primary antibody was washed away 3x 5min using Wash/Block Buffer. The secondary antibody was diluted in Wash/Block Buffer with Hoechst 33342 (Biotrend 1:3000) and incubated for 1 hour at room temperature. Next the secondary antibody was washed away 3x 5min using Wash/Block Buffer and the tissue was mounted with Fluoromount G. TUNEL staining was done according to manufacturer's protocol (Promega). Following antibodies were used: Amylase (Rabbit anti-α-Amylase, 1:200, Sigma-Aldrich #A8273), CK19 (Rat anti-Cytokeratin 19, 1:100, Troma III, Hybridoma Bank, Iowa University), E-cadherin (Rat anti-E-cadherin, 1:1000, Invitrogen #13-1900), Insulin (Mouse anti-Insulin, 1:200, Sigma-Aldrich #I2018), Ki67 (Mouse anti-Ki67, 1:100, BD Bioscience #556003), pH3 (Rabbit anti-phospho-Histone H3, 1:500, Millipore #06-570), STMN1 (Mouse anti-OP18 (A-4), 1:200, Santa Cruz Biotechnology #sc-48362), YFP (Chicken anti-GFP, 1:1000, Aves #1020 – cross-reactive with YFP)

2.2.6 Hematoxylin and Eosin staining

Cryosection specimens of the pancreas were fixed in acetone for 2 mins and air dried for 5 seconds. The slides were then incubated in Hematoxylin solution (Mayer's hemalum from Merck, 1:1 diluted with tap water) for 90 seconds and dipped in 1% HCl (concentrated HCl diluted in 70% ethanol) for 30 seconds. With running tap water, excessive Hematoxylin was washed. After a single dip in Eosin solution (Merck, 1% Eosin dissolved in tap water with 2 drops of acetic acid per 50ml solution), slides were rapidly washed under running tap water until water turned clear. To remove excessive Eosin, slides were washed with 100% ethanol for at least 40 times. Clearing in xylene for 15 seconds was necessary before mounting the slides with mounting medium.

2.2.7 Quantitative Real-Time PCR

Reverse transcription reaction was performed using the Superscript III First Strand Synthesis SuperMix from Invitrogen according to the manufacturer's instructions. Quantitative real-time PCR was performed with Power SYBR® Green PCR Master Mix according to the manufacturer´s protocol in a 96 well plate with a ABO 7500 Fast Real-Time PCR System Cycler (Applied- Biosystem). Relative levels of gene expression were quantified, using the $2^{-\Delta\Delta CT}$ method.

2.2.8 Cerulein Treatment

Accute pancreatits was induced as previously described(Carrière et al., 2011). Briefly, adult mice were intraperitoneally injected with Cerulein (Sigma-Aldrich) in PBS (50μg/Kg of body weight) hourly for seven hours on two consecutive days. The last injection on day two was defined as time point 0 and mice were sacrificed 28 days later.

2.2.9 Image analysis

Cells from images of recombined NesCreERT2 rainbow2 mice were segmented using a modified version of the Fiji segmentation from (Cervero et al., 2013). For each segmented cell the RGB values and pixel coordinates were recorded. Next, the RGB values were converted to HSV colour space. For each image obtained from a given microscopy session a cell in which the Cre recombinase didn't recombine (which only expresses dTomato) was used for normalization of HSV values. Next, we clustered the segmented cells based on the similarity of its HSV values. In order to discover the number of colours in a bottom up fashion we decided to utilize a clustering algorithm that doesn´t require a priori determination of the number of clusters. For this purpose we decided to use affinity propagation clustering (Frey and Dueck, 2007). The affinity propagation clustering algorithm defines a certain amount of colours (clusters) as well as an example cell for this colour (exemplars) autonomously. However, in contrast to e.g. the *k-means* clustering algorithm this algorithm simultaneously considers all cells to be potential exemplars for clusters. Thus, it doesn´t require initially randomly defined exemplars which the result is quite sensitive to (Frey and Dueck, 2007). The number of clusters the algorithm detects depends on input preference values (q-values). Depending on the q-values we got a colour range from 14-108 clusters. Next, we aimed to find out which cluster number most likely represents the true amount of colours. For this purpose we supervised the clustering. We examined the exemplars of each cluster by eye and clustered them according to their similarity. Although the number of clusters linearly increases as a function of the q- values, our manual analysis showed that the number of supervised clusters saturates. We therefore considered the supervised cluster number at q = 0.5 to be closest to the true amount of colours we detect in our setup since an even higher q-value will be very unlike to provide more colours in the supervised clustering analysis.

2.2.10 Clone fusion probability estimation

In order to get an estimate of how likely the probability of clone fusion is we determined the x-y coordinates of 573 segmented cells in which the Cre recombinase induced a rainbow2 color. Since cells with overrepresented colors will have higher fusion probability, the clone-fusion probability had to be considered for each color separately. We determined the largest

diameter of the biggest clone of each color group at one year after labeling. Next, we analyzed how frequently cells with the same color were within this distance at 1 DPI. For any analyzed picture the ration between the maximum number of potentially fused clones and the total number of fused clones determines the clone fusion probability.

2.2.11 Single cell RNA seq

Single cell RNA seq library preparation protocol was based on the SMART seq2 protocol (Picelli et al., 2014) with following modifications:
Acinar cells were isolated as described in the section "Acinar Cell Isolation and Culture" and resuspended in DPBS without Ca^{2+} and Mg^{2+} (PAN-Biotech). Cells were collected in a volume of 0.5μl and transferred to a reaction tube containing 4μl of 6M Guanidine-HCl (Sigma-Aldrich) and 0.1% (vol/vol) Triton X-100 (Sigma-Aldrich). The tube was immediately transferred into liquid nitrogen and kept there for the duration of cell collection. Next, 2.2x RNA SPRI beads (Beckman Coulter) was added directly to the lysis buffer and incubated for 5 min at room temperature. The beads were washed twice with 70% Ethanol. Air-dried beads were resuspended in a solution containing 2μl H20, 1 μl oligo-dT primer and 1μl dNTP mix (primer and nucleotides used as in (Picelli et al., 2014)). 24 cells contained ERCC Spike-In RNAs (1:10 000 – Mix2, Ambion) Mix in addition to primer and nucleotides. Beads were incubated for 3 min at 72°C and reverse transcription and PCR (19 cycles) were performed as described (Picelli et al., 2014). PCR product was cleaned up using 0.8x DNA SPRI beads (Beckman Coulter) and air dried beads were resuspended in 15μl H_2O. Quality of cDNA library was assessed for each cell on a high sensitivity DNA Bioanalyzer chip. Subsequent steps (tagmentation, amplification, multiplexing) were done as previously described (Llorens-Bobadilla et al., 2015). DKFZ Genomics and Proteomics Core Facility conducted sequencing on an Illumina HiSeq2000 sequencer (paired-end 100bp).

2.2.12 Single-cell RNA-seq data analysis

In total, we did single-cell RNA-seq on 108 acinar cells. Dr. Sheng Zhao performed data analysis. The following steps are described by him:
Read trimming and mapping:

Quality of raw reads was checked by FASTQC (http://www.bioinformatics.babraham.ac.uk/projects/fastqc/). Before alignment, adapter sequences in raw reads were trimmed by Btrim64 (http://graphics.med.yale.edu/trim)(Kong, 2011). Trimmed reads were mapped to mouse genome (ENSEMBL Release 80) using STAR_2.4.2a. Genome mapping results were visualized by using Integrative Genome Viewer (www.broadinstitute.org/igv/).

RNA-seq data quality metrics:

RNA-seq data quality metrics of each cell, including total reads, transcriptome mapped reads and transcriptome mapped rate was calculated by picard-tools-1.123 (https://broadinstitute.github.io/picard/).

Gene Expression Matrices:

Gene expression matrices were generated as previously described (Llorens-Bobadilla et al., 2015; Shalek et al., 2013; 2014) with slight modifications. Briefly, expression level of each gene was quantified in unites by transcript per million (TPM) using RSEM 1.2.21 (Li and Dewey, 2011) with bowtie2-2.2.6 using default parameters. To compare expression levels of different genes across samples, we performed an additional TMM (trimmed mean of M-values) normalization on TPM using Trinity (Haas et al., 2013) (http://trinityRNA-seq.github.io/) based on edgeR (Robinson and Oshlack, 2010) (abbreviated TMM-TPM). The purpose of this normalization is to account for differences in total cellular RNA production across all cells.

Validation Single-cell RNA-seq data using ERCC spike-in controls, technical replicates and population RNA-seq data:

We assessed the quality of single-cell RNA-seq data by comparing the results with known quantities of 92 ERCC spike-in RNA transcripts. Briefly, 92 ERCC spike-in RNA transcripts were randomly add to 19 single cells when preparing library. Expression levels of 92 ERCC spike-in controls in these 19 cells were quantified in units of TPM by RSEM.

Principal component analysis (PCA):

We developed custom R scripts based on FactoMineR library (http://factominer.free.fr/) performing PCA analysis on gene expression matrices. PCA analysis was performed on cells passed quality control using all genes expressed in more than two cells and with a variance in log2 (TMM-TPM) across all single cells greater than 0.5. In total, 4, 628 genes in 108 cells were used. Subsequently, genes with the highest correlation coefficient with one of the first three or four principal components were identified using dimdesc function in FactoMineR.

Hierarchical clustering was performed on cells and on the genes identified by PCA using Euclidean distance or correlation metric.

GO analysis:

Gene ontology analysis was done using the DAVID database (v6.7) (Dennis et al., 2003)

3 Results

3.1 Characterization of multicolour lineage tracing tools in the adult pancreas

The aim of this project was to decipher the functional heterogeneity among adult acinar cells with respect to their capacity to proliferate and produce new acinar cells. We hypothesized two scenarios: a) all acinar cells have the capacity to divide or b) only a small subset of acinar cells retains proliferative capacity. In order to distinguish between the two scenarios we had to label individual acinar cells and trace their progeny over time. For this purpose we used multicolour lineage tracing based on the Cre/LoxP system (Livet et al., 2007; Tabansky et al., 2013). This approach labels cells with different colours, which are inherited by the daughter cells. The size of acinar cell clones sharing the same colour indicates whether and to which extent the labelled acinar cell (and its progeny) divided. In order to label acinar cells in the pancreas, we chose an inducible Cre line under the Nestin regulatory elements ($NesCreER^{T2}$), which has been previously demonstrated to label acinar cells (Carrière et al., 2011). Two of the most prominent multicolour lineage tracing reporter are the confetti mouse (Snippert et al., 2010) and the rainbow2 mouse (Tabansky et al., 2013). We crossed the $NesCreER^{T2}$ mice with both multicolour reporters to test whether the systems works in the adult pancreas. We observed faithful labelling of pancreatic cells with multiple colours after injection of tamoxifen for both reporter lines (Fig. 5a,b). The confetti mouse line labelled pancreatic cells with 4 colours whereas the rainbow2 line offered a much greater variety of colours (Fig. 5a,b). The reason for this discrepancy is the fact that the confetti construct is integrated only once in the ROSA26 locus (Snippert et al., 2010), whereas the rainbow2 construct is randomly integrated as a tandem of several constructs (Tabansky et al., 2013). Furthermore, the cells in the rainbow2 system express dTomato as a default colour without recombination of the Cre recombinase. This is – in contrast to the confetti line - due to the lack of a stop codon upstream of the rainbow2 cassette (Tabansky et al., 2013). Our goal was to label acinar cells on a clonal level so that we could distinguish one cell from another. We therefore chose to use the rainbow2 line for all subsequent experiments. The large variety of colours decreases the chance of two neighbouring acinar cells being labelled with the same colour and is thus more suitable for clonal analysis. Interestingly, we observed that the nuclei of cells labelled with the rainbow2 construct displayed strong autofluorescence (Fig. 5c). We took

advantage of the notion and determined the size of all acinar clones by estimating the number of nuclei in each clone.

With these mouse lines at hand we wondered whether we could also perform clonal analysis of pancreatic tumour cells. Previously, it has been demonstrated that expression of mutated K-*Ras* ($Kras^{G12D}$) in the pancreas leads to formation of precursor lesions for pancreatic ductal adenocarcinoma (Hingorani et al., 2003). The induction of these so-called pancreatic intraepithelial neoplasia (PanIN) lesions can be further accelerated by induction of pancreatitis (Carrière et al., 2011; Guerra et al., 2007). We tested whether we could induce PanIN lesions by crossing the $NesCreER^{T2}$ rainbow2 mice with mice expressing $Kras^{G12D}$ while additionally inducing pancreatitis (Fig. 5d). We observed PanIN lesions in all mice tested 8 weeks after induction of pancreatitis (Fig. 5d). Curiously, none of the PanIN lesions were labelled with rainbow2 colours, which impeded clonal analysis of neoplastic cells (data not shown). We speculate that epigenetic changes as a result of oncogenic transformation might have silenced the rainbow2 construct.

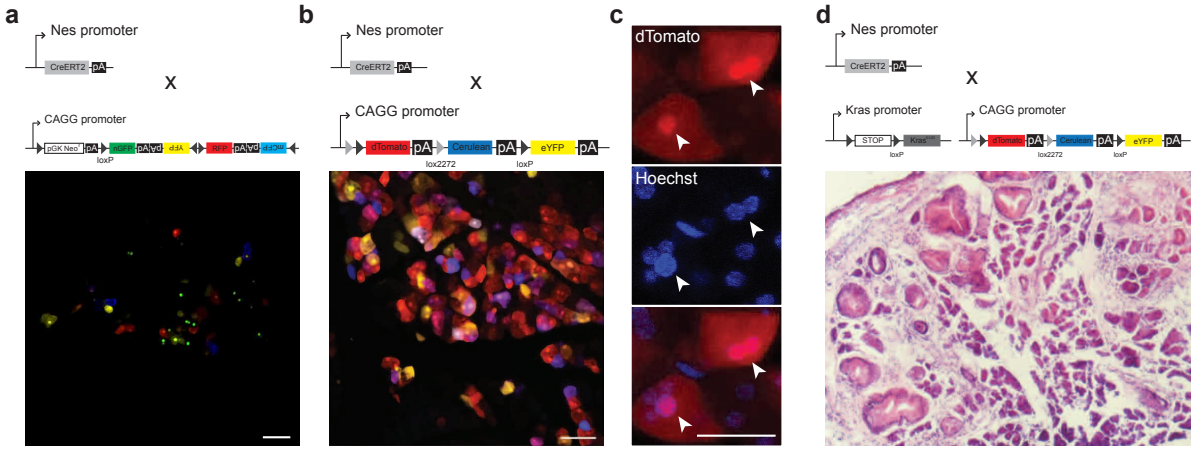

Figure 5. Evaluation of multicolour lineage tracing constructs and $NesCreER^{T2}$ recombination in the adult pancreas. (**a**) $NesCreER^{T2}$ mice crossed with CAG-Confetti mice (upper panel) revealed acinar specific expression of confetti colours (lower panel). (**b**) $NesCreER^{T2}$ mice were crossed with CAG-Rainbow2 mice (upper panel) to obtain acinar specific rainbow2 expression (lower panel). (**c**) Hoechst 33342 counterstaining indicates nuclear identity of bright subcellular structure upon rainbow2 expression (arrowheads). Scale bar = 25μm. (**d**) $NesCreER^{T2}$ mice crossed with $Kras^{G12D}$ mutant mice induces early neoplastic lesions in the adult pancreas.

Next, we aimed to determine the number of colours offered by the rainbow2 line in our setup. It has been described that the rainbow2 construct labels embryonic cells with 21 distinct colours (Tabansky et al., 2013). This spectral variety is, however, not universal for all tissues since we detected only few colours in the adult brain (data not shown). We computationally segmented 2420 acinar cell from pictures obtained from $NesCreER^{T2}$ rainbow2 mice. The

acinar cells were clustered according to the similarity of their colours by the affinity propagation (AP) clustering algorithm (Frey and Dueck, 2007)(Methods – Image analysis). The number of clusters that the algorithm detects linearly increased with the stringency (q value) of the algorithm (Fig. 6a). We estimated which q-value reflects the true amount of colours that we can distinguish by supervising the AP clustering (Methods – Image analysis). Supervision of the clustering revealed that number of clusters saturates with increasing q-value (Fig. 6a). We determined a maximum of 17 distinct colours (Fig. 6b). Recently, it has been demonstrated that the confetti reporter line has a bias for certain colours (Lescroart et al., 2014). Therefore, we had to determine whether the 17 detected colours are equally represented in our system. Among the 2420 analysed cells we detected 77% expressing the "Group1" default colour red (Fig. 6b,c). This indicates that the Cre recombinase was either only expressed in a subset of acinar cells or recombined very inefficiently. Analysis of the other colour groups indicated that the colours are not equally represented (Fig. 6d). This finding is important with respect to subsequent consideration of clonality. Thus, the unequal representation of colours seems to be a general issue for multicolour lineage tracing.

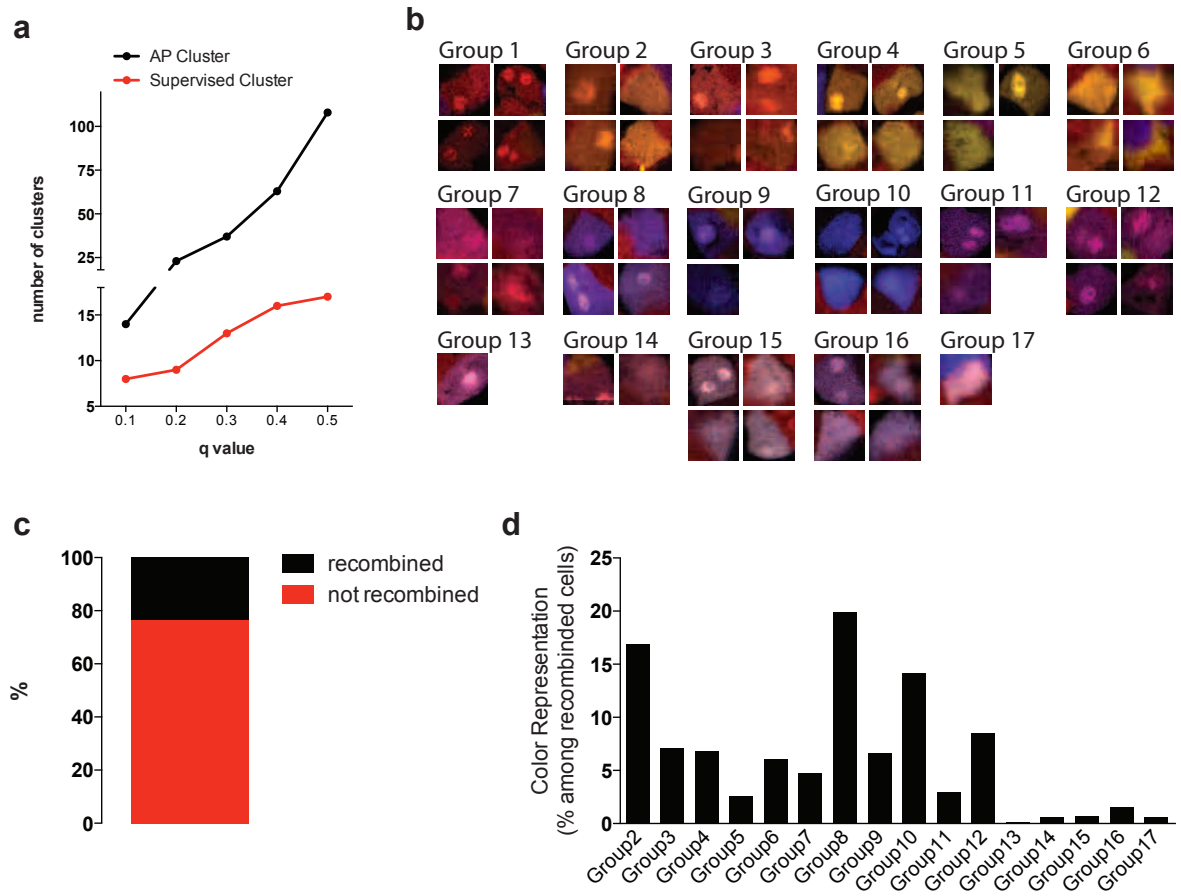

Figure 6. Characterization of rainbow2 colour spectrum in the adult pancreas. (**a**) Estimation of the number of rainbow2 colours by affinity propagation (AP) clustering and supervised AP clustering analysis. (**b**) Computational image segmentation of 2420 cells was conducted to determine the number of colours (17) using the rainbow2 system in the adult pancreas. Pictures of segmented cells are representative examples. (**c**) Quantification of recombination efficiency of the NesCreER^{T2} rainbow2 system in the adult pancreas. The segmentation algorithm randomly selected 2430 acinar cells. Based on the supervised clustering, cells were divided into non-recombined cells that exclusively expressed dTomato (Group 1 – 1857 cells) and recombined cells (Group 2-17 – 573 cells).

3.2 Identification of proliferative acinar subpopulation *in vivo*

The results thus far demonstrate that the NesCreER^{T2} rainbow2 line can be used for clonal analysis of pancreatic acinar cells. Therefore, we investigated the proliferative potential of single acinar cells over time in a pulse-chase experiment. We injected tamoxifen to induce the rainbow2 colours and sacrificed the animals at the indicated time points (Fig. 7). At the first day post injection (DPI) of tamoxifen we primarily found acinar clones with one or two nuclei per clone (Fig. 7). The surprisingly large number of two-nuclei clones is unlikely due to proliferation in such a short time frame given the quiescent nature of the organ (Magami et

al., 1990). Rather, these cells represent a pool of binuclear acinar cells that have previously been described in rats (Oates and Morgan, 1986; P S Oates, 1989). In the three subsequent time points (7 DPI, 28 DPI, 84 DPI) the number of acinar cells with two nuclei steadily increased (Fig 7).

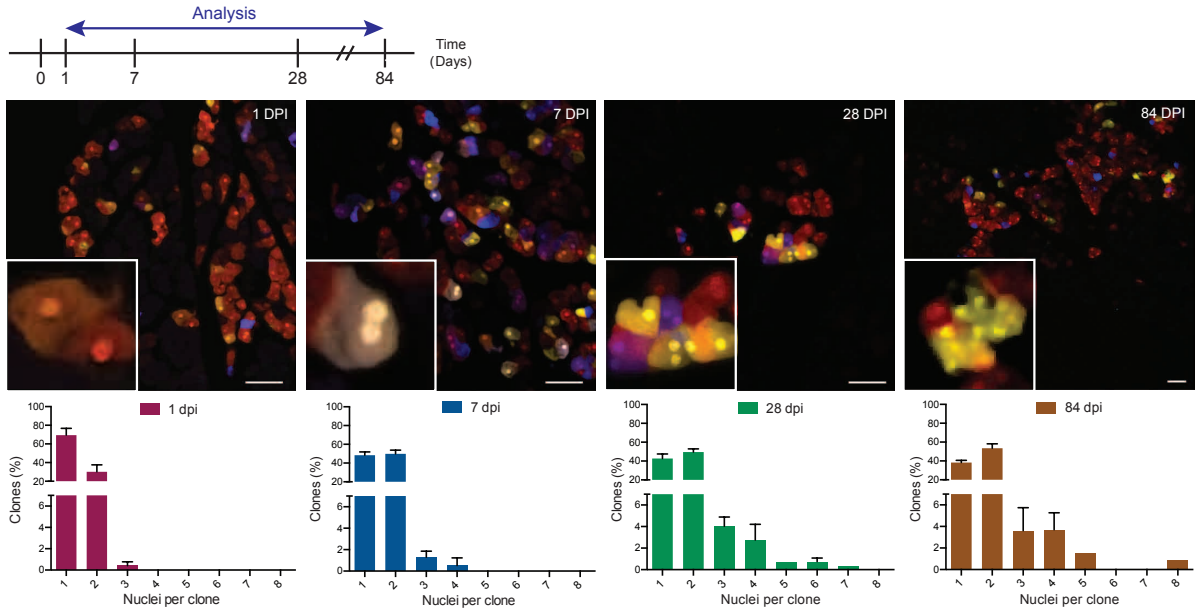

Figure 7. Multicolour lineage tracing of adult acinar cells reveals clonal heterogeneity. Quantitative analysis of the clone size distribution (fraction of clones with a certain number of nuclei) at the given time points after induction of the rainbow2 system. For 1 DPI n = 885 clones from 3 mice; 7 DPI n = 1185 clones from 5 mice, 28 DPI n = 681 clones from 3 mice, 84 DPI n = 274 clones from 3 mice were analysed. Scale bars = 50μm. Data represent mean ± SD.

This indicates a potential transition from a mono- to a binuclear acinar cell state. Interestingly, a subset of acinar cells produced clones of larger size over time as indicated by the tail of the distribution from 28 DPI on (Fig. 7).

This finding suggested that only a small subset of acinar cells exhibits proliferative capacity. Another possible explanation for the obtained clone size distribution was that some acinar cells stochastically proliferate more than others. This was previously observed for progenitor cells in mouse tail epidermis (Clayton et al., 2007). In this system, all cells are equipotent and thus all have the capacity to divide. Subsequently, with time all cells start to form large clusters of clones. If this was also the case for the acinar cells, the peak of the distribution should shift towards larger clones after long periods of time as it was observed for epidermis progenitor cells (Clayton et al., 2007). We therefore induced the rainbow2 colours and chased the cells for one year. Upon microscopic examination of the pancreas we observed that the majority of the cells did not proliferate even after one year of chase (Fig. 8a). The clone size distribution after one year of chase looked similar compared to shorter chase periods (Fig.

8b). Interestingly, we observed clones of acinar cells of exceptional large size (Fig. 8a,b). This suggests that only a small subset of acinar cells continuously gave rise to new cells in the course of the observed time. We found large clones of different colours and no sign of morphological abnormalities after the one-year chase (Fig. 8c). This argues against cytotoxicity of certain fluorophore combinations.

One concern, however, was that the large clones might arise from two (or more) cells that were initially labelled with the same colour and in close proximity. Infrequent division of these cells might lead to a so-called "clone-fusion" event. This would contradict our interpretation of the data claiming that the large clones arise from a distinct acinar subpopulation. We showed that the 17 colours of the rainbow2 system are not equally represented in the tissue (Fig. 8d). Thus, the clone-fusion likelihood had to be considered for each colour separately because cells labelled with overrepresented colours are more likely to be in close proximity. In order to get a quantitative estimate of how likely clone-fusion for each colour was, we measured the diameter of the largest clone from each colour at 365 DPI and tested how many times we find cells of the respective colour within this particular distance at one day after induction of the colours (Fig. 8d - scheme). We found large clones from the majority of all observed colours (Fig. 8e– red arrows). We compared the relative number of cell pairs within this distance (or a shorter distance) with the number of cells that are further apart from each other. This estimate indicated that for most colours there is a relatively low clone-fusion probability (Fig. 8e). Importantly, for some of the large clones (Colour Group 6, 11, 15) the clone-fusion probability was 0. This indicates that these large clones arose with very high likelihood from a single cell. This observation serves as a proof of principle that a single acinar cell can proliferate continuously within one year and thus give rise to the large clones and resemble progenitor cells from other tissues.

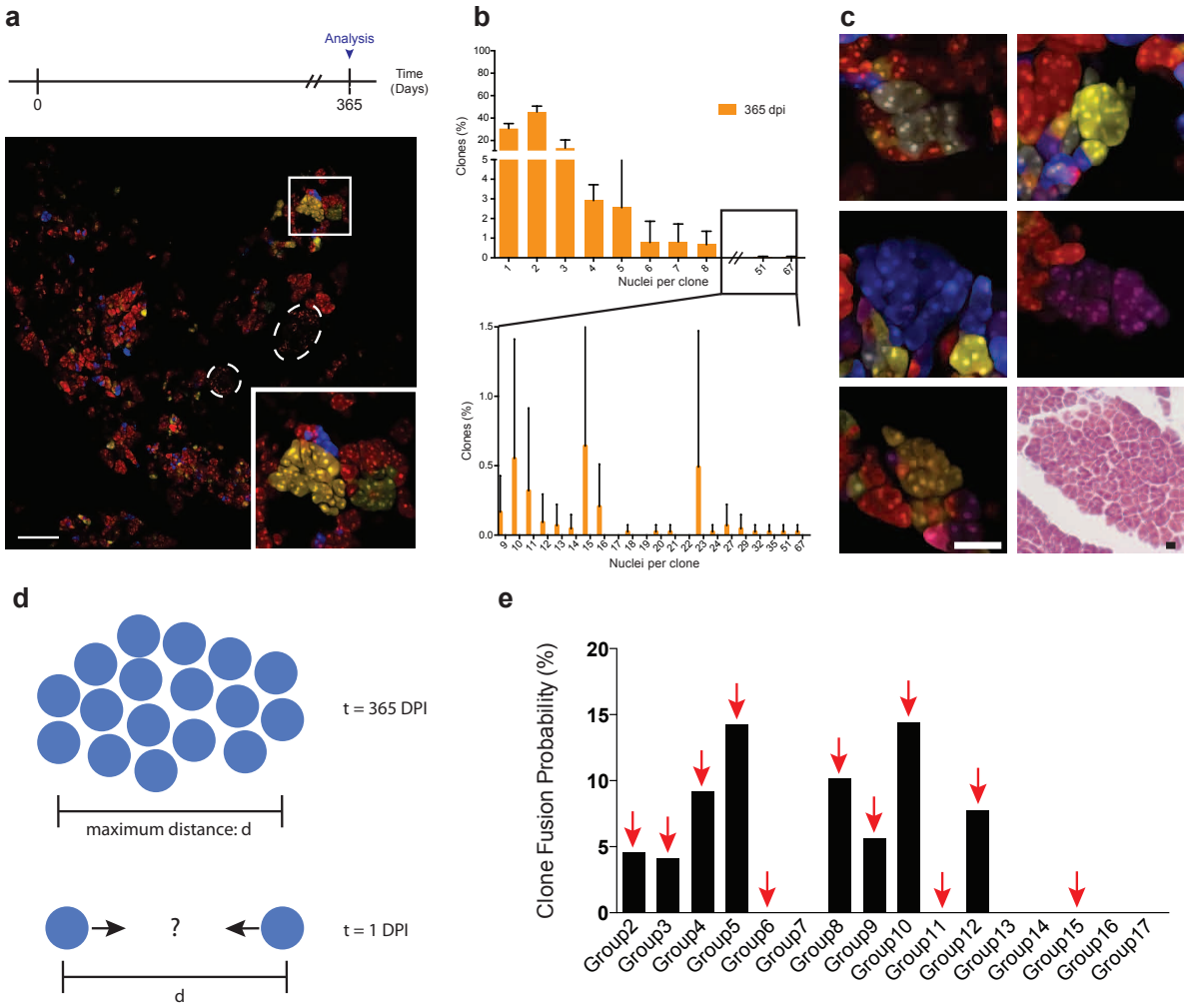

Figure 8. Clonal tracing reveals acinar subpopulation with long-term proliferative capacity. (**a**) Acinar cells are traced for a one-year period post rainbow2 induction. Representative example of rainbow2 labelled acinar cells one-year post label induction. Dashed circles indicate Islets of Langerhans. Scale bar = 50µm. (**b**) Quantitative analysis of clones traced for one year following label induction (n = 1283 clones from 5 mice). Data represent mean ± SD. (**c**) Representative examples of large clones arising independent of fluorophore expression. Images were acquired at 365 DPI. H&E staining of pancreas sections at 365 DPI indicates no morphological abnormalities. Scale bar = 50μm. (**d**) Relative abundance of cells with a distinct colour among recombined acinar cells (Group 2-17). (**e**) Schematic Representation of the determination of the clone fusion distance. (**f**) Relative clone fusion probability for acinar cells of a distinct colour. Red arrows denote colours for which large clones of acinar cells (<3 nuclei) were present.

Another hypothesis challenging our interpretation of the data was that we could not fully exclude the possibility that the large clones we observed at 365 DPI were a result of stochastic mitotic events of a uniform cell population. We addressed this question by mathematic modelling. For this purpose Monte Carlo simulation based on the Gillespie algorithm (Gillespie, 1976) was used to simulate clone size distributions after stochastic proliferation of a uniform cell population. After testing a variety of parameters, a good fit of the experimental data was not possible under the assumption that acinar cells are a uniform cell population (data by U. Kummer et al. – not shown).

Since we found a subpopulation of progenitor-like cells we wanted to test whether this subpopulation also gives rise to other pancreatic cell types. We stained pancreatic tissue from rainbow2 mice for YFP, in order to detect cells in which the NesCreER^{T2} line recombined. Co-staining of YFP with Insulin, CK19 and E-cadherin revealed that the NesCreER^{T2} line labels exclusively acinar cells (Fig. 9a). Further, after tracing acinar cells for 365 days we did not find YFP^{+} cells within Islets of Langerhans or ducts (Fig. 9b). These results indicate that acinar cells are a unipotent, lineage restricted entity. This finding is in line with previous findings of acinar cells that have been traced for shorter chase periods (Desai et al., 2007).

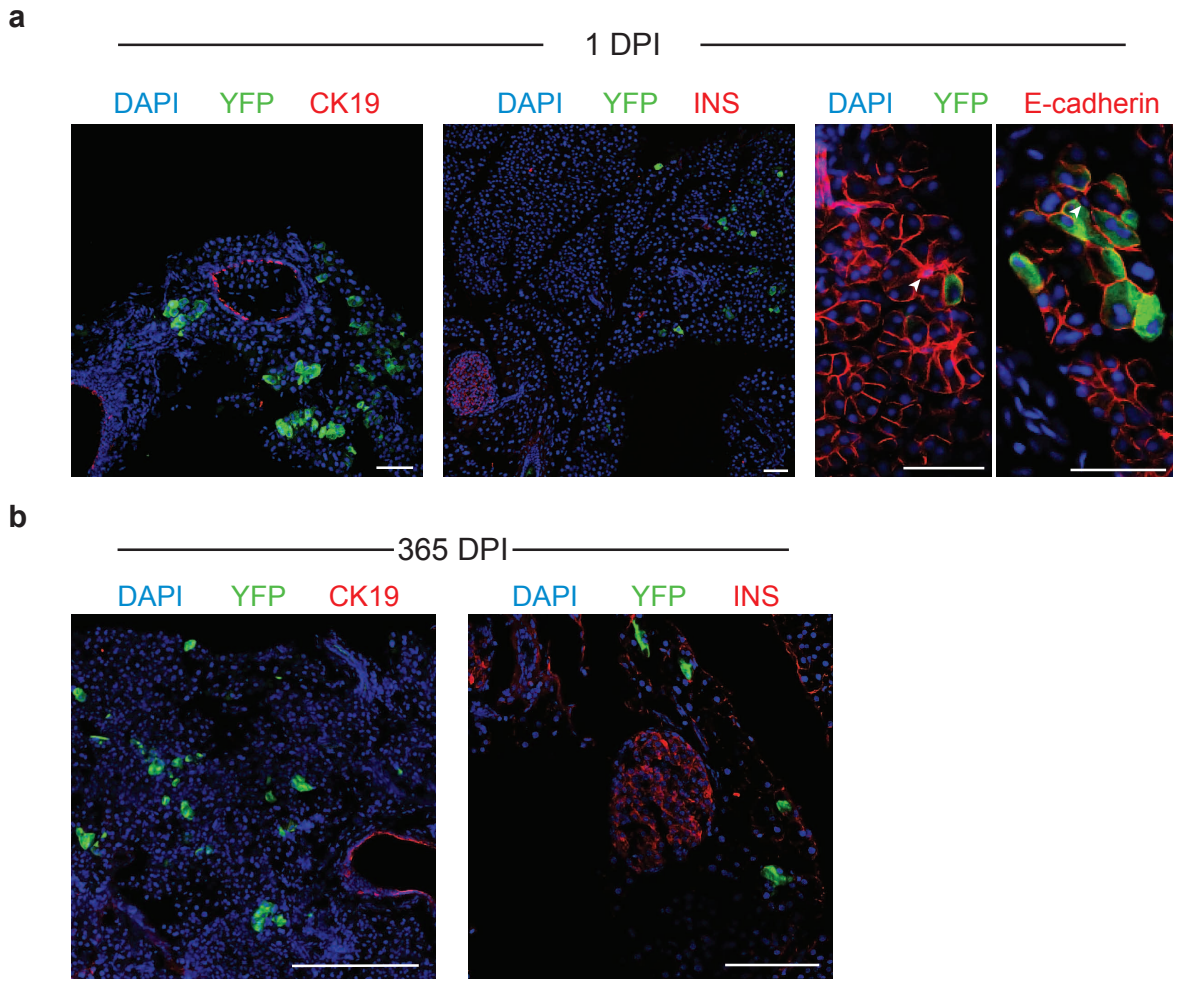

Figure 9. NesCreER^{T2} recombination and analysis of Nestin-derived progeny. (**a**) Pancreatic sections of rainbow2 mice 1 DPI stained for YFP. Anti-YFP antibody detects all rainbow-induced clones. Anti-Cytokeratin 19 (CK19) and anti-Insulin staining was conducted to indicate duct cells and Islets of Langerhans. Anti-E-cadherin staining was used to identify centroacinar cells by morphology. (n = 391 cells from 2 mice) Scale bars = 50μm. (**b**) Pancreatic sections of rainbow2 mice 365 DPI stained for YFP, Cytokeratin 19 (CK19) and Insulin (Ins). Scale bars = 200μm (left panel) and 100μm (right panel).

3.3 Clonal dynamics of acinar cells upon injury

The data acquired thus far suggested that an acinar subpopulation retains proliferative capacity in order to compensate for dying acinar cells during homeostasis. In the healthy pancreas the turnover has been described to be very low (Magami et al., 1990). In contrast, cell death and replacement after injury is markedly increased (Fukuda et al., 2011; Nagashio et al., 2004). Thus, we wanted to test, whether the proliferative acinar subpopulation also compensates for injury-induced cell death. An alternative scenario would be that acinar cells outside the pool of the proliferative subpopulation would gain the ability to enter the cell cycle in order to compensate for the loss of acinar cells upon injury. In order to distinguish between these two scenarios, we induced the rainbow2 colours in adult mice followed by a chemically induced acute pancreatitis as previously described (Carrière et al., 2011). If the proliferative acinar subpopulation would compensate for acinar cell death we would expect to find larger clones at a given time point as compared to the naive condition (Fig. 10a – right scenario). If, on the other hand, other acinar cells start to proliferate we would expect to observe larger average clone sizes (Fig. 10a – left scenario). We chose 28 DPI as the time point for tissue analysis since this is the first time point where we reliably detect large clones derived from the proliferative subpopulation (Fig. 10).

Compared to acinar cells from naive animals, the injury-induced clonal expansion led to an increase in average clones size (Fig. 10b,c). Specifically, we observed an increase in three and five cell clones at 28 DPI (Fig. 10c). No increase in maximal clone size was observed indicating that the injury induces a proliferative response, which is not restricted to small acinar subpopulations (Fig. 10a – left scenario). Furthermore, there was no change in two-nuclei clones as a result of the injury (Fig. 10c). Given that the majority of the two-nuclei clones represent binuclear acinar cells (Fig. 7) this result suggests that binuclear cells are not able to respond to the injury by proliferation.

This data raises the question whether the acinar cells that started to proliferate will continue to do so through time and essentially convert into the acinar cell type that retains proliferative capacity. Another possibility is that the injury-induced proliferation is only of transient nature. We aimed to distinguish between these two scenarios by repeating the previous experiment while analysing the tissue at 365 DPI instead of 28 DPI. If the injury response is not transient then we expect to find more large clones at 365 DPI in comparison to the homeostatic situation. Analysing the pancreas of rainbow2 mice at 365 DPI revealed that the clone size distributions of the injured and naïve groups are almost identical (Fig. 10d). We neither

observed an increased number of large clones, which would be reflected at the tail of the distribution, nor an increase regarding the average clone size. These experiments demonstrate that injury induces a transient proliferative response of acinar cells.

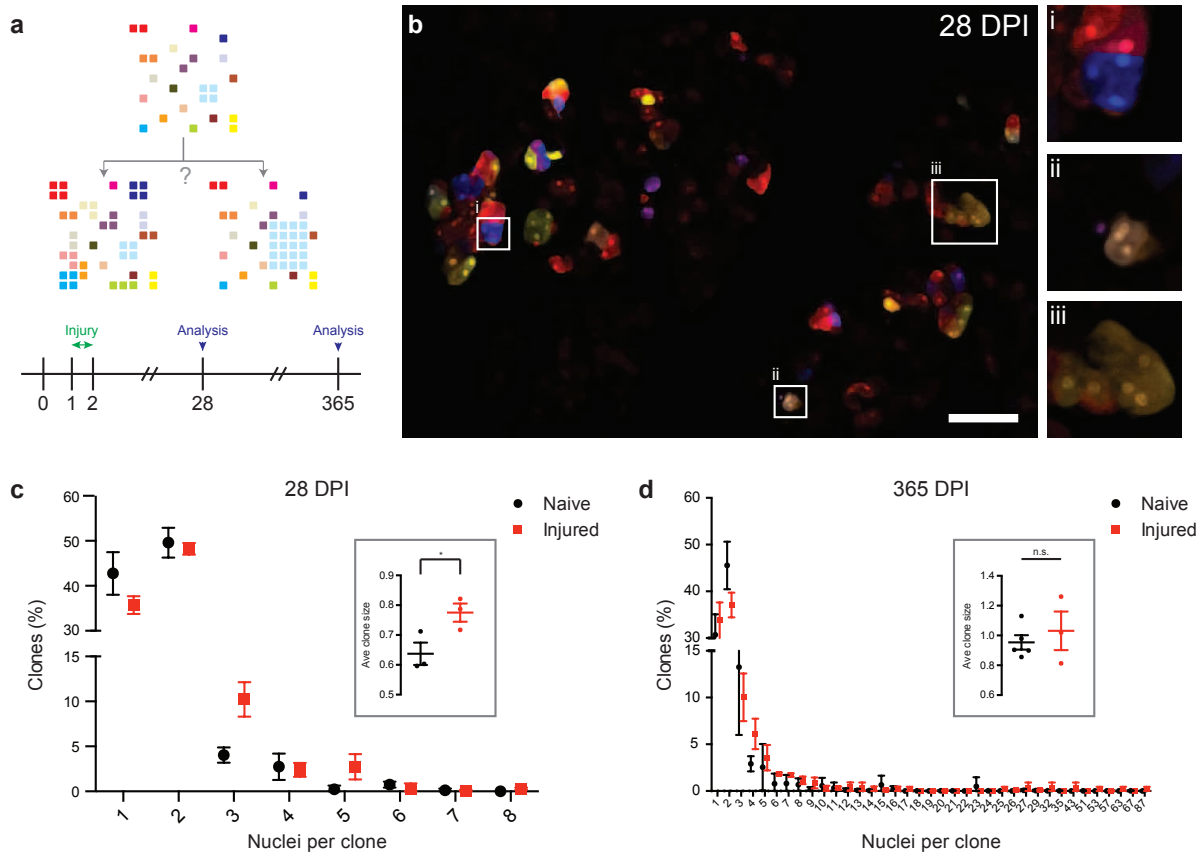

Figure 10. Injury transiently activates a broad range of acinar cells. (**a**) Experimental Design and schematic illustration of potential changes of clone size distribution upon injury. Squares represent clonal clusters of acinar cells. Hypothesized outcome scenarios are clone size expansion of many previously dormant clones (left matrix) versus clone size expansion of few clones which are actively proliferating under homeostatic conditions (right matrix). Pancreatic tissue was analysed 28 and 365 days post injection. (**b**) Representative illustration of clonal distribution 28 days after rainbow2 induction. Scale bar = 50µm (**c, d**) Quantification of clone size distribution from naive and injured mice. For 28 DPI n = 1307 clones from 3 injured mice; 365 DPI n = 2805 from 3 injured mice. Data represent mean ± SD. Insets: Average clone size comparison between naïve and injured animals. Log2 of clone sizes were calculated to obtain normal clone size distribution. Average clone size data are presented as mean ± SEM; *p < 0.05.

3.4 Proliferative capacity of acinar cells *in vitro*

Stem and progenitor cells of various organs have been described to have the capacity to form organoids under 3D culture conditions (Sasai, 2013). Considering that the acinar subpopulation that we discovered resembles lineage-restricted progenitors, we hypothesized that some acinar cells would form organoids. In order to carefully characterise the organoid formation capacity of individual acinar cells *in vitro* we purified acinar cells from adult mice in which the Histone H2B is genetically tagged to a mcherry fluorophore. With this tool at hand, we could microscopically track the number of nuclei at any time during organoid formation. When we plated acinar cells in matrigel at a density of 500 cells per well we detected a subpopulation of acinar cells that was able to form organoids, mirroring the functional heterogeneity we observed *in vivo* (Fig. 11a).

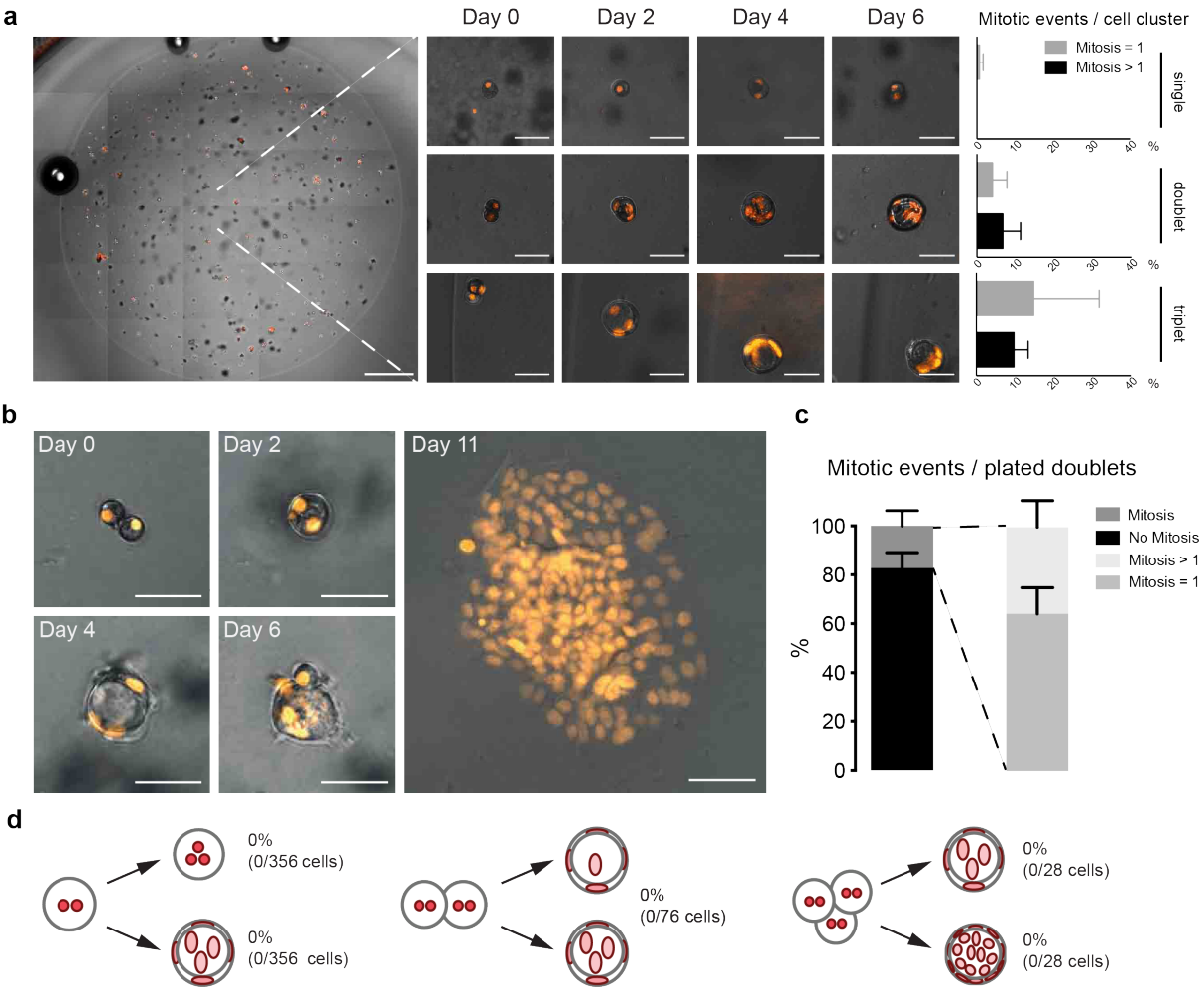

Figure 11. An acinar subpopulation forms organoids *in vitro*. (**a**) Representative image of spontaneously formed organoids 0 - 6 days after isolation of adult pancreatic cells. 500 cells isolated from H2B-mcherry mice were plated in matrigel and the rate of divisions from single cells, doublets or triplets at day 0 was followed over a period of 11 days. Representative pictures of mitotic events of single cells (top row), doublets (middle row) and triplets (bottom row) are shown. Quantification of number of mcherry^{+} nuclei is plotted on the right of the respective row. Scale bars = 500µm (overview) and 50μm (close up). N = 1899 cell clusters from 3 mice. (**b**) Representative image of handpicked acinar doublets isolated from H2B-mcherrry mice that were cultured for 11 days and quantified on the last day. Scale bars = 50µm. (**c**) Quantification of handpicked acinar doublets undergoing a single mitotic event or multiple mitotic events (n = 682 doublets derived from 4 mice). (**d**) Quantification of proliferation capacity of binuclear acinar cells from (**a**). Data acquired in collaboration with Isabelle Everlien. Data in part presented in her master thesis.

Single acinar cells were infrequently able to undergo a single mitotic event but were not able to further proliferate and form organoids (Fig. 11a). In contrast, multiple mitotic events were observed in mononuclear acinar doublets 6.70 ± 4.61%, triplets 9.72 ± 3.67% and clusters 12.14 ± 5.08% of acinar cells (Fig. 11a). Hence, at least two cells in contact are required to initiate organoid formation accompanied by more than one mitotic event. Interestingly, we observed 2 modes of proliferation in doublets and triplets. Acinar doublets/triplets were able to either undergo only a single mitotic event (and subsequently stop to proliferate) or

continuously proliferate and give rise to organoids (Fig. 11a). These results suggest that the proliferative acinar subpopulation might contain cells capable of limited and unlimited proliferative capacity. Thus, the proliferative acinar subpopulation might represent a heterogeneous pool of cells in itself.

The organoid formation assay suggests that acinar cells need at least one supporting cell in order to form organoids and proliferate. To test whether cell-cell contact between acinar cells is not only necessary but also sufficient to form organoids, we handpicked a total of 682 acinar doublets from 4 mice and cultured them as single doublets. Among the acinar doublets 4.53 ±1.55% were able to form organoids and proliferate considerably (Fig. 11b,c). Similarly, to clusters of acinar cells within a cell suspension we again observed two modes of proliferation in which acinar cells underwent a single or multiple mitotic events (Fig. 11c). This finding is reminiscent of studies of the small intestine where $Lgr5^+$ stem cells need short-range niche signals from paneth cells to form organoids (Sato et al., 2010), possibly indicating that acinar cells receive signals from specific niche-like acinar cells.

Importantly, while examining binuclear acinar cells we discovered that binuclear cells did not undergo mitosis, independent of their association with other binuclear cells as doublets or triplets (Fig 11d). This result underscores the finding that binuclear cells are proliferation-deficient as also suggested by the fact that two-nuclei clones do not display proliferative response upon injury *in vivo* (Fig. 10c).

It was previously demonstrated that pancreatic duct cells are able to form organoids in 3D culture conditions (Huch et al., 2013a). Therefore, we aimed to investigate whether duct cell contaminations might be the source of the organoids we observe. First, we stained freshly isolated acinar cells for the duct marker CK19 and analysed the cells by flow cytometry. The analysis of 10.000 events showed that all cells express the acinar marker Amylase (Fig. 12a). Furthermore, we could not detect a single $CK19^+$ cell strongly suggesting that our isolation protocol ensures high purity (Fig. 12a). Interestingly, we found a population of cells (12%) that expressed acinar and duct markers (Fig. 12a). This finding is likely due to the fact that acinar cells undergo acinar-to-ductal metaplasia (ADM) during the organoid formation (unpublished data by Xiaokang Lun).

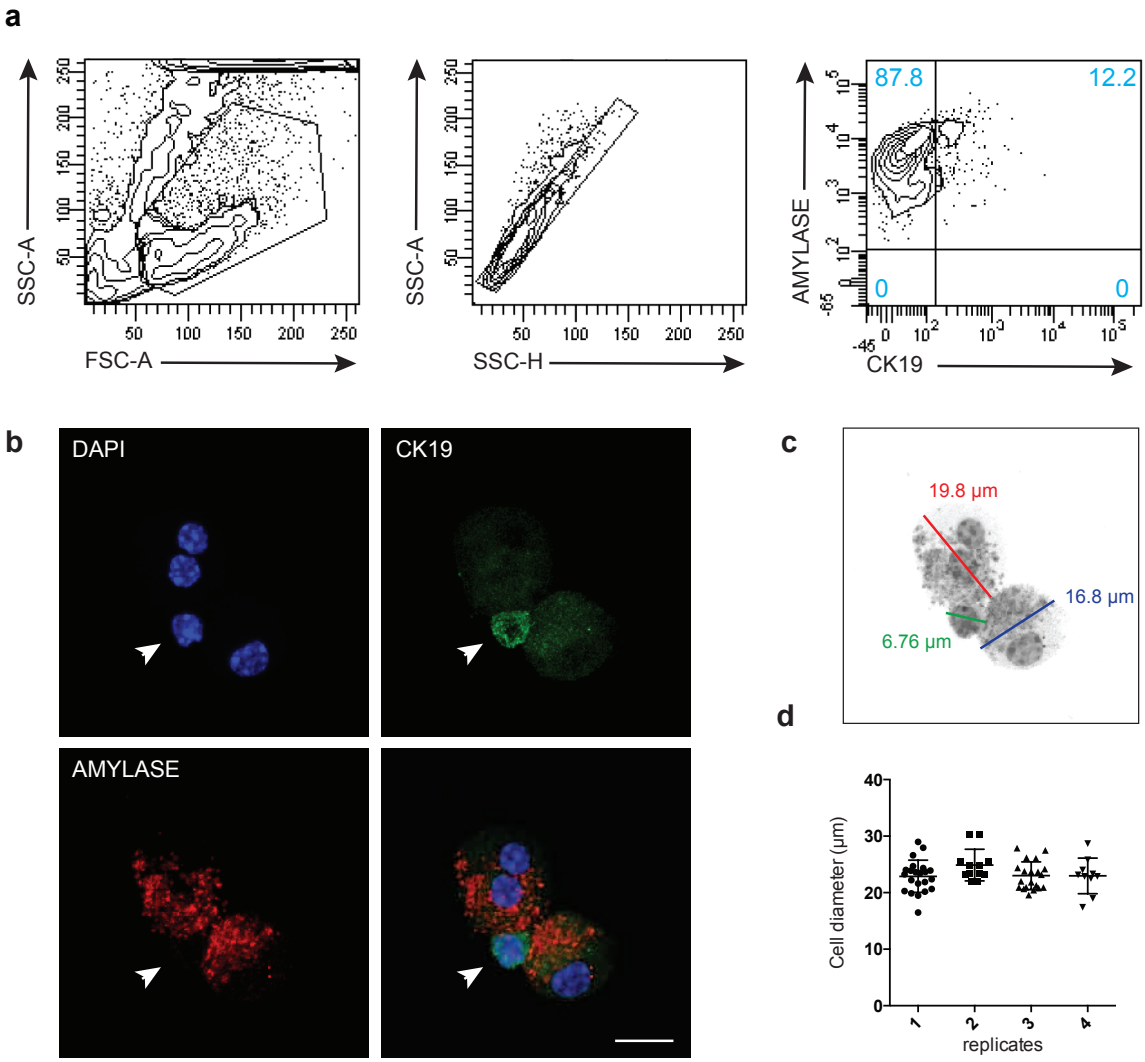

Figure 12. Characterisation of acinar purity after isolation. (**a**) Flow cytometry analysis of pancreatic cells directly after isolation confirms high purity of acinar cells. Acinar cells were purified by differential centrifugation and stained for CK19 and Amylase to detect duct and acinar cells, respectively. (**b**) Immunofluorescence staining of Amylase and CK19 confirming acinar and ductal identity after cell isolation. Scale bar = 10μm. (**c**) Measurements of acinar and ductal cell diameter after isolation. (**d**) Quantification of the cell diameter of all cells that gave rise to organoids in Fig. 2b,c. 1-4 denote biological replicates.

To further assure that pancreatic organoids arose from acinar cells, we took advantage of the significant size difference between acinar and duct cells (Fig. 12b). The diameter of acinar cells is approximately 3-fold larger as compared to duct cells (Fig. 12c). Next, we revisited the experiment in which we handpicked acinar doublets that formed organoids (Fig. 12b). We measured the diameter of all cells that gave rise to organoids at day 0. The size range of all analysed cells was between 20 and 30 μm excluding ductal origin of organoids (Fig. 12d). Furthermore, we can exclude contamination of other cell types in this experiment since we used H2B-mcherry mice. Any living cell potentially contaminating our culture would have been detected due to the fluorescence of the nuclei.

3.5 Characterisation of binuclear acinar cells

We found that binuclear acinar cells display marked deficiency in proliferation (Fig. 10 & 11). Therefore, we aimed at characterizing binuclear acinar cells. The existence of binuclear cells in the pancreas of rats has been described in 1968 (D S Longnecker, 1968). Quantification of mono- and binuclear cells revealed that the pancreas of adult rats contained 64% binuclear cells (Oates and Morgan, 1986). We stained tissue of adult murine pancreas for E-cadherin in order to mark cell borders of acinar cells (Fig. 13a). We determined that the pancreas of an adult mouse contains 44±1% binuclear acinar cells (Fig. 13a). Next, we quantified the number of mono- and binuclear acinar cells, which stained positive for the proliferation marker pH3. Under homeostatic conditions the proliferation rate of acinar cells is too low for feasible characterization by immunohistochemistry (Magami et al., 1990). Thus, we increased the proliferation rate by chemically inducing pancreatitis by Cerulein injection as previously described (Carrière et al., 2011). We observed that the majority of proliferating cells were mononuclear, while no difference regarding cells death was detected (Fig. 13b,c). Similarly, we did not observe proliferation of binuclear cells *in vitro* despite the high concentration of mitogens in culture (Fig. 11d). It is possible that the pH3 positive binuclear cells that we observed *in vivo* could represent mononuclear acinar cells that just completed telophase and therefore still stain positive for pH3. Another possibility is that a fraction of binuclear cells start to enter cell cycle in response to injury.

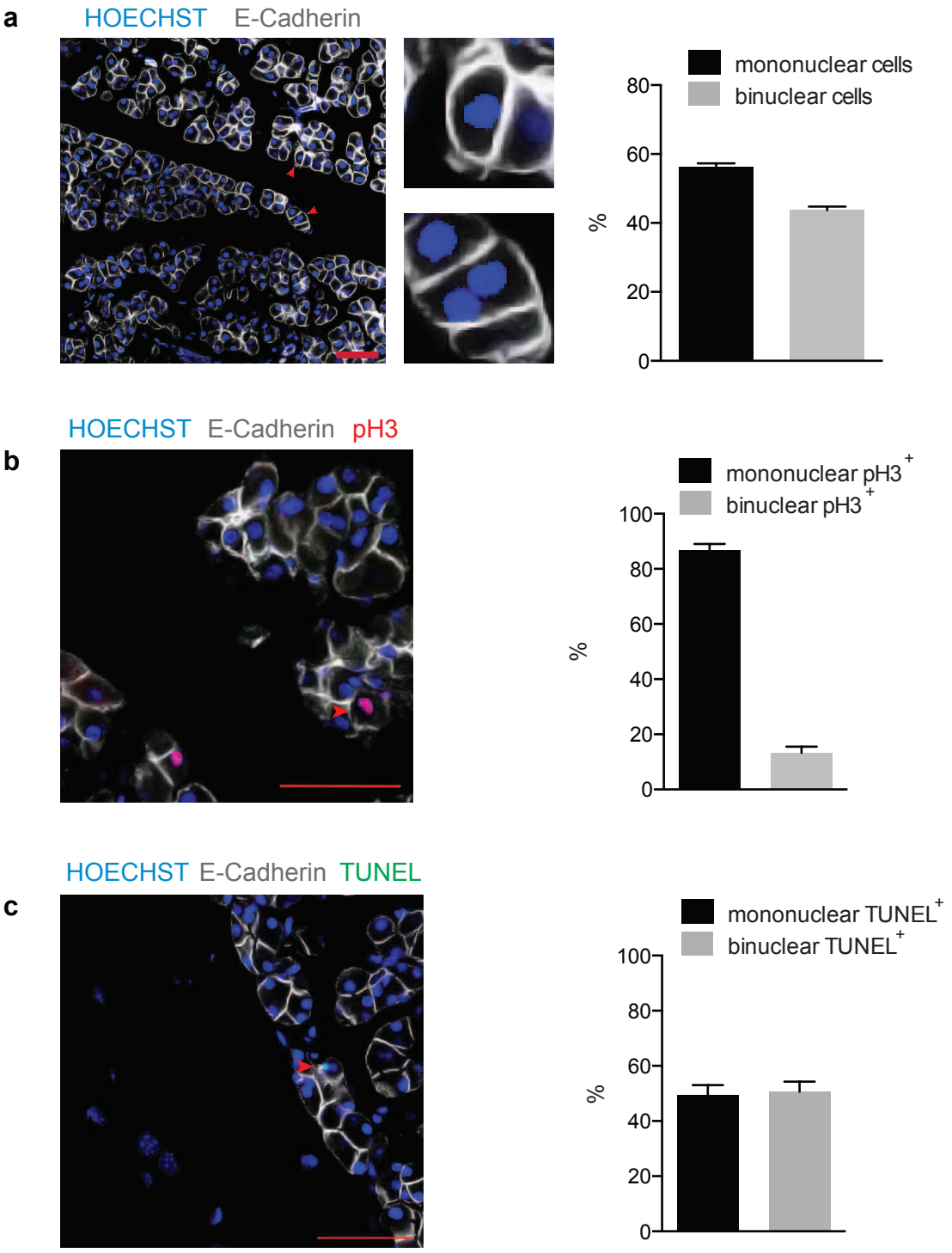

Figure 13. Analysis of proliferation and cell death of mono- and binuclear acinar cells. (**a**) Representative images of pancreas sections stained for E-cadherin and counterstained for Hoechst 33342. Numbers of mono- and binuclear acinar cells were quantified (Right panel). Data represent mean ± SD for 560 cells from 2 mice. Scale bar = 50μm. (**b,c**) Quantification of proliferating and dying mono- and binuclear acinar cells was assessed by phospho-Histone H3 (pH3) and TUNEL staining 3 days post injury. Data represent mean ± SD for 172 $pH3^+$ and 72 $TUNEL^+$ cells from 2 mice.

Even though binuclear cells have been reported to exist in rats (D S Longnecker, 1968) it has not been determined whether the human pancreas also contains binuclear cells. We stained

human pancreatic tissue sections, which did not show any pathological abnormalities for E-cadherin to determine the nuclei number of human acinar cells. We found binuclear acinar cells in each of the 15 observed tissue samples (Fig. 14). Thus, we demonstrated that the adult human pancreas contains binuclear acinar cells and expose human acinar as a morphologically heterogeneous entity.

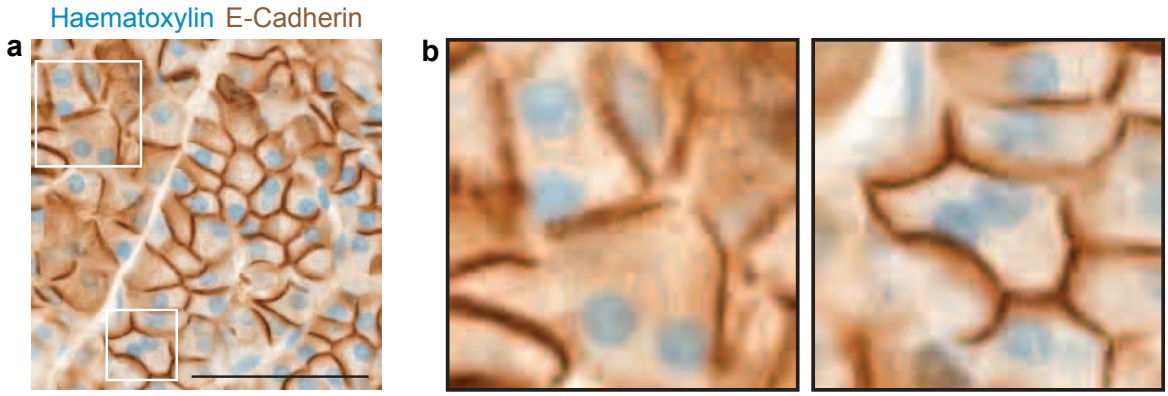

Figure 14. The adult human pancreas contains binuclear acinar cells. (**a**) E-cadherin staining of paraffin-embedded human pancreatic sections reveals binuclear acinar cells. Haematoxylin was used for nuclear counterstaining. Scale bar = 50μm. (**b**) Magnification of insets from (**a**). Staining was performed by the Institute of Pathology, University of Heidelberg

3.6 Development of library preparation protocol for single acinar cell RNA-seq

The data acquired thus far strongly suggested that acinar cells are not a pool of homogenous cells but contain (at least) one subpopulation. This subpopulation, albeit being morphologically indistinguishable from other acinar cells, displays long-term proliferative capacity similar to progenitor cells from other tissues. We hypothesized that the functional difference of this subpopulation would be reflected on the molecular level. In order to test this hypothesis, we aimed to perform single cell RNA sequencing of randomly selected acinar cells. This unbiased, bottom-up approach should reveal the molecular basis of acinar subpopulations if this pool of cells is as heterogeneous as our previous experiments suggest.

There are a number of protocols for RNA sequencing of single cells that have recently been established (Saliba et al., 2014). Our laboratory established the SMART-Seq2 protocol for library preparation and sequencing of mRNA from single neural stem cells (Llorens-Bobadilla et al., 2015). This protocol is based on two major steps: a) reverse transcription of mRNA and cDNA amplification and b) adaptor ligation through Tn5 tagmentation and library amplification. The first step starts by cell lysis using hypotonic lysis buffer containing

oligodT primers and free dNTPs (Fig. 15a). After annealing of the primer, the addition of the Moloney murine leukemia virus (M-MLV) reverse transcriptase permits cDNA synthesis in the same reaction tube where the cell was lysed. This approach avoids the purification of RNA, which frequently leads to loss of RNA as well as RNA degradation (Picelli et al., 2014). The M-MLV reverse transcriptase inherently adds 2-5 untemplated nucleotides (mostly cytosines) to the 3´ end of the cDNA (Schmidt and Mueller, 1999). This feature grants a template switch, which offers high coverage of the RNA 5´ end and subsequently full-length coverage across the transcript (Fig. 15). After cDNA amplification by PCR, the quality of the cDNA library can be tested via capillary electrophoresis using a 2100 Agilent Bioanalyzer (Fig. 15b,c). Successful cDNA library preparation results in an average library size of 1.5 - 2 kb (Fig. 15b). In contrast, library preparation from degraded RNA is characterized by a shift towards shorter fragments resulting in a broader peak distribution (Fig. 15d).

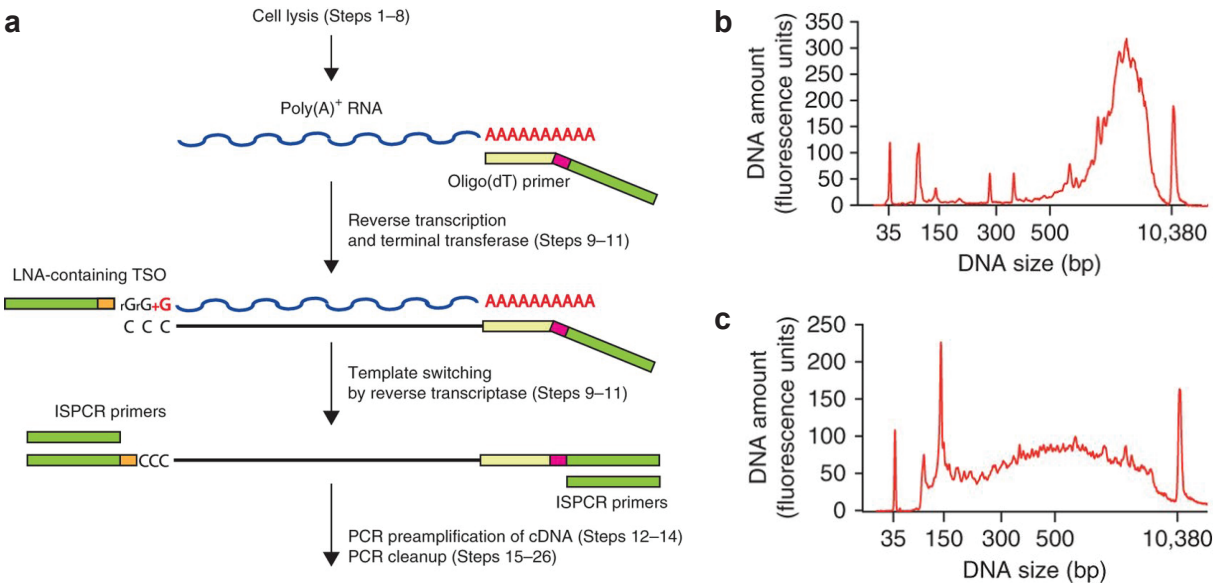

Figure 15. cDNA library preparation using SMART-Seq2. (**a**) Schematic representation of the cDNA preparation. (**b,c**) Representative Bioanalyzer profiles of cDNA libraries upon successful preamplification (a) and RNA degradation before cDNA preparation (c). Figures were obtained from Picelli et al., 2014.

Library preparation from single acinar cells using standard conditions led to cDNA libraries of very small size and low concentration (Fig. 16a-c – "normal cond."). The shift towards smaller fragments indicated degradation of the input material. RNA isolation from the pancreas is classically considered to be very challenging due to the high RNAse content of the tissue (Chirgwin et al., 1979). The RNAses are produced in vast amounts by acinar cells in order to digest the nucleic acids within the diet (Barnard, 1969).

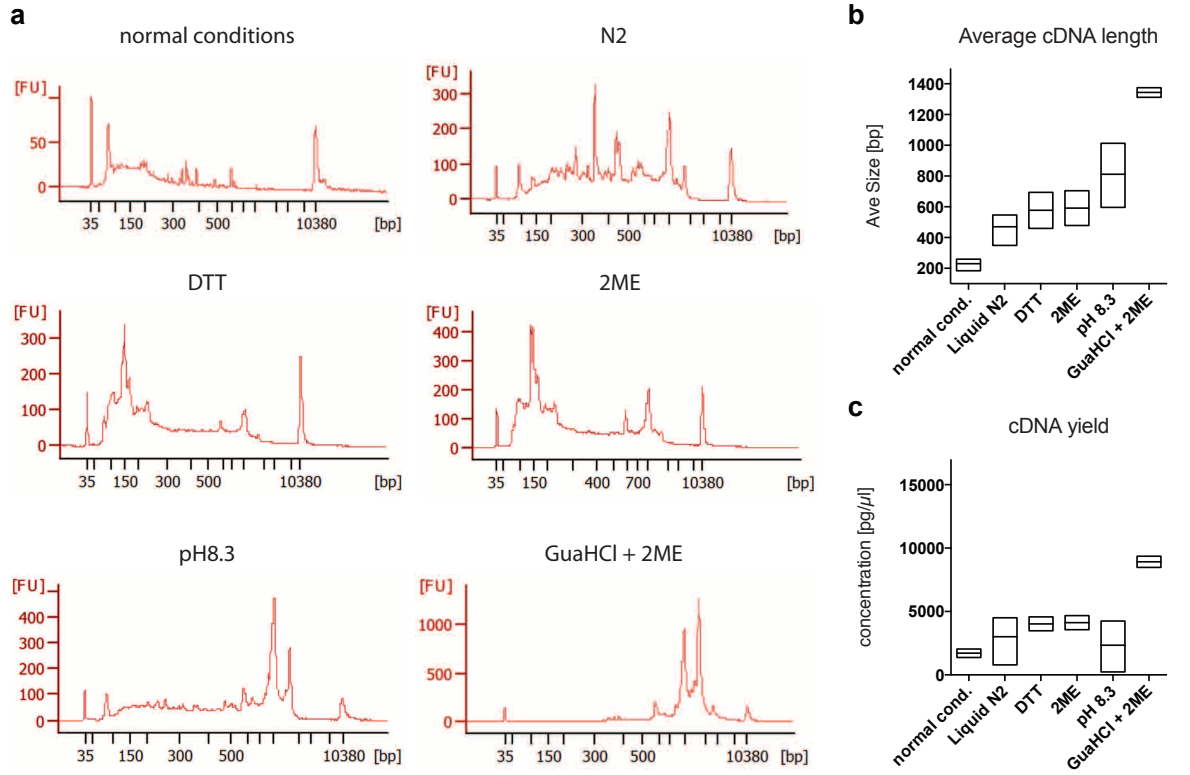

Figure 16. Protocol development for cDNA library preparation from single acinar cells. (**a**) Representative Bioanalyzer profiles of cDNA libraries obtained from single acinar cells under varying cell lysis conditions. (**b**) Average size of cDNA library length obtained under conditions described in (a). (**c**) cDNA yield produced under conditions described in (a).

We hypothesized that acinar derived RNAses would rapidly degrade mRNA prior to reverse transcription. Although the lysis buffer contains RNAse inhibitors, the extensive amount of RNAses will likely exceed the inhibitor concentration. In order to hold RNA degradation upon lysis, we transferred the reaction tube to liquid nitrogen directly after the cell lysis until we proceeded with cDNA synthesis. Although this increased the average cDNA length and yield, the broad peak distribution suggested persistent RNA degradation impeding full-length cDNA synthesis (Fig. 16a-c – "N2"). The secondary structure of RNAses strongly depends on disulfide bridges (Klink et al.). We therefore supplemented our lysis buffer with either dithiothreitol (DTT) or β-mercaptoethanol (2ME) to reduce the disulfide bonds. The addition of either reducing agent resulted in slightly higher average library size and consistently higher cDNA yield as compared to previous buffer compositions (Fig. 16a-c – "DTT" / "2ME"). However, the peak of the library distribution was at ~150bp indicating substantial RNA degradation (Fig. 16a). Next, we tried to target the pH dependent catalytic activity of ribonucleases. The enzyme activity of RNAse A has a pH optimum at ~7.4, which is declining at alkaline and acidic conditions (Findlay et al., 1962). In contrast, the cDNA synthesis using M-MLV reverse transcriptase is performed at a pH of 8.3 (Kotewicz, 1988).

Since the protocol does not involve purification steps between cell lysis and reverse transcription, we hypothesized that shifting the pH to 8.3 at the point of cell lysis would substantially hamper RNAse activity, but not affect reverse transcription. In contrast to all previous conditions the cDNA libraries obtained through pH shift of the lysis buffer demonstrate a peak at long fragments for a number of libraries (Fig. 16a – "pH8.3"). Although this indicates successful library preparation, the cDNA length and yield varied considerably from sample to sample (Fig. 16b,c). Thus, pH optimization might be a more attractive, low-cost approach for cDNA synthesis from tissues other than the pancreas. Previously, RNA isolation from large amounts of pancreatic tissues has been successful by making use of chaotropic agents (Chirgwin et al., 1979). In this approach, RNA degradation was prevented by lysing the cells using high concentration of guanidine hydrochloride (Chirgwin et al., 1979). Chaotropic agents such as guanidine hydrochloride or urea lead to denaturation of proteins (Chirgwin et al., 1979). Subsequently, RNA could be isolated by phenol chlorophorm extraction (Chomczynski and Sacchi, 1987). Although promising, this approach was not directly applicable to our low input protocol because an essential component of the protocol was the avoidance of purification steps before cDNA amplification (Picelli et al., 2014). A lysis buffer containing high concentrations of guanidine hydrochloride would also denature all enzymes subsequently added for reverse transcription and amplification. To circumvent this problem, we combined the chaotropic protein denaturation with solid-phase reversible immobilization (SPRI) technology (Fig. 17).

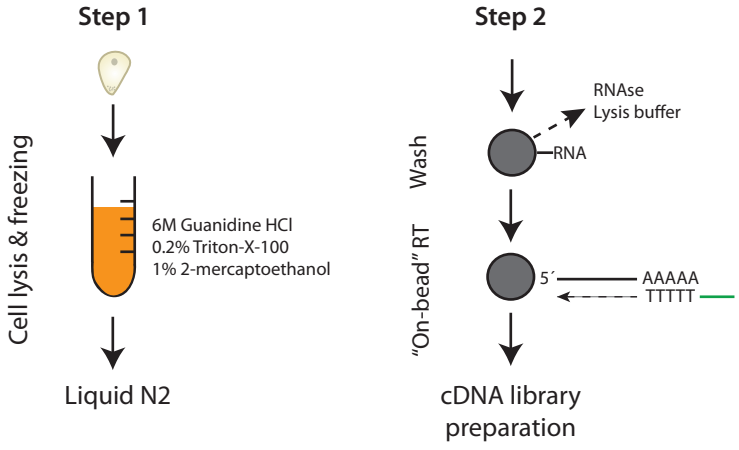

Figure 17. cDNA library preparation protocol for single acinar cells. Schematic representation of the step-by-step protocol for cDNA library production from single acinar cells. Grey circles represent SPRI beads.

We prepared a buffer containing 6M guanidine hydrochloride and 0.2% Triton X-100 to lyse the cells and denature the released proteins. We added reducing agents to the lysis buffer as a result of the small but consistent enhancement in cDNA yield and length that we observed (Fig. 16a-c – "DTT" / "2ME"). After cell lysis we directly transferred the reaction tube into liquid nitrogen for the time of cell collection. Next, we added SPRI beads to the lysate. SPRI beads are carboxyl-coated magnetic particles, which are dissolved in polyethylene glycol (PEG) (Hawkins et al., 1994). Application of high PEG concentrations leads to the precipitation of RNA and DNA onto the carboxylated beads at nearly 100% efficiency (Hawkins et al., 1994). Subsequent washing steps remove the guanidine hydrochloride containing lysis buffer as well as acinar cell derived RNAses. It should be noted that PEG could also be used for protein precipitation (Lis, 1980). However, efficient protein precipitation onto carboxylated beads requires acetonitrile treatment (Hughes et al., 2014). Therefore, PEG precipitation of RNAses might be not sufficient for degradation of RNA. After the final washing steps, the elution step was avoided to trap RNA on the beads for cDNA synthesis as previously described (Shalek et al., 2013). The protocol led to highly increased average cDNA length and yield with very limited sample-to-sample variablilty (Fig. 16a-c "GuaHCl + 2ME"). We observed indistinguishable results by using dithiothreitol instead of β-mercaptoethanol (data not shown). This data strongly indicated successful and robust cDNA library preparation from single acinar cells.

In order to test the quality of the cDNA libraries on a global scale we sequenced libraries from 108 single acinar cells. We obtained 5.4 million total reads on average of which 77.9% mapped to the transcriptome (Fig. 18a,b). The number of reads we recovered as well as the mapping rate are both similar to previously published results indicating high quality of the sequenced libraries (Llorens-Bobadilla et al., 2015; Treutlein et al., 2014). To test linear amplification of our transcripts we spiked in a mixture of 92 polyadenlyated transcripts of known quantity as recommended by the External RNA Controls Consortium (ERCC) into the lysate of 19 cells. We then correlated the known abundance of the transcripts with the transcript levels ($\log_2$(TPM)) detected by sequencing (Fig. 18c). None of the 19 tested libraries displayed a Pearson correlation lower then r = 0.9 indicating linear amplification of cDNA by our protocol (Fig. 18d). The SMART-seq2 protocol starts cDNA synthesis at the 3´end by priming at the poly(A) tail (Fig. 15a) (Picelli et al., 2014). Therefore, it is possible that some libraries display a 3´ bias if, for instance, the RNA would be partially degraded. We tested the coverage of the sequencing reads along the transcripts and found no 3´ bias for any of the sequenced libraries (Fig. 18e). All sequenced cells expressed extremely high levels of

digestive enzymes ensuring that all sequenced libraries are derived from acinar cells (Fig. 18f). These data demonstrated that we were able to obtain high quality sequencing data from single acinar cells. Since we used a NesCreER^{T2} mouse line for lineage tracing of acinar cells we wanted to test how many acinar cells showed detectable levels of *Nestin*. Among the pool of cells that we profiled we detected (TPM > 1) *Nestin* in 22% of all acinar cells (Fig. 18g). This result is in excellent agreement with the recombination efficiency of our Cre line in the pancreas, which we determined to be 23% (Fig. 6c). Thus, the number of cells that recombine in our lineage tracing setup is likely limited by the expression of Nestin among acinar cells rather than recombination efficiency of the NesCreER^{T2} line.

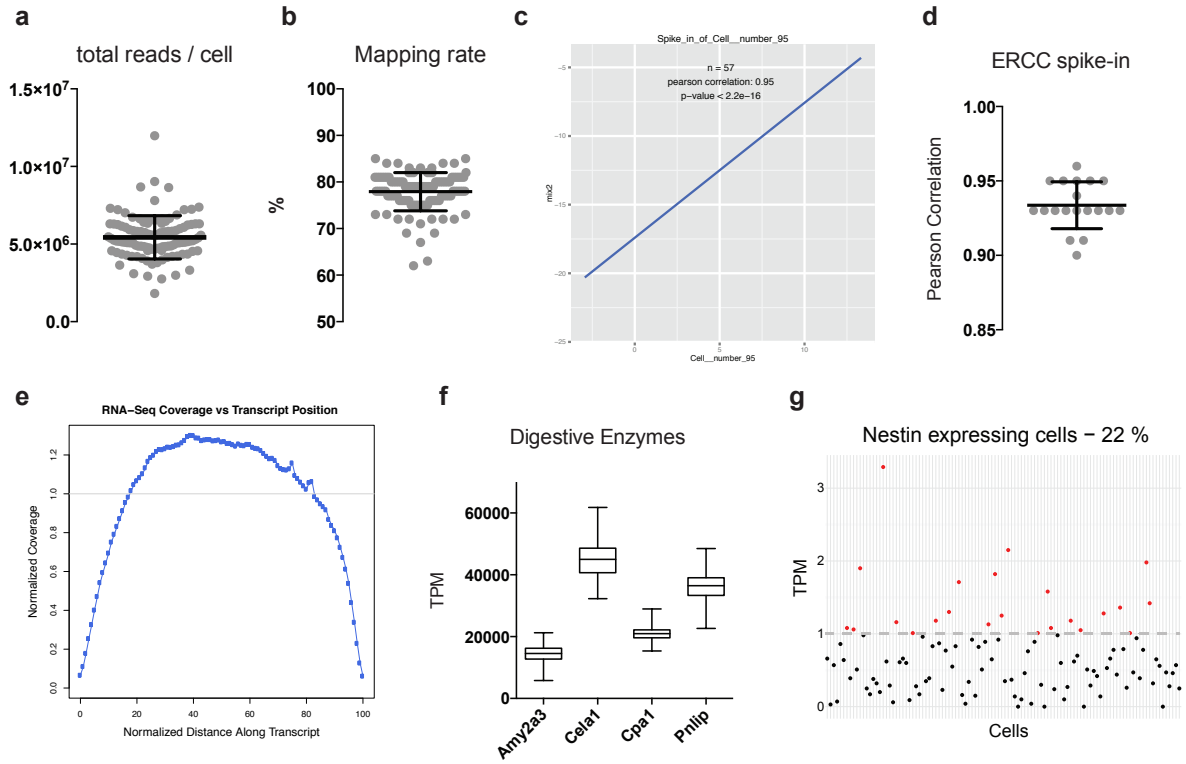

Figure 18. Quality control of acinar single cell sequencing data (**a**) Total number of reads obtained for each cell. (**b**) Rate of reads mapping to exons of genes. (**c**) Representative example (Cell #95) displaying correlation between ERCC RNA abundance and detection by sequencing. (**d**) Pearson correlation of 19 cells containing ERCC spike-ins. (**e**) Representative example (Cell #98) of normalized 3´ and 5´ coverage of sequenced reads along the transcripts. (**f**) Expression values of selected digestive enzymes expressed in acinar cells. (**g**) Expression values of *Nestin* in all sequenced cells.

3.7 Molecular heterogeneity of acinar cells

With the data at hand, we aimed to discover whether the acinar cells represent a molecularly heterogeneous entity. We compared the similarity of all sequenced transcriptomes by

comparing the Euclidian distance in the gene expression matrix. We found that the majority of the 108 sequenced acinar cells are very similar on the transcriptome level (Fig. 19a).

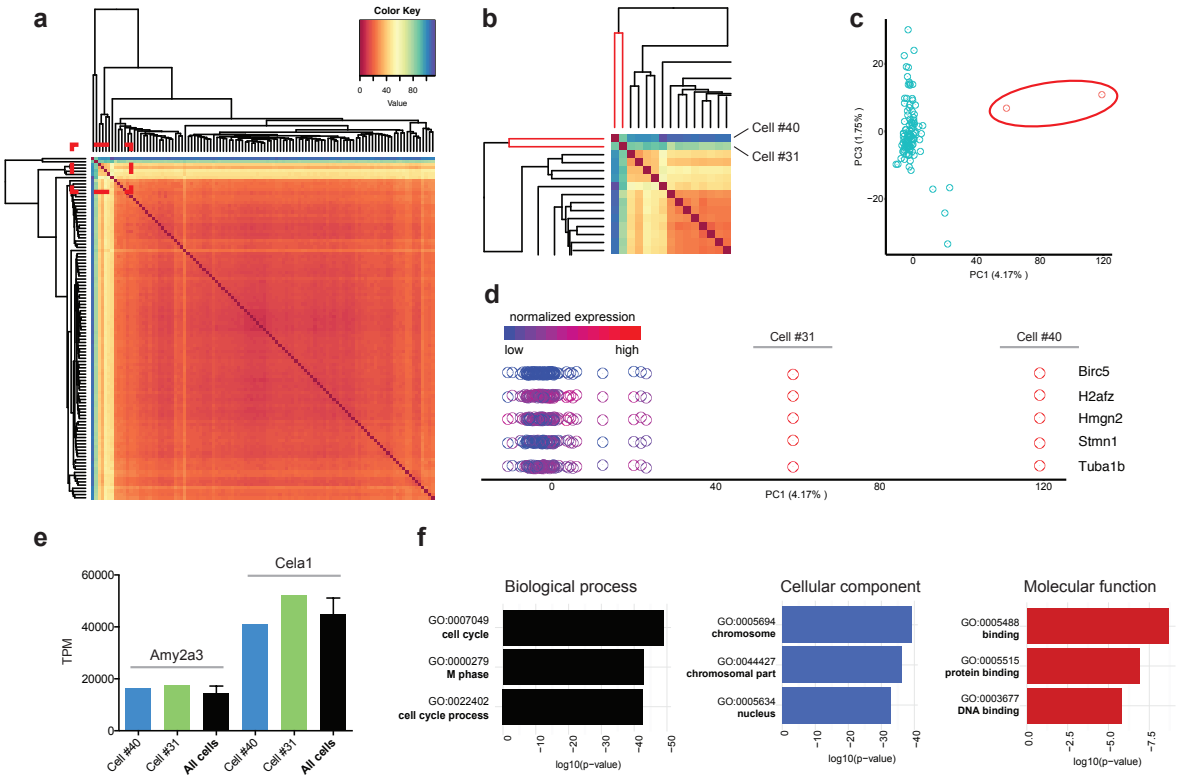

Figure 19. Single cell sequencing reveals molecularly distinct acinar subpopulations. (**a**) Heat map indicating 108 single-cell transcriptome similarities measured by the Euclidean distance of the gene expression matrix. (**b**) Magnification of heat map inset. (**c**) Principle component analysis of single-cell transcriptomes of 108 acinar cells. (**d**) One-dimensional PCA of 108 acinar cells. Each point corresponds to one cell, the colour on each cell corresponds the scaled expression value of the respective gene in each single cell and the position of each point corresponds the coordinate value of each cell on selected component from PCA. (**e**) Expression values of Amylase (*Amy2a3*) and Elastase (*Cela1*) for Cell #40, Cell #31 and the average (±SD) of all acinar cells. TPM = transcript per million. (**f**) GO category of genes highly expressed in Cell #31 and Cell #40.

Within the pool of the cells that we sequenced we found two cells that displayed a distinct transcriptional profile by hierarchical clustering (Fig. 19a inset, 19b). These cells (Cell #40 and Cell #31) were also confirmed to be distinct by principle component analysis (Fig. 19c). This analysis showed that the outlier population differed from the other profiled cells mainly by genes within the principle component 1 (PC1), which comprises 4,17% of the transcriptome (Fig. 19c). We then reduced the dimensionality of the components to one dimension (PC1) and revealed that the two outlier cells express high levels of genes involved in chromatin remodelling (*H2afz*, *Hmgn2*), microtubule maintenance (*Stmn1*, *Tuba1b*) and proliferation (*Birc5*) (Fig. 19d). Given the difference between the outlier cells and the other acinar cells, we wondered whether the outlier cells represent a cross-contamination from

another cell type. To test this, we evaluated the expression levels of two acinar marker genes: Amylase and Elastase. We found that both outlier cells expressed levels of these markers that are comparable to the average of all other acinar cells (Fig. 19e). We conclude that the outlier cells are acinar cells, since no other cell in the mammalian body expresses such high levels of digestive enzymes (Logsdon and Ji, 2013). Next, we performed gene ontology (GO) analysis of genes, which are highly expressed in the outlier cells. We found that the three most significant categories were related to proliferation. Furthermore, GO category analysis revealed that the genes highly expressed in the outlier population are related to binding of DNA and proteins and thus localized in the nucleus (Fig. 19f).

These results suggest that acinar cells harbour a molecularly distinct subpopulation with the feature of cell cycle activity. This is in accordance with our finding of proliferative heterogeneity as illustrated by the lineage tracing experiments. Since we found only two cells with this molecular profile, we aimed to find a marker for this subpopulation in order to validate the existence *in vivo*. We filtered out all genes, which are differentially expressed between Cell #40 / Cell #31 and all other profiled acinar cells. Next, we plotted the most differentially expressed genes of both outlier cells against each other to find common markers (Fig. 20a). Among the most highly differentially expressed genes in both cells was *Stmn1*. STMN1, also known as Oncoprotein 18 or Stathmin, is a highly conserved protein, which regulates microtubule dynamics (Cassimeris, 2002). Interestingly, STMN1 has recently been described to be a novel marker for early intermediate progenitor cells in the adult hippocampal subgranular zone (Shin et al., 2015). Furthermore, it was shown to be a marker for proliferating cells in a variety of tissues (Cassimeris, 2002). We took advantage of the Human Protein Atlas (Uhlen et al., 2015) to see whether STMN1 was expressed in the healthy human pancreas. Staining of human pancreatic sections for STMN1 (performed by the Human Protein Atlas) indicated strong expression of STMN1 in a subset of pancreatic cells (Fig. 20b). According to morphological features, the majority of these cells could be identified as acinar cells (Fig. 20b – inlet). We stained murine pancreatic tissue to test whether we could identify a $STMN1^+$ acinar subpopulation. A subset of acinar cells expressed STMN1, validating the existence of an STMN1 subpopulation *in vivo* (Fig. 20c,d). Although we occasionally found $STMN1^+$ acinar cells that expressed the proliferation marker pH3, the vast majority of $STMN1^+$ cells did not stain positive for pH3 (Fig. 20c,d). This demonstrates that STMN1 is not expressed solely because the cell is actively cycling. Instead, this data is in line with previous findings illustrating that STMN1 is post-translationally regulated during the cell cycle (Cassimeris, 2002).

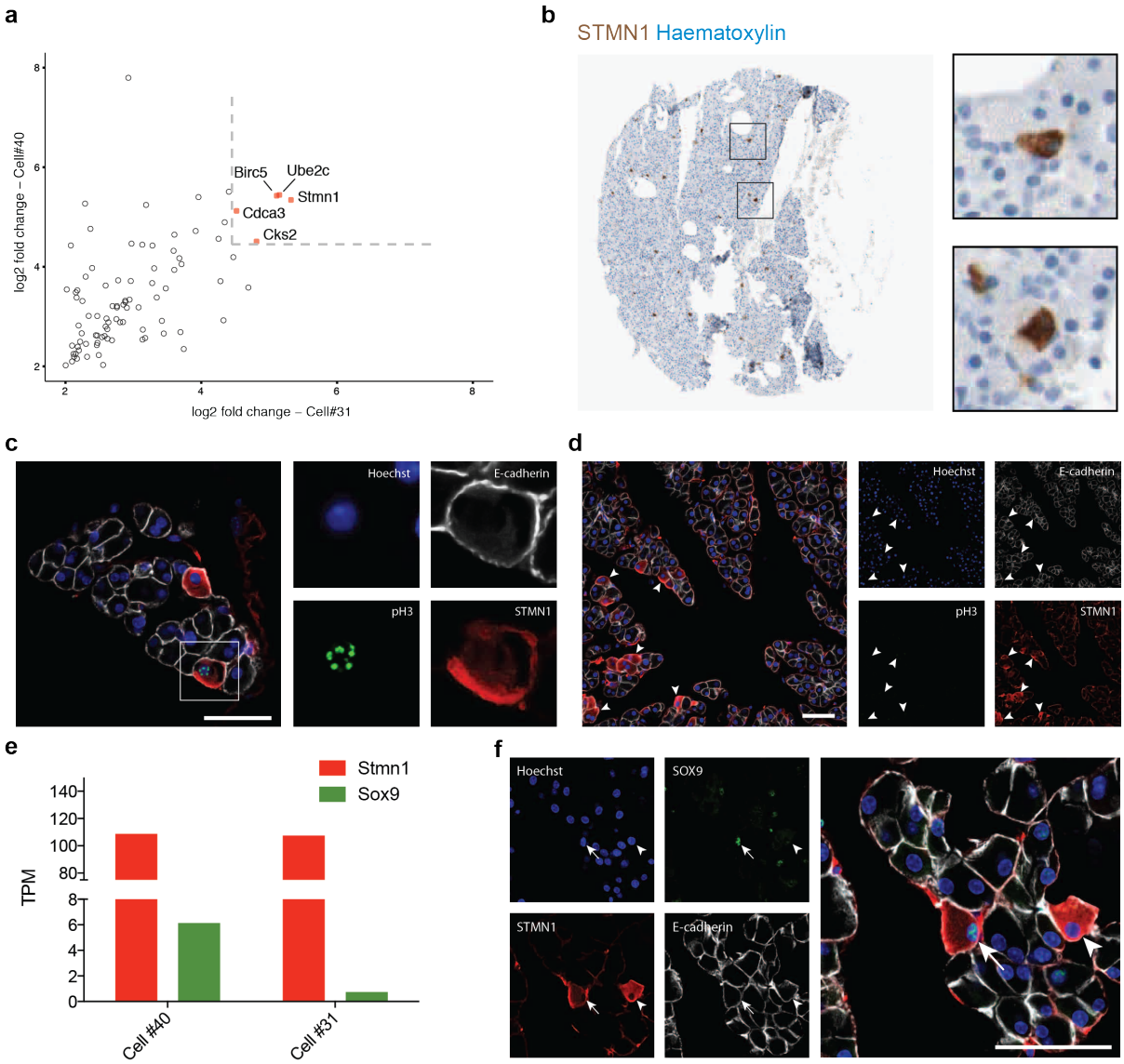

Figure 20. Description of a STMN1$^+$ acinar subpopulation in the murine and human pancreas. (**a**) Log_2 fold change of differentially expressed genes in Cell #40 and Cell #31 over average expression of all acinar cells. (**b**) STMN1 staining on human pancreatic section performed by the Human Protein Atlas (Uhlen et al., 2015). Picture was taken from http://www.proteinatlas.org/ENSG00000117632-STMN1/tissue/pancreas. (**c,d**) Immunofluorescence staining of STMN1, phospho-Histone H3 (pH3) and E-cadherin. Scale bars = 50μm. (**g**) Expression values of STMN1 and SOX9 for Cell #40, Cell #31. TPM = transcript per million. (**f**) Immunohistochemical analysis of STMN1 and SOX9 coexpression in acinar cells. Scale bar = 50μm.

Sox9 has previously proposed to be a progenitor marker in the adult pancreas (Furuyama et al., 2011). We found that one of the STMN1 expressing outliers (Cell #40) expressed the highest *Sox9* levels of all profiled acinar cells, whereas the other outlier cell (Cell #31) did not express *Sox9* (Fig. 20e). We therefore stained for STMN1 and SOX9 to validate the existence of STMN1$^+$/SOX9$^+$ acinar cells. SOX9 expression was detected in a subset of STMN1$^+$ cells (Fig. 20f). However, we also found STMN1$^+$/SOX9$^-$ cells as predicted by the RNA

sequencing results (Fig. 20e,f). This result suggests that further heterogeneity might exist within the STMN1$^+$ subpopulation.

While examining the spatial distribution of STMN1$^+$ acinar cells, we noticed that these cells are primarily found at the periphery of pancreatic lobes (Fig. 20d). Given the molecular profile of STMN1-expressing cells, we hypothesized that STMN1$^+$ cells might give rise to the large clones, which we found in the lineage tracing experiments (Fig. 8). If this was the case, then we should find large clones at the periphery of the pancreatic lobes. Re-analysis of the images taken from the long-term tracing experiment uncovered that large clones were frequently found in the periphery of tissue lobes (Fig. 21a-c). Although not providing direct evidence, this result suggests that STMN1$^+$ cells might be the source of long-term proliferating acinar cells. Performing clonal analysis of the STMN1$^+$ subpopulation in the future will likely provide the most direct test of this hypothesis.

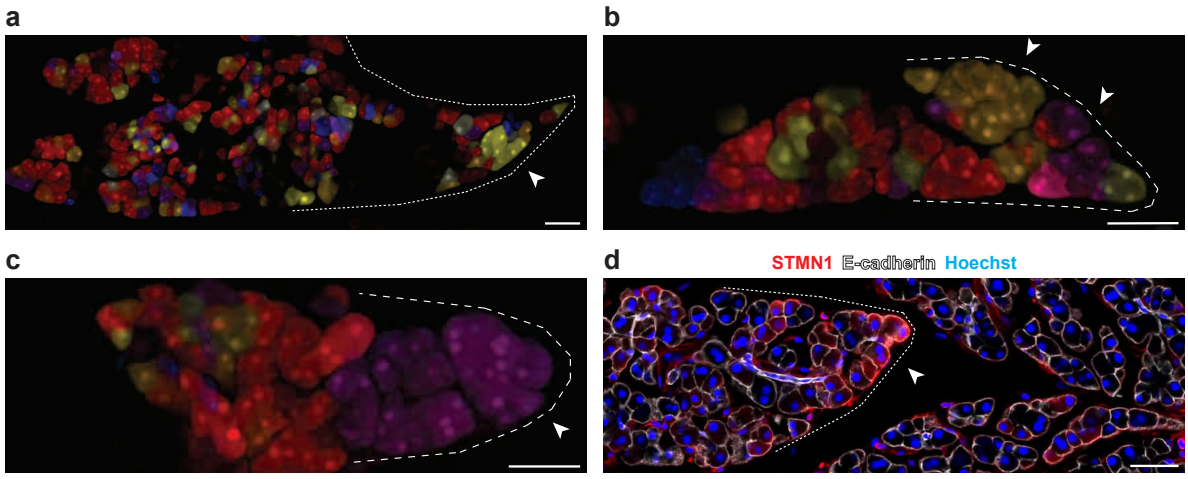

Figure 21. Large clones and STMN1$^+$ acinar cells are frequently located at the periphery of pancreatic lobes. (a-c) Peripheral locations of large clones obtained from 365 DPI multicolour lineage tracing. (d) Representative example of peripheral STMN1$^+$ acinar cell location. Scale bars = 50μm.

Transcription factors play a crucial role in the determination of cellular fate and cellular identity (Alberts et al., 2014). To identify possible transcriptional heterogeneity among acinar cells, we restricted our analyses to transcription factors. Global sample-to-sample comparison revealed two populations of acinar cells (Fig. 22a). The two large clusters were mainly separated by early response genes like *Jun*, *Fos* and *Egr1*, the stress response genes *Xbp-1* and *Atf3* as well as Klf6 (Fig. 22b – red boxes). Acinar lineage confined transcription factors such as *Ptf1a* and *Bhlha15* were robustly expressed in all profiled acinar cells, confirming the acinar nature of the cells (Fig. 22b – green box). The size of the two main clusters roughly corresponds to the ratio of mono- and binuclear acinar cells that we determined (Fig. 22b &

13a). Therefore, we hypothesized that acinar subpopulations defined by transcription factors might represent mono- and binuclear acinar cells. In order to test this, we chose *Fosb* as a marker to distinguish between the two populations since the *Fosb* expression was closest to a binary expression pattern (Fig. 22c). Immunostaining of *Fosb* revealed expression in both, mononuclear as well as binuclear acinar cells (Fig. 22d). Exocytosis of secreted acinar proteins depends on the increase of intracellular Ca^{2+} (Yule, 2010). $Ca2^{+}$ responsive transcription factors like *Jun*, *Fos* and *Egr1* might therefore distinguish cells actively secreting from non-secreting acinar cells. Thus, the two transcription factor derived clusters might be of only transient nature.

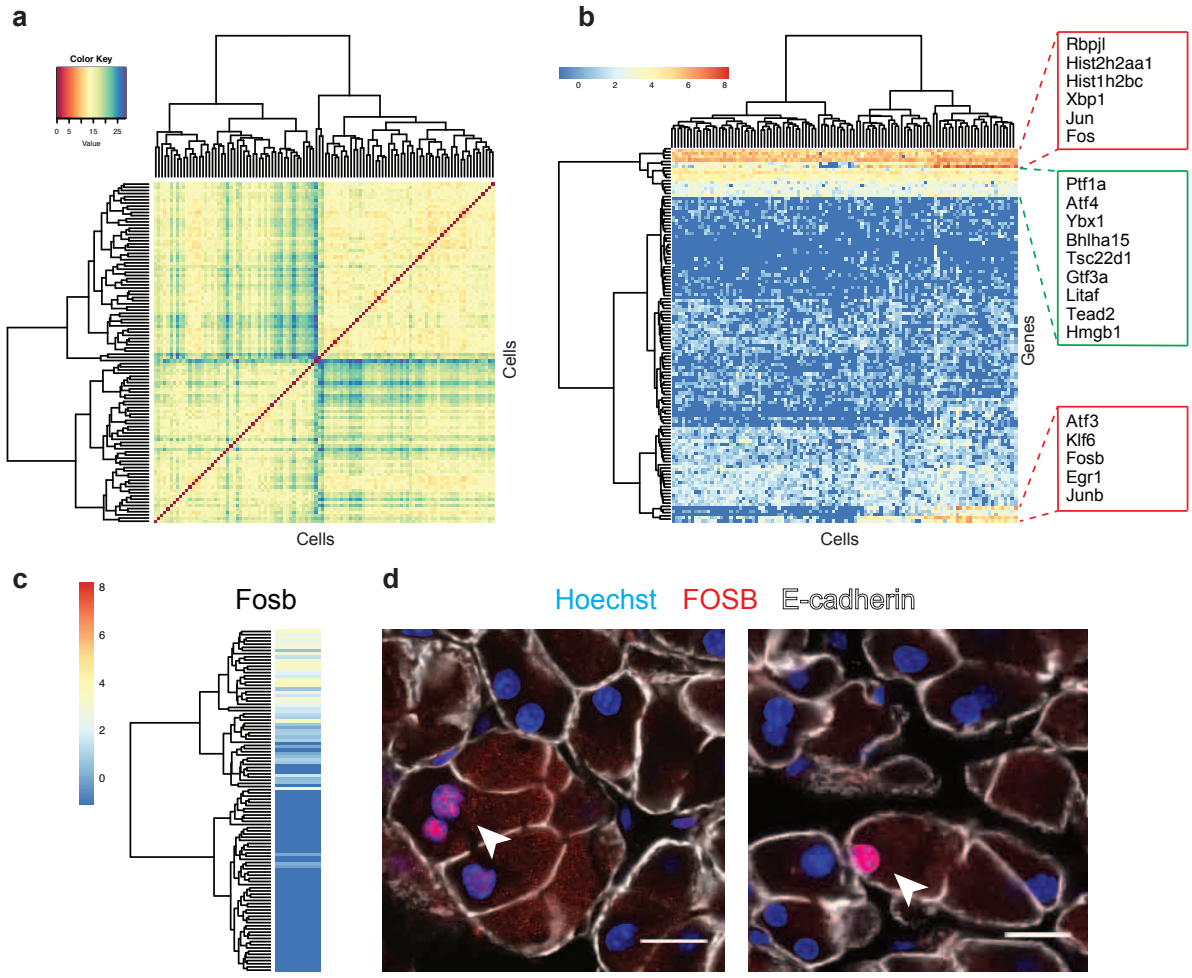

Figure 22. Analysis of transcription factor heterogeneity reveals two populations within acinar cells. (**a**) Sample-to-sample plot comparing similarity of transcription factor expression among acinar cells. (**b**) Analysis of transcription factors defining the two main acinar clusters. (**c**) Binary *Fosb* expression in the two acinar clusters. (**d**) *Fosb* expression analysis in mono- and binuclear acinar cells.

4 Discussion

The results obtained in the course of this dissertation indicate that the decade-old notion of acinar cells representing a single, homogenous pool of cells might be too simplistic. We find that murine and human acinar cells are morphologically different, with acinar cells being mono- or binuclear. Further, we demonstrate that binuclear acinar cells display a marked deficiency in proliferation, thus connecting the morphological discrepancy with a previously unknown functional difference. Although mononuclear acinar cells appear morphologically similar, we found major differences in their capacity to give rise to new acinar cells for long periods of time. On top of the morphological and functional differences we showed that acinar cells are also different on the molecular level as assessed by single cell RNA sequencing. In order to perform single cell sequencing from acinar cells we had to develop a modified version of the SMART-seq2 protocol which enables single cell RNA sequencing from cell types with high RNAse content.

4.1 How many pancreatic cell types exist?

4.1.1 Binuclear acinar cells

In order to find out how many cell types exist in an organ, one has to consider how a cell type is defined. As already discussed in the introduction, the definition of a cell type is surprisingly ambiguous, even today (Trapnell, 2015). The cell types described in the adult pancreas have been determined by morphological differences (Langerhans, 1869). Since the form frequently determines a cell´s function, this has been the prevailing approach of cell type classification to date (Achim and Arendt, 2014). Although acinar cells are classified as a single cell type, morphological differences in the form of mono- and binuclear cells have been already described in rats in the 1960s (D S Longnecker, 1968). Whether the binuclear acinar cells are functionally different remaines unknown, which is likely the reason why these cells were not considered to be a distinct type of acinar cell. Binuclear cells have also recently been described in mammary epithelial cells from five different species (Rios et al., 2016). The authors speculate that the increase in binuclear mammary epithelial cells at lactation favours

milk production (Rios et al., 2016). At lactation the main function of alveolar epithelial cells of the mammary gland is the production of protein, lipids and carbohydrates for the offspring (Anderson et al., 2007). Thus, it is plausible that binuclear cells, given that both nuclei are transcriptionally active, are able to produce and secrete more molecules. Similarly, the main purpose of pancreatic acinar cells is to produce and secrete digestive enzymes (Cleveland et al., 2012). Rios and colleagues also noted that binuclear mammary epithelial cells are larger and speculate that this cytoplasmic extension corresponds to increase in endoplasmic reticulum occupancy (Rios et al., 2016). Although binuclear acinar cells of the pancreas also contain large amounts of endoplasmic reticulum, it is difficult to infer a causal relationship between the ploidy of the cell and the amount of organelles. Particularly, given that mononuclear acinar cells clearly also harbour large amounts of endoplasmic reticulum (D S Longnecker, 1968). In order to make statements regarding this issue, the ratios between cell size, ploidy and endoplasmic reticulum have to be accurately measured. It would be interesting to investigate how acinar cells and lactating mammary epithelial cells regulate the amount of endoplasmic reticulum in the cell. So far, it is not known how the amount of endoplasmic reticulum in a cell is regulated (Alberts et al., 2014). Comparing gene expression profiles among cell types with increased amounts of endoplasmic reticulum might therefore shed light into the elusive mechanism.

As mentioned above, the diversity in morphology and subcellular anatomy of a cell type is often closely connected to the function it fulfils. Thus, the binuclear state might be functionally different from mononuclear cells. We found that binuclear acinar cells do not divide *in vitro* despite culture conditions, that promote proliferation (Fig. 11). Interestingly, the connection between the binuclear state and cell proliferation has been previously discussed in the field of heart development. The murine heart loses its regenerative potential within 7 days after birth (Porrello et al., 2011). The reason for the lack of regenerative potential is that cardiomyocytes become postmitotic after birth. This proliferation deficiency coincides with postnatal binucleation of cardiomyocytes (Walsh et al., 2010). Notably, the kinetics of early postnatal binucleation are similar between acinar cells and cardiomyocytes (Oates and Morgan, 1986; Walsh et al., 2010). Thus, it was speculated that binuclear cells represent a terminally differentiated form of cardiomyocytes (Porrello et al., 2011). This hypothesis is further supported by the fact that zebrafish cardiomyocytes are entirely mononuclear and retain their proliferative and regenerative capacity throughout their lives (Poss, 2007). The concept of terminal differentiation of binuclear cardiomyocytes was recently challenged by a study investigating the proliferation kinetics of cardiomyocytes

during development (Naqvi et al., 2014). The authors found a brief but intense burst in cardiomyocyte proliferation on postnatal day P15 which could not be explained by proliferation of mononuclear cells alone (Naqvi et al., 2014). Proliferation analysis of cardiomyocytes at P15 demonstrated that 90% of all cells in prophase were binuclear, as assessed by punctated aurora kinase B staining in the nucleus (Naqvi et al., 2014). The authors proposed a "2+1 cell cycle" model, in which binuclear cells which enter M phase give rise to two mononuclear- and one binuclear cell could explain the observed proliferation kinetics (Naqvi et al., 2014). The binuclear state might therefore not *per se* mark a cell as postmitotic. In the regenerating liver, aurora kinase B staining suggested that binuclear hepatocytes undergo cytokinesis to generate two mononuclear hepatocytes (Miyaoka et al., 2012). Similarly, we found that a small subset of $pH3^+$ binuclear cells upon injury, possibly suggesting similar mechanisms of activation during regeneration in the liver and pancreas (Fig. 13). Despite the role of proliferative potential of binuclear cells during early postnatal development in cardiomyocytes or during injury in the liver and pancreas, it is possible that these cells are proliferation deficient in the respective adult, healthy organ. Although our *in vitro* experiments support this notion, long-term label-retaining assays will be needed to provide *in vivo* evidence. Assuming the outcome would support our *in vitro* data, then binuclear acinar cells should be considered as a separate acinar subtype, given their morphologically and functionally distinct characteristics.

4.1.2 Long-term proliferating acinar cells

While it is relatively easy to discover novel cell types by morphological differences it is possible that cells which are similar in their appearance might have different functions. As mentioned in the introduction, hematopoietic stem cells were discovered by their potential to give rise to colonies harbouring several different cell types found in the blood (BECKER et al., 1963; Siminovitch and McCULLOCH, 1963). The main function of stem- and progenitor cells is to produce new cells in order to compensate for cell loss during the lifespan of an organism. Whether a cell (population) has this capacity or not might not necessarily be reflected by morphological differences. Yet, these cells are still considered to be a distinct cell type. Our data suggests that acinar cells harbour a subpopulation of acinar cell with the capacity to proliferate for long periods of time (Fig. 8). It is thus possible that the proliferating acinar subpopulation represents a "progenitor-like" population in the pancreas. If future

research confirms this interpretation, then this population should also be considered a distinct acinar subtype. Future experiments leading to a more detailed molecular characterization will be needed to fully exclude the possibility that our data might be explained by stochastic proliferation of a equipotent population as described for organs (Klein and Simons, 2011a). Interestingly, hematopoietic stem cells as well as the epidermal system were both first described solely based on their proliferative capacities (Barrandon and Green, 1987; BECKER et al., 1963). Subsequent studies identified markers for the prospective isolation and characterization of these stem cell populations (Jones and Watt, 1993; Spangrude et al., 1988). Thus, clonal proliferation assays might be a promising tool for unbiased identification of stem- or progenitor cells in a variety of tissues. Cardiomyocytes of the mammalian heart represent a candidate population, which might harbour such hidden subpopulation. Cardiomyocytes, similar to acinar cells, are morphologically similar and only differ in their ploidy. By combining lineage tracing with multi-isotope imaging mass spectrometry, it was demonstrated that new cardiomyocytes are produced by pre-existing cardiomyocytes at a very low rate (Senyo et al., 2012). It is possible that this proliferative capacity is confined to a previously neglected cardiomyocyte subpopulation, which might be resolved by clonal analysis.

During development, multipotent pancreatic progenitors reside at the tip of the epithelial branches and subsequently develop into acinar cells (Fig. 3) (Zhou et al., 2007). Adult acinar cells have therefore been suggested to be most closely related to the multipotent pancreatic progenitor during development (Puri et al., 2015). Interestingly, we also frequently find large clones to be located at the tip of pancreatic lobes (Fig. 21). This raises the interesting question whether it is possible that the proliferating acinar cells in the adult pancreas are remnants of embryonic development. An elegant study useing male-female chimera mice with subsequent fluorescence *in situ* hybridization (FISH) against the Y chromosome to determine the developmental clonality of different cell types (Swenson et al., 2009). The authors found large patches of Y-positive acinar cells surrounded by Y-negative cells (Swenson et al., 2009). This suggests that pancreatic development is driven by clonally dominant progenitors similar to heart development in zebrafish (D S Longnecker, 1968; Gupta and Poss, 2012). These patches are reminiscent of the large clones we found after long-term lineage tracing of acinar cells (Fig. 8). It is therefore possible that a subset of the clonally dominant progenitors, which drive pancreatic organogenesis, retain their proliferative capacity to become adult progenitors-like acinar cells. A similar mechanism was found in studies investigating the embryonic origin of adult neural stem cells (NSCs) in the subventricular zone (Fuentealba et al., 2015; Furutachi

et al., 2015; Porrello et al., 2011). Two studies independently discovered with the help of label retaining assays (Furutachi et al., 2015) and retroviral barcoding (Fuentealba et al., 2015) that adult NSCs in the subventricular zone arise from embryonic progenitors that become quiescent between embryonic day (E) 13.5 and E15.5. In the course of the lifetime of a mouse these cells get reactivated to maintain homeostasis in the adult brain. It would be desirable to use similar approaches in the developing pancreas in order to determine whether a similar mechanism applies to the pancreas.

4.1.3 Injury responsive acinar cells

Pancreatitis, an inflammation of the pancreas, is the most common experimentally induced injury model (Lerch and Gorelick, 2013). As a result of the injury, a massive increase in proliferation of pancreatic cells compensates for the loss of cells (Fukuda et al., 2011; Nagashio et al., 2004; Porrello et al., 2011). We asked whether the progenitor-like acinar cells, which maintain homeostasis in naïve animals, are also the source of new cells upon injury. We found that injury induces transient proliferation of a pool of cells distinct from the progenitor-like population we discovered (Fig. 10). Given the transient nature of the response, it is possible that the proliferative response is unselective and thus not confined to a distinct subpopulation. One argument against this interpretation is that the proportion of 2-nuclei per clone did not change in response to injury (Fig. 10c). This population likely represents binuclear cells, which were less responsive to injury with regard to proliferation (Fig. 13b). Another interpretation of the data is that the acinar cell compartment contains a reservoir of acinar cells that only gets activated after injury. Stem cells in the hematopoietic system are divided into long-term and short-term stem cells (Poss, 2007; Weissman, 2000). It was shown that long-term hematopoietic stem cells are dormant but efficiently get activated by interferon-α (IFNα) upon injury to replenish lost cells (Essers et al., 2009; Naqvi et al., 2014; Wilson et al., 2008). A recent study suggests that a distinct population of quiescent, *Dclk1*-expressing acinar cells get activated upon injury, analogue to the hematopoietic system (Naqvi et al., 2014; Westphalen et al., 2016). The authors demonstrate that $Dclk1^{+}$ acinar cells make up the majority of responding acinar cells and that this subpopulation is more efficient in generating pancreatic tumour lesions (Naqvi et al., 2014; Westphalen et al., 2016). In the light of our data, this finding suggests that the acinar cell compartment harbours a

subpopulation of injury responsive acinar cells, which are distinct from the progenitor-like cells that proliferate under homeostatic conditions.

4.2 What are the molecules underlying the acinar heterogeneity?

4.2.1 The molecular role of STMN1

Given the fact that we find a subpopulation of acinar cells with the capacity for long-term proliferation, we hypothesized that this subpopulation would be molecularly distinct. Thus, we performed single cell mRNA sequencing of acinar cells that were handpicked in an unbiased fashion. Based on transcriptome analysis, we found a small subpopulation of acinar cells that displayed a proliferative signature (Fig. 19). One of the differential expressed genes that was highly abundant in this acinar subpopulation was STMN1, suggesting that STMN1 might represent a possible marker for this newly discovered acinar progenitor-like cells (Fig. 20).

The molecular role of STMN1 (also known as Oncoprotein 18, OP18 or Stathmin1) remained elusive until a landmark study in the 1990s discovered its microtubule-depolymerizing activity (Belmont and Mitchison, 1996; Naqvi et al., 2014). Expression analysis of STMN1 in several tissues from mice and humans revealed that STMN1 is ubiquitously expressed in almost any tissue tested (Bièche et al., 2003; Koppel et al.; Miyaoka et al., 2012). However, not all cells within these tissues expressed this protein, indicating an important role for STMN1 in only a subset of cells (BECKER et al., 1963; Bièche et al., 2003; Koppel et al.; Siminovitch and McCULLOCH, 1963). It was subsequently demonstrated that STMN1 expression is restricted to the proliferating compartment of most tissues (Klein and Simons, 2011a; Rowlands et al., 1995). Further, embryonic tissues expressed higher levels of STMN1 as compared to the adult counterpart (Barrandon and Green, 1987; BECKER et al., 1963; Bièche et al., 2003; Chen et al., 2003; Koppel et al.). These findings suggest a role for STMN1 in cell proliferation. Overexpression of STMN1 increased the number of cells in G2/M transition of the cell cycle and consequently its downregulation locked cells in post-metaphase stage of mitosis (Jones and Watt, 1993; Larsson et al., 1997; Mistry and Atweh, 2001; Spangrude et al., 1988). In the following years, a large number of other studies confirmed STMN1´s role in cell cycle progression (Belletti and Baldassarre, 2011; Senyo et

al., 2012). Our data suggest that, similar to other tissues, STMN1 labels acinar cells with the capacity to proliferate. Thus, the question arises whether STMN1 is expressed in these cells solely as a consequence of being actively proliferating. If so, STMN1 would not be a stable marker for this progenitor-like population. Co-staining of the mitosis marker pH3 with STMN1 demonstrated that the vast majority of $STMN1^+$ acinar cells are not actively cycling (Fig. 20). The expression of STMN1 might therefore be a prerequisite for cells to proliferate, which in turn raises the question how STMN1 itself is regulated.

The regulation of STMN1 on the transcriptional level was suggested to be cell cycle dependent in cancer cells since a putative binding site for the transcription factor E2F was found (Melhem et al., 1991; Zhou et al., 2007). More direct evidence was provided by a microarray screen for genes regulated by E2F during mitosis (Ishida et al., 2001; Puri et al., 2015). This study demonstrated that STMN1 was downstream of E2F in serum-stimulated fibroblasts (Ishida et al., 2001; Swenson et al., 2009). Furthermore, E2F dependent STMN1 expression was confirmed in other cancer cell lines (Polager and Ginsberg, 2003; Polzin et al., 2004; Swenson et al., 2009). Although these studies clearly demonstrate that the STMN1 expression might be E2F-dependent, our data argues against a cell cycle-dependent STMN1 expression (Fig. 10). In addition to that, we find expression of E2F1 in only one of the $STMN1^+$ acinar cells (data not shown). This indicates that the expression of STMN1 might be differently regulated depending on the cell type. An example for tissue specific regulation of STMN1 transcription is provided by its negative regulation. It was shown that p53 is a transcriptional repressor of STMN1 in various cancer cell lines (Ahn et al., 1999; Johnsen et al., 2000; Murphy et al., 1999). In the hepatic cancer cells, however, the wild-type form of p53 does not influence the expression of STMN1 (Singer et al., 2007).

Besides the transcriptional control of STMN1 a large body of data has been acquired regarding its post-translational regulation. STMN1 has four phosphorylation sites: S^{16}, S^{25}, S^{38}, S^{63}, each phosphorylated by a different kinase (Belletti and Baldassarre, 2011). The phosphorylation of these serins inhibits STMN1´s ability to destabilize microtubules (Belletti and Baldassarre, 2011). CDK1, the master regulator of M phase progression, phosphorylates S^{25} and S^{38}, followed by phosphorylation of S^{16} and S^{63} by Aurora kinase B (Beretta et al., 1993; Brattsand and Marklund, 1994; Larsson et al., 1997; Luo et al., 1994). These phosphorylation events are critical for mitotic spindle formation in order to separate sister chromatids (Beretta et al., 1993; Brattsand and Marklund, 1994; Luo et al., 1994). Furthermore, phosphorylation of S^{16} has also been demonstrated to facilitate T-helper cell differentiation and axon development in neurons (Tanaka et al., 2007; Watabe-Uchida et al.,

2006). In the light of these findings it is tempting to speculate that STMN1 expression is required for acinar cells in order to be able to divide. The actual trigger leading to acinar cell mitosis might act on STMN1 on the post-translational level. Further experiments are needed to confirm this hypothesis. If this assumption holds true, STMN1 might be a faithful marker of progenitor-like acinar cells.

4.2.2 The role of Sox9 in the developing and adult pancreas

Single cell mRNA sequencing revealed that the STMN1 expressing subpopulation is heterogeneous with regards to the expression of Sox9 (Fig. 20). The transcription factor Sox9 is labelling stem cells of various organs such as hair bulge, the intestine as well as the neural crest (Blache et al., 2004; Cheung and Briscoe, 2003; Vidal et al., 2005). Similarly, Sox9 is expressed in the earliest multipotent cells during pancreatic organogenesis (Kopp et al., 2014). During the developmental transition towards tip-trunk morphology, Cpa-1$^+$ tip cells are known to harbour multipotent progenitors, which drive organogenesis from E10.5 on (Zhou et al., 2007). Cells within the trunk region, however, have also been shown to harbour Sox9 expressing multipotent stem cells during pancreatic development (Kopinke et al., 2011; Kopp et al., 2011). In embryonic stem cells of the pancreas, Sox9 directly regulates the expression of a transcriptional network for maintaining the stem cell identity and activates the expression of Neurogenin3, whereby it directs endocrine differentiation (Lynn et al., 2007). The importance of Sox9 for embryonic pancreatic stem cells is further supported by investigations regarding pancreatic development in Sox9 deficient mice (Seymour et al., 2007). Pancreas-specific deletion of Sox9 resulted in severe pancreatic hypoplasia, indicating that the Sox9 dependent transcriptional network is essential for development of the pancreas (Seymour et al., 2007).

Given the data obtained from the developing pancreas Sox9 has been a promising candidate for potential adult pancreatic stem-/progenitor cells. A comprehensive lineage tracing study aimed to test this assumption by tracing the fate of Sox9$^+$ cells in the adult liver, pancreas and intestine (Furuyama et al., 2011). The authors found that Sox9 expressing duct cells were able to give rise to acinar cells over time, suggesting that Sox9 expressing duct cells might serve as adult exocrine progenitor cells (Furuyama et al., 2011). Surprisingly, an independent attempt to determine the multi-lineage potential of Sox9$^+$ duct cells revealed that Sox9-expressing cells of adult mice only gave rise to duct cells, contradicting the exocrine progenitor

hypothesis (Kopp et al., 2011). It has been speculated that differences in the strategies for the creation of the transgenic mice might explain the difference (Kopp et al., 2014). The investigators of one study created Sox9CreER^{T2} mice by targeting the endogenous gene (Furuyama et al., 2011), while the other study used an bacterial artificial chromosome (BAC) to deliver the transgene (Kopp et al., 2011). Thus, one of these strategies might more faithfully recapitulate the expression of the endogenous gene as compared to the other. Another possible explanation could be the different dosages of tamoxifen used in these studies (Kopp et al., 2014). This interpretation is particularly plausible in the light of the fact that Kopp and colleagues demonstrated labelling of acinar cells when higher dosages of tamoxifen were used (Kopp et al., 2011). Furuyama and colleagues used similarly high concentrations of tamoxifen (Furuyama et al., 2011). Thus, it is possible that a subpopulation of acinar cells express low levels of Sox9, which are only labelled when a high dosage of tamoxifen is used. However, high dosages of tamoxifen might also lead to unspecific recombination of the Cre recombinase (unpublished observation). Our data derived from single cell mRNA sequencing of acinar cells provided evidence for Sox9 expression of acinar cells, which we were able to confirm by immunohistochemistry (Fig. 20). Thus, our data offers an explanation for the controversy of Sox9 expression in the adult pancreas. It is therefore possible that the multi-lineage capacity of Sox9^{+} duct cells as demonstrated by Furuyama and colleagues might be a misinterpretation of labelling of Sox9^{+} acinar cells induced by high tamoxifen levels. This is further confirmed by the fact that lineage tracing of adult pancreatic duct cells with other duct specific CreER^{T2} lines do not display multi-lineage potential of duct cells (Kopinke et al., 2011; Solar et al., 2009).

4.2.3 Transcription factor heterogeneity among acinar cells

The transcription factor Sox9 is a typical example of how transcription factors control transcriptional networks and thus maintain cell identity. The power of these factors is demonstrated by recent years establishment and advances of iPS technology (Xu et al., 2016). As revealed by the Nobel prize winning proof of principle study, overexpression of four transcription factors, which became known as the Yamanaka factors, were sufficient to change a cell´s identity (Takahashi and Yamanaka, 2006). Since we were interested in determining the cellular heterogeneity among acinar cells, we aimed to uncover the transcription factor heterogeneity within the sequenced acinar cells. We discovered that the

profiled acinar cells separate into two main groups depending on which transcription factors are expressed (Fig. 22). The size of the clusters resembled the ratio between mono- and binuclear acinar cells in adult mice (Fig. 13). However, staining of Fosb, the most binary differentially expressed transcription factor, revealed that the clustering of transcription factors are not likely to reflect mono- and binuclear acinar cells (Fig. 22). Thus, the question arises which class of transcription factors separate these clusters. We found that the clusters were mainly separated by so-called early response genes such as *Jun*, *Fos* and *Egr1* (Fig. 22 – red box). Previously, it was discovered that the expression of early response genes such as *c-Fos* and *c-Jun* was increased in pancreatic acinar cells upon cholinergic stimulation (Turner et al., 2001). As described above, pancreatic acinar cells are secretory cells, responsible for producing and secreting large amounts of digestive proteins (Logsdon and Ji, 2013). The exocytosis of secretory granules is a controlled process. Secretion happens upon secretagogue-induced increase of intracellular Ca^{2+} concentration (Low et al., 2010; Yule, 2010). The main secretagogues responsible for stimulus-dependent secretion of digestive enzymes are the neurotransmitter acetylcholine (Ach) and the peptide hormone cholecystokinin (CCK) (Petersen, 1992). Cholecystokinin stimulation has been shown to increase expression of Egr-1 and c-Jun in pancreatic acinar cells (Guo et al., 2012; Kaufmann et al., 2014). In the light of these findings it is likely that the acinar cell cluster that is separated by high levels of early response genes might be in the process of stimulus-mediated exocytosis. This would indicate that the clustering of transcription factors is not representing a stable acinar subpopulation, but rather a transient state of acinar cells. Similarly, expression analysis of several hundred single brainstem neurons displayed transcriptional heterogeneity which is reflected by diverse input responses based on the environmental experiences of the neurons (Park et al., 2014).

Despite these findings it is surprising that binuclear cells could not be distinguished by our unbiased single cell mRNA sequencing approach, particularly given the fact that we find functional differences between mono- and binuclear acinar cells (Fig. 11). One possible explanation would be that the transcriptional difference between mono- and binuclear cells are below our level of detection. It was noted before that transcription factors are expressed at much lower levels as compared to secreted proteins such as hormones (Wen and Tang, 2015). Hence, more sensitive methods might be needed to detect potential transcription factors that might determine binuclear cell identity.

4.3 What is an adult stem cell?

In the course of this study, we described an acinar subpopulation with the capacity to proliferate for long periods of time, resembling stem-/progenitor cells from other tissues. Hence, we termed these acinar cells "progenitor-like". The classic definition of stem-/progenitor cells dates back to the discovery of hematopoietic stem cells (BECKER et al., 1963). Since then, hematopoietic stem cells have become the archetype of a hierarchically organized stem cell system, engraining our understanding of how to define a stem cell. The question then arises how the progenitor-like acinar cells fit into the framework of hierarchically organized stem cells.

Recently, the provocative question arose whether our classically defined understanding of how stem cell systems maintain homeostasis is out-dated (Clevers, 2015). In the light of recent findings, arising from efforts to find stem cells in a multitude of adult tissues, it is possible that tissues might use different mechanisms to replace lost cells (Clevers, 2015).

4.3.1 Multipotency and self-renewal of adult stem cells

Hematopoietic stem cells are multipotent and have the ability to self-renew (Weissman, 2000). Based on the example of the hematopoietic stem cell system, multipotency and self-renewal have since served as dogmatic prerequisites for stem cells in adult tissues. However, examples from other organs, including recent findings from the hematopoietic system itself, challenge the concept that multipotency and long term self-renewal are two stringently coupled processes. With the help of a labour-intensive single-cell transplantation assay, a myeloid-restricted progenitor population with long-term repopulating activity was discovered (Yamamoto et al., 2013). This example demonstrates that long-term self-renewal might be a property, which stem cells share with certain cells lower in the hierarchy such as progenitor cells. In the adult liver, mature hepatocytes are terminally differentiated cells making up the majority of all cells in the liver (Alberts et al., 2014). Axin2 expressing pericentral hepatocytes were identified as a self-renewing subpopulation which maintains hepatocyte homeostasis (Wang et al., 2015). This study argues that the property of self-renewal might not just be restricted to stem-/progenitor cells, but possibly also apply to terminally differentiated cells. The properties of the progenitor-like acinar subpopulation that we identified closely resemble the self-renewing hepatocytes (Fig. 8). Thus, the liver and the pancreas might have

evolved similar mechanisms of maintaining homeostasis, which depend on the self-renewal capacity of fully differentiated cells. In support of this hypothesis, both organs do not harbour multipotent cells (Yanger et al., 2014). Hepatocytes and pancreatic acinar cells are very similar in their function as both cell types are producing und secreting large amounts of protein (Barnard, 1969; Grieninger and Granick, 1978). Another resemblance is the occurrence of binuclear cells in both cell types, indicating a relation between protein production and DNA content (Wang et al., 2015). Interestingly, Axin2 expressing hepatocytes were shown to be largely diploid. Together with the finding that binuclear acinar cells are proliferation deficient (Fig. 11) these results suggest that the binuclear state might render both cell types terminally differentiated with no self-renewal capacity (Wang et al., 2015).

Multipotency, the second main property of stem cells, is frequently observed during development of organs as exemplified by $Pdx1^+$ or $Cpa\text{-}1^+$ multipotent stem cells in the developing pancreas (Gu et al., 2002; Zhou et al., 2007). Similarly, adult hematopoietic stem cells were shown to be multipotent early after their identification (BECKER et al., 1963). Hence, the stem cell community took advantage of genetic tools such as lineage tracing to directly test multipotency of several adult cell types in situ (Kretzschmar and Watt, 2012; Snippert and Clevers, 2011). Adult neural stem cells reside in two niches: the subventricular zone in the walls of the lateral ventricles and the in the subgranular layer of the dentate gyrus (Kriegstein and Alvarez-Buylla, 2009). Although stem cells in both niches were shown to be multipotent, the question remained, whether all cells within the stem cell populations were multipotent (Gage, 2000; Kriegstein and Alvarez-Buylla, 2009). If a population of unipotent cells were lineage traced, multiple cell types would be labelled. In this case, the traced individual cells might not be “truly” multipotent cells, as compared to the early hematopoietic stem cell studies which able to trace cells at the single cell level (BECKER et al., 1963). Recently, clonal analysis of neural stem cells aimed to address this issue in order to determine whether single neural stem cells in the respective niches are truly multipotent. With the help of a sparse genetic labelling approach, Bonaguidi and colleagues were able to trace the fate of single neural stem cells in the dentate gyrus (Bonaguidi et al., 2011). The results of the clonal analysis demonstrated self-renewal as well as multipotency on the single cell level (Bonaguidi et al., 2011). Interestingly, clonal analysis of neural stem cells in the second neurogenic niche revealed a bias in the fate specification towards deep granule neurons (Calzolari et al., 2015). This study indicates that the multipotency of neural stem cells in the subventricular zone on the population level is not fully recapitulated on the single cell level. The phenotypic heterogeneity of neural stem cells from the two niches is particularly surprising as recent

single cell sequencing studies have demonstrated that neural stem cells from both niches are similar on the transcriptome level (Llorens-Bobadilla et al., 2015; Shin et al., 2015).
The above-discussed evidence argues that, despite the fact that many tissues harbour cells that are multipotent or have the ability to self-renew, few adult organs seem to contain cells that integrate both properties.

4.3.2 Quiescence of adult stem cells

The concept that tissue resident adult stem cells are quiescent is demonstrated in several tissues such as hair follicle or striated muscle (Brack and Rando, 2012; Jaks et al., 2010). The idea of quiescence of stem cells seems counterintuitive since the main purpose of a stem cell is to produce daughter cells to counter homeostatic or injury-induced cell loss (Clevers, 2015). Further, many terminally differentiated cells are non-dividing, making quiescence a rather unspecific hallmark of stemness (Clevers, 2015). A rational for the quiescence of adult stem cells was provided by the hematopoietic system. The most quiescent stem cells, termed dormant stem cells, were shown to provide a silent reservoir, which gets reversibly activated upon injury (Wilson et al., 2008). The small intestine is a tissue with high cellular turnover, similar to the hematopoietic system. Yet, the $Lgr5^+$ stem cells of the small intestine are constantly cycling and get stochastically activated (Barker et al., 2007; Snippert et al., 2010).
Recently, $Dclk1^+$ pancreatic cells were proposed to be quiescent progenitor cells which get activated in several injury models (Westphalen et al., 2016). It was speculated for many years that the pancreas and the liver might harbour facultative stem cells (Yanger and Stanger, 2011). These cells were proposed to be terminally differentiated cells which dedifferentiate into stem cells upon injury (Yanger and Stanger, 2011). $Dclk1^+$ pancreatic cells might be a first candidate for this elusive population. The authors convincingly demonstrate that $Dclk1^+$ cells are necessary for the regeneration of the pancreas after injury (Westphalen et al., 2016). Yet, whether quiescence is a particular feature of these cells is questionable, since we show that ~ 90% of all acinar cells are quiescent (Fig. 8). However, our data demonstrate that injury activates a pool of pancreatic cells distinct from the progenitor-like acinar cells we discovered (Fig. 10). It is therefore tempting to speculate that the pool of acinar cells contains two progenitor populations: continuously proliferating progenitors, similar to intestinal stem cells, as well as a distinct dormant pool of injury-induced progenitors, resembling dormant hematopoietic stem cells. Our single cell mRNA sequencing results suggest that STMN1

might be a marker for the continuously proliferating progenitor-like acinar cells. With this marker at hand, future experiments can directly address whether two functionally distinct progenitor-like acinar cells exist.

4.3.3 Coexistence of stem cell pools

The above discussed question of coexisting quiescent and active acinar progenitor-like cells aimed to decipher acinar heterogeneity. Although the pancreas mainly consists of acinar cells, other cell types are also present in the pancreas, which might contain their own progenitor population. The notion of coexisting progenitors within the same organ is particularly interesting considering that multipotency is lost in the adult pancreas (Desai et al., 2007; Dor et al., 2004; Kopp et al., 2011). Thus, every tissue compartment needs to autonomously maintain homeostasis.

An example for cell types, which independently maintain homeostasis, is given by the adult mammary gland. Although transplantation experiments suggested the existence of multipotent mammary stem cells, lineage tracing experiments demonstrated that basal and luminal cells are not multipotent when traced *in situ* (Shackleton et al., 2006; Stingl et al., 2006; Van Keymeulen et al., 2011). Similar results were obtained by fate mapping experiments of the adult prostate and sweat glands (Lu et al., 2012; Ousset et al., 2012). These studies elucidate a concept of tissue homeostasis in a unipotent fashion for several adult organs. Yet, it is not clear if homeostasis is maintained by stochastic proliferation of all cells, or only a small subset of e.g. basal or luminal cells. By clonal analysis of adult acinar cells we were able to show that only a small subset of acinar cells maintains homeostasis of the acinar cell compartment (Fig. 8, 11). Brennand and colleagues aimed to uncover whether such a subpopulation also exists among endocrine β-cells using a label retaining assay (Brennand et al., 2007). The authors found that all β-cells contribute equally to growth and maintenance (Brennand et al., 2007). This result is particularly surprising in light of our finding showing that there is clear heterogeneity among acinar cells with regard to how many of these cells contribute to growth and homeostasis in the adult animal (Fig. 8). These findings indicate that two distinct mechanisms for maintenance of homeostasis can coexist within the same organ. It would be interesting for future studies to investigate which mechanism the other cell types in the pancreas use to maintain homeostasis. Furthermore, it would be interesting to investigate

whether β-cells might be equally susceptible to tumour formation given their equal capacity to proliferate.

4.4 Organs in a dish – what can we learn from 3D cultures?

4.4.1 Advantages of organoid cultures

Adult stem-/progenitor cells from varies organs, once cultured in three dimensional hydrogels, can form miniature versions of the respective organs which were termed organoids (Sasai, 2013). We hypothesized that progenitor-like acinar cells would also form organoids in 3D cultures. Thus, we aimed to use organoid formation as a surrogate for identification of progenitor-like acinar cells. We found a subpopulation of acinar cells, which form organoids, once in direct cell-cell contact with supporting acinar cells, and simultaneously undergo acinar-to-ductal metaplasia (Fig. 11).

Organoid assays provide a useful addition to the assays for stem cell research. For a long time, the only stem cell that could be propagated *in vitro* was the epidermal stem cell (Barrandon and Green, 1987). The development of organoid assays opened the door to long-term in vitro cultures for stem cells from a large variety of organs such as intestine (Sato et al., 2009), stomach (Barker et al., 2010), lung (Lee et al., 2014), liver (Huch et al., 2013b), salivary gland (Lalitha S Y Nanduri, 2014), tongue (Hisha et al., 2013) and many more. In addition to that, and in contrast to the 2D cultures of epidermal stem cells, the organoid assay provides means for studying mechanisms of tissue morphogenesis. The cultures recapitulate many features of organ morphogenesis as stem cells interact with their progeny in order to form organoids. This is impressively demonstrated by organoid formation of optic cups and cerebral organoids (Eiraku et al., 2011; Lancaster et al., 2013).

Another advantage of the organoid assay is that it could, in combination with iPS technology, in principle be performed for all human organs for which iPS protocols are available. Morphogenesis is almost exclusively studied in model organism, but signals that are important for organ formation might differ between species. An example is given by organoids derived from adult human liver cells, which, in contrast to mouse liver organoids, need inhibition of TGF-β signalling for long-term culture (Huch and Koo, 2015). Moreover, adult stem cells in mammalian organs were mainly studied in mice. The organoid formation

assay might provide a fast and cost-effective way of identifying stem cells in human tissue. Although we find organoid-forming acinar cells, supporting our discovery of progenitor-like acinar cells *in vivo*, we have no indication whether this organoid forming acinar population exists in the human pancreas. It would therefore be interesting to perform the organoid assay using human acinar cells. Similar to studies of organ formation, many diseases are studied using mouse models, which, despite individual achievements, frequently fall short of predicting human disease response (Shanks et al., 2009). Pancreatic ductal adenocarcinoma (PDAC) is a very good example for this problem. Several years of extensive studies on mouse models of PDAC has increased our understanding of the disease, but completely failed to improve treatment efficacy (Hwang et al., 2015; Perez-Mancera et al., 2012). Recent efforts to model PDAC using organoid assays might provide more faithful recapitulation of the disease (Boj et al., 2015; Huang et al., 2015). Yet, these organoid models for PDAC will need to be improved in order to mimic micro environmental signals which were shown to be critical for modelling therapeutic response of PDAC (Olive et al., 2009). Furthermore, this assay could directly test whether the progenitor-like acinar population that we find might be the cell-of-origin for human PDAC.

4.4.2 Using organoids to define stem cell niches

Adult stem cells receive signals from cells, which are frequently in close proximity and orchestrate their differentiation or maintain their stemness (Fuchs et al., 2004). The microenvironment that controls the fate of stem cells is called “stem cell niche” (Fuchs et al., 2004). The importance of the niche signals for stem cells is illustrated by the fate determination of embryonic stem cells as a function of the environmental signals. Embryonic stem cells, once transplanted into an adult mouse, form tumours that contain multiple cell types (Przyborski, 2005). This result illustrates the pluripotency of embryonic stem cells and their transplantation was subsequently used as a reliable readout for true pluripotency (Takahashi and Yamanaka, 2006). However, the uncontrolled differentiation into multiple cells was not an inert attribute of embryonic stem cells upon isolation. This was demonstrated by a study in which embryonic stem cells were transplanted into blastocytes, providing the native niche of embryonic stem cells (Mintz and Illmensee, 1975). The chimeric blastocyst developed into a normal, healthy organism and therefore demonstrates the importance of specially and temporally controlled signals for stem cells (Mintz and Illmensee, 1975).

Adult stem cells of the small intestine reside at the bottom of anatomically well-defined regions termed crypts (Barker et al., 2007). The confinement of their location and their lack of migratory capacity argues that the niche signals for stem cell might come from neighbouring cells close by. In fact, it was believed that subepithelial myofibroblasts provide a cellular niche for epithelial stem cells, given their anatomical location (Sato et al., 2009). This idea was refuted by a set of elegant studies demonstrating that paneth cells are the niche cells (Farin et al., 2016; Sato et al., 2009; 2010; van Es et al., 2012). The authors of these studies used the organoid formation assay as a readout for the stem cells capacity to form organ-like structures in vitro (Sato et al., 2009). $Lgr5^+$ cells share a large part of their surface contact area with paneth cells at the bottom of the crypt (Sato et al., 2010). Thus, incomplete digestion upon stem cell isolation led to clusters of cells recapitulating the physiological cellular interaction in the organ (Sato et al., 2010). The authors developed a FACS strategy to sort "doublets" of stem cells and paneth cells and demonstrated drastically increased efficiency in organoid formation (Sato et al., 2010). Our finding that acinar cells only grow organoids once in direct cell-cell contact to a supporting acinar cell closely resembles these finding (Fig. 11). It is therefore possible that the acinar cell compartment does not only harbour a subpopulation of progenitor-like acinar cells but also a subpopulation of acinar cells that acts as a niche cell. At first sight it seems surprising that acinar cells provide the niche for its own cell type, considering that many stem cell driven organs demonstrate that cell types other than the stem-/progenitor provide the niche signals for adult stem cells (Fuchs et al., 2004). However, our data *en bloc* suggests that the acinar cell compartment consists of many (sub)cell types and the existence of a niche-like cell might support this concept.

If niche signals from supporting acinar cells control the proliferation of progenitor-like acinar cells the most obvious question is: What is the molecular identity of the niche signals? At this point, this remains an open question. Further experiments elucidating the signalling pathways that activate progenitor-like acinar cells might provide a clue on which ligands to look for. We find that direct cell-cell contact is necessary to induce proliferation, indicating that short-range signals promote organoid formation similar to the recently described mechanism for intestinal stem cells niches (Farin et al., 2016). Identification of candidate molecules will be the most straightforward way to directly test what are the signals that progenitor-like acinar cells depend on. The acinar cells that are the source of these signals could subsequently be identified and further characterized *in vivo*. Furthermore, the identification of the elusive niche factors would prove the existence of niche-like acinar cells. Although our data is very reminiscent of the data that led to the identification of the intestinal stem cell niche, we have

not isolated and characterised niche like acinar cells yet and thus had no means to manipulate them. Further experiments are needed to exclude the possibility that the proliferative capacity of progenitor-like acinar cells is completely inert trade.

Overall, the discovery of the intestinal stem cells niche in combination with our data regarding niche-like acinar cell suggest that the organoid assay is a valuable tool for discovering stem-/progenitor niches in other systems. This is particularly important for tissues in which the niche is not as clearly anatomically defined as for the small intestine. On the other hand, the progenitor-like acinar cell might reside in a previously neglected anatomically defined structure. Although stem cells in the mammalian brain were known to reside in the subventricular zone, it was not until recently that it was demonstrated that the stem cells reside in "pinwheel-like" structures (Mirzadeh et al., 2008). The adult pancreas might harbour similar, not yet identified microanatomial structures where progenitors reside, and advances in three-dimensional, whole-tissue imaging approach might facilitate their identification.

4.5 What is the acinar cell of origin for pancreatic ductal adenocarcinoma (PDAC)?

As described in the introduction (1.4 Pancreatic cancer), mouse models for pancreatic cancer demonstrated that acinar cells most likely represent the cell of origin for PDAC. Our data suggests that acinar cells are a heterogeneous population that consists of several sub-cell types. This raises the question whether these subpopulations differ in their susceptibility to tumour initiation and, if so, which of the acinar subtypes is most vulnerable.

4.5.1 From tissue turnover to tumorigenesis

Cancer is frequently diagnosed in patients at a late stage, which, in addition to the resulting poor prognosis, provides little information about the early events during tumour formation. Elegant studies from the 1960s analysed genetic abnormalities to retrospectively infer tumour cell clonality of chronic myelogenous leukaemia (BAIKIE et al., 1960). The authors demonstrated that dividing leukaemia cells shared the same genetic abnormalities, suggesting clonal origin of the tumour (BAIKIE et al., 1960). Although these studies, and subsequently several others, demonstrated that most cancers arise from a single cell, it remained unknown,

which cell within an organ is the root of the disease. The laboratory of John Dick discovered the first leukaemia initiating cell, and further provided evidence that leukaemia cells are hierarchically organized (Bonnet and Dick, 1997; Lapidot et al., 1994). The leukaemia initiating cell showed an immunophenotype, which closely resembled normal hematopoietic stem cells, suggesting that hematopoietic stem cells might be the cell of origin for acute myeloid leukaemia (Wang and Dick, 2005). Subsequently, genetic mouse models enabled researchers to directly test how susceptible different cell types within the blood or other organs are towards malignant transformation. For many tissues, introducing oncogenic mutation in stem- or progenitor cells was necessary in order to efficiently generate tumours (Visvader, 2011). These studies argue that stem-/progenitor cells likely represent the cell of origin for many cancers.

The applicability of this concept to the pancreas was long questioned, as the adult pancreas does not harbour multipotent stem cells (Kopp et al., 2016). More recently, it was hypothesized that the susceptibility for malignant transformation might depend on the most rudimentary feature of stem- and progenitor cells: the ability to renew the organ (or parts of it) for long periods of time (Kong et al., 2011). The progenitor-like acinar cells that we discovered might therefore represent a suitable candidate for the acinar cell of origin for PDAC. Although this acinar subpopulation is not multipotent, it is able to renew and produce new acinar cells for at least one year (Fig. 8, 9). Proliferation has been suggested to induce carcinogenesis through a mechanism involving homologous recombination mediated genetic rearrangement (Bishop and Schiestl, 2001). In fact it has been shown that murine pancreatic tissue accumulates recombinant cells with age and ageing has been recognized as a critical risk factor for pancreatic cancer (Li et al., 2004; Wiktor-Brown et al., 2006). It is therefore possible that progenitor-like acinar cells might acquire mutations as a consequence of their continuous proliferation in the course of time.

Our single cell mRNA sequencing results suggest that STMN1 might be a marker for the progenitor-like acinar cells that we discovered in our lineage tracing experiments (Fig. 20). STMN1 is also known as Oncoprotein 18 (Op18) after it was shown to be highly overexpressed in acute leukaemia cells (Hanash et al., 1988). STMN1 expression has since been determined in a large number of cancer samples (Belletti and Baldassarre, 2011). STMN1 was overexpressed in most, if not all analysed samples, despite the large variety of samples from different tumours (Belletti and Baldassarre, 2011). Furthermore, high expression levels of STMN1 was associated with poor survival and increased metastasis in a large number of cancers (Belletti and Baldassarre, 2011) including PDAC (Li et al., 2015).

These findings resemble the above-described phenotypic similarity of leukaemia initiating cells and hematopoietic stem cells. Yet, it is not possible to say whether the expression of STMN1 in pancreatic (as well as other) tumour cells mirrors the tumour cell´s origin or whether STMN1 was transiently upregulated. Although a similar mechanistic relationship has been previously established between the STMN1 and cell cycle activity, we did not find STMN1 expression as a consequence of mitosis, potentially arguing against transiently regulated expression of STMN1 in the pancreas (Cassimeris, 2002)(Fig. 20). Nevertheless, further experiments will be necessary to resolve this issue. In addition to STMN1´s role in cell cycle progression, a large body of evidence links STMN1 to migratory capacity of several cell types. High expression of STMN1 was observed at the invasive fronts of several cancers such as gastric cancer, colorectal cancer, non-small cell lung carcinoma and glioblastoma (Belletti and Baldassarre, 2011). The migration of non-cancer cells such as *Drosophila* ovary border cells and neurons were demonstrated to be STMN1-dependent (Borghese et al., 2006). It is conceivable that STMN1 might be a marker for metastasis initiating cells, given the cell´s dependence on STMN1. Yet, the idea that $STMN1^+$ pancreatic cells represent tumour-/metastasis-initiating cells needs experimental confirmation and remains purely speculative at this point.

Alternatively, the fact that injury increases the proliferative burden of acinar cells suggests the possibility that a pool of acinar cells distinct from $STMN1^+$ cells becomes susceptible to malignant transformation. This is particularly important in light of the fact that pancreatitis is another risk factor for pancreatic cancer (Hidalgo, 2010; Li et al., 2004). A recently discovered subpopulation of Dclk1 expressing acinar cells was shown to regenerate the pancreas after experimentally induced injury (Westphalen et al., 2016). Interestingly, this population was demonstrated to be particularly susceptible to tumour initiation upon pancreatic injury (Westphalen et al., 2016). According to our data, this population is likely to be distinct from the progenitor-like acinar cells that we discovered (Fig. 10). It will be interesting to directly compare the tumour initiating capacity of $Dclk1^+$ and $STMN1^+$ cells under different conditions, similar to the comparison of acinar and duct cell tumour susceptibility (Kopp et al., 2012). Such studies would help to further unravel which among the acinar subpopulations is most likely to be the true acinar cell of origin for PDAC.

4.5.2 The role of polyploid cells in tumour initiation

Our data suggests that binuclear acinar cells are proliferation deficient (Fig. 11, 13). The idea that these cells might be at the heart of pancreatic tumour formation seems therefore counterintuitive. However, a large body of literature suggests that tetraploid cells are genetically unstable and tumourigenic (Davoli and de Lange, 2011; 2012; Fujiwara et al., 2005; Ganem et al., 2007). Genome instability is described to underlie all hallmarks of cancer (Hanahan and Weinberg, 2011). So the question arises whether (and how) binuclear acinar cells might be able to escape their cell cycle arrest and start to proliferate uncontrollably as a result of their mutational burden.

In the 1960s a study addressing the effect of a group of fungal metabolic derivatives called cytochalasins on mammalian cells discovered that these molecules inhibited cytokinesis of dividing fibroblasts (CARTER, 1967). Interestingly, these cells display reduced mitotic rates and subsequent studies showed that p53 mediates cell cycle arrest in tetraploid cells (Andreassen et al., 2001; Kuffer et al., 2013). Recently, an RNAi screen identified the Hippo pathway kinase LATS2 as a regulator of tetraploid-induced G1 arrest in fibroblasts by stabilizing p53 (Ganem et al., 2014). Inactivating mutations of the tumour suppressor p53 are present in more than 50% of all PDACs and mouse models demonstrated that loss of p53 is necessary for progression of early lesion to aggressive, metastatic tumours (Bardeesy and DePinho, 2002; Guerra et al., 2007). It is therefore possible that p53 mutation erase the roadblock for binuclear acinar cell proliferation. Further support for this model is provided by the fact that tetraploid mammary epithelial cells isolated from $p53^{-/-}$ mice gave rise to malignant mammary epithelial cancers in contrast to diploid cells (Fujiwara et al., 2005, Nature).

It needs to be determined whether the molecular mechanism controlling cell cycle arrest in acinar cells is also p53 dependent. In contrast to fibroblasts or mutated cells, cultured normal hepatocytes show high levels of p53 independent of the ploidy, which does not hinder progression through S phase (Guidotti et al., 2003, JBC). This result argues that different mechanisms might govern tetraploid mediated cell cycle arrest in different cell types. Another potential argument against binuclear acinar cells as the source for PDAC is the fact that the pancreas is most prone to PDAC formation during pancreatic development (Guerra et al., 2007). Mouse models demonstrated that introduction of $Kras^{G12D}$ mutation before postnatal day P10 resulted in 100% PDAC incidence, as compared to 12% when the mutation was introduced after P10 (Guerra et al., 2007). However, in rodents between 5-17 days of age 95%

of all acinar cells are mononuclear (Oates and Morgan, 1986). Although the latter study was performed in rats and has yet to be confirmed in mice, the close evolutionary relationship between the species argues that similar kinetics might be observed in mice. A similarly high proportion of mononuclear acinar cells in the early postnatal murine pancreas would indicate, that mononuclear acinar cells might be more susceptible to malignant transformation.

Whether binuclear acinar are potential cells of origin for PDAC or if their proliferation deficiency mirrors the resistance to tumour formation observed in neurons or cardiomyocytes remains to be tested. Since binuclear cells also exist in human pancreatic tissue (Fig. 14), mouse models addressing this issue would be important in order to facilitate our understanding of human PDAC formation.

5 References

Achim, K., and Arendt, D. (2014). Structural evolution of cell types by step-wise assembly of cellular modules. Curr. Opin. Genet. Dev. *27*, 102–108.

Ahn, J., Murphy, M., Kratowicz, S., Wang, A., Levine, A.J., and George, D.L. (1999). Down-regulation of the stathmin/Op18 and FKBP25 genes following p53 induction. Oncogene *18*, 5954–5958.

Alberts B, Johnson A, Lewis J, Raff M, Roberts K, Walter P. 2014. Molecular biology of the cell. 6th edn. New York: Garland Science.

Anderson, S.M., Rudolph, M.C., McManaman, J.L., and Neville, M.C. (2007). Key stages in mammary gland development. Secretory activation in the mammary gland: it's not just about milk protein synthesis! Breast Cancer Research 2007 9:1 *9*, 1.

Andreassen, P.R., Lohez, O.D., Lacroix, F.B., and Margolis, R.L. (2001). Tetraploid state induces p53-dependent arrest of nontransformed mammalian cells in G1. Mol. Biol. Cell *12*, 1315–1328.

Arendt, D. (2008). The evolution of cell types in animals: emerging principles from molecular studies. Nat Rev Genet *9*, 868–882.

Babu, V., Paul, N., and Yu, R. (2013). Animal models and cell lines of pancreatic neuroendocrine tumors. Pancreas *42*, 912–923.

Baeyens, L., Lemper, M., Leuckx, G., De Groef, S., Bonfanti, P., Stangé, G., Shemer, R., Nord, C., Scheel, D.W., Pan, F.C., et al. (2013). Transient cytokine treatment induces acinar cell reprogramming and regenerates functional beta cell mass in diabetic mice. Nat Biotechnol.

BAIKIE, A.G., COURT-BROWN, W.M., BUCKTON, K.E., HARNDEN, D.G., JACOBS, P.A., and TOUGH, I.M. (1960). A Possible Specific Chromosome Abnormality in Human Chronic Myeloid Leukæmia. Nature *188*, 1165–1166.

Bardeesy, N., and DePinho, R.A. (2002). Pancreatic cancer biology and genetics. Nat Rev Cancer *2*, 897–909.

Barker, N., Huch, M., Kujala, P., van de Wetering, M., Snippert, H.J., van Es, J.H., Sato, T., Stange, D.E., Begthel, H., van den Born, M., et al. (2010). Lgr5(+ve) stem cells drive self-renewal in the stomach and build long-lived gastric units in vitro. Cell Stem Cell *6*, 25–36.

Barker, N., van Es, J.H., Kuipers, J., Kujala, P., van den Born, M., Cozijnsen, M., Haegebarth, A., Korving, J., Begthel, H., Peters, P.J., et al. (2007). Identification of stem cells in small intestine and colon by marker gene Lgr5. Nature *449*, 1003–1007.

Barnard, E.A. (1969). Biological function of pancreatic ribonuclease. Nature *221*, 340–344.

Barrandon, Y., and Green, H. (1987). Three clonal types of keratinocyte with different capacities for multiplication. Proc. Natl. Acad. Sci. U.S.a. *84*, 2302–2306.

Beck, B., and Blanpain, C. (2013). Unravelling cancer stem cell potential. Nat Rev Cancer *13*, 727–738.

BECKER, A.J., McCULLOCH, E.A., and Till, J.E. (1963). Cytological demonstration of the clonal nature of spleen colonies derived from transplanted mouse marrow cells. Nature *197*, 452–454.

Belletti, B., and Baldassarre, G. (2011). Stathmin: a protein with many tasks. New biomarker and potential target in cancer. Expert Opinion on Therapeutic Targets.

Belmont, L.D., and Mitchison, T.J. (1996). Identification of a protein that interacts with tubulin dimers and increases the catastrophe rate of microtubules. Cell *84*, 623–631.

Beretta, L., Dobránsky, T., and Sobel, A. (1993). Multiple phosphorylation of stathmin. Identification of four sites phosphorylated in intact cells and in vitro by cyclic AMP-dependent protein kinase and p34cdc2. J. Biol. Chem. *268*, 20076–20084.

Bièche, I., Maucuer, A., Laurendeau, I., Lachkar, S., Spano, A.J., Frankfurter, A., Lévy, P., Manceau, V., Sobel, A., Vidaud, M., et al. (2003). Expression of stathmin family genes in human tissues: non-neural-restricted expression for SCLIP. Genomics *81*, 400–410.

Bishop, A.J., and Schiestl, R.H. (2001). Homologous recombination as a mechanism of carcinogenesis. Biochim. Biophys. Acta *1471*, M109–M121.

Blache, P., van de Wetering, M., Duluc, I., Domon, C., Berta, P., Freund, J.-N., Clevers, H., and Jay, P. (2004). SOX9 is an intestine crypt transcription factor, is regulated by the Wnt pathway, and represses the CDX2and MUC2genes. J. Cell Biol. *166*, 37–47.

Boj, S.F., Hwang, C.-I., Baker, L.A., Chio, I.I.C., Engle, D.D., Corbo, V., Jager, M., Ponz-Sarvise, M., Tiriac, H., Spector, M.S., et al. (2015). Organoid Models of Human and Mouse Ductal Pancreatic Cancer. Cell *160*, 324–338.

Bonaguidi, M.A., Wheeler, M.A., Shapiro, J.S., Stadel, R.P., Sun, G.J., Ming, G.-L., and Song, H. (2011). In Vivo Clonal Analysis Reveals Self-Renewing and Multipotent Adult Neural Stem Cell Characteristics. Cell *145*, 1142–1155.

Bonnet, D., and Dick, J.E. (1997). Human acute myeloid leukemia is organized as a hierarchy that originates from a primitive hematopoietic cell. Nat Med *3*, 730–737.

Boraas, M.E., Seale, D.B., and Boxhorn, J.E. (1998). Phagotrophy by a flagellate selects for colonial prey: a possible origin of multicellularity. Evolutionary Ecology.

Borghese, L., Fletcher, G., Mathieu, J., Atzberger, A., Eades, W.C., Cagan, R.L., and Rørth, P. (2006). Systematic analysis of the transcriptional switch inducing migration of border cells. Developmental Cell *10*, 497–508.

Brack, A.S., and Rando, T.A. (2012). Tissue-specific stem cells: lessons from the skeletal muscle satellite cell. Cell Stem Cell *10*, 504–514.

Brattsand, G., and Marklund, U. (1994). Cell-cycle-regulated phosphorylation of oncoprotein 18 on Ser16, Ser25 and Ser38. European Journal of ….

Brembeck, F.H., Schreiber, F.S., Deramaudt, T.B., Craig, L., Rhoades, B., Swain, G., Grippo, P., Stoffers, D.A., Silberg, D.G., and Rustgi, A.K. (2003). The mutant K-ras oncogene causes pancreatic periductal lymphocytic infiltration and gastric mucous neck cell hyperplasia in transgenic mice. Cancer Research *63*, 2005–2009.

Brennand, K., Huangfu, D., and Melton, D. (2007). All beta cells contribute equally to islet growth and maintenance. Plos Biol *5*, e163.

Bullock, T.H., Bennett, M., and Johnston, D. (2005). The neuron doctrine, redux. ….

Buss, L.W. (1983). Evolution, development, and the units of selection.

Buss, L.W. (1987). The Evolution of Individuality (Princeton University Press).

Cajal, S.R.Y., Swanson, N., and Swanson, L.W. (1899). Histology of the nervous system of man and vertebrates.

Calzolari, F., Michel, J., Baumgart, E.V., Theis, F., Götz, M., and Ninkovic, J. (2015). Fast clonal expansion and limited neural stem cell self-renewal in the adult subependymal zone. Nat Neurosci.

Carr, M., Leadbeater, B., and Hassan, R. (2008). Molecular phylogeny of choanoflagellates, the sister group to Metazoa.

Carrière, C., Seeley, E.S., Goetze, T., Longnecker, D.S., and Korc, M. (2007). The Nestin progenitor lineage is the compartment of origin for pancreatic intraepithelial neoplasia. Proc. Natl. Acad. Sci. U.S.a. *104*, 4437–4442.

Carrière, C., Young, A.L., Gunn, J.R., Longnecker, D.S., and Korc, M. (2011). Acute Pancreatitis Accelerates Initiation and Progression to Pancreatic Cancer in Mice Expressing Oncogenic Kras in the Nestin Cell Lineage. PLoS ONE *6*, e27725.

CARTER, S.B. (1967). Effects of Cytochalasins on Mammalian Cells. Nature *213*, 261–264.

Cassimeris, L. (2002). The oncoprotein 18/stathmin family of microtubule destabilizers. Current Opinion in Cell Biology *14*, 18–24.

Cervero, P., Panzer, L., and Linder, S. (2013). Podosome reformation in macrophages: assays and analysis. Methods Mol. Biol. *1046*, 97–121.

Chen, W., Ji, J., Xu, X., He, S., and Ru, B. (2003). Proteomic comparison between human young and old brains by two-dimensional gel electrophoresis and identification of proteins. Int. J. Dev. Neurosci. *21*, 209–216.

Chera, S., Baronnier, D., Ghila, L., Cigliola, V., Jensen, J.N., Gu, G., Furuyama, K., Thorel, F., Gribble, F.M., Reimann, F., et al. (2014). Diabetes recovery by age-dependent conversion of pancreatic [dgr]-cells into insulin producers. Nature *514*, 503–507.

Cheung, M., and Briscoe, J. (2003). Neural crest development is regulated by the transcription factor Sox9. Development.

Chirgwin, J.M., Przybyla, A.E., MacDonald, R.J., and Rutter, W.J. (1979). Isolation of biologically active ribonucleic acid from sources enriched in ribonuclease. Biochemistry *18*, 5294–5299.

Chomczynski, P., and Sacchi, N. (1987). Single-step method of RNA isolation by acid guanidinium thiocyanate-phenol-chloroform extraction. Analytical Biochemistry *162*, 156–159.

Clayton, E., Doupé, D.P., Klein, A.M., Winton, D.J., Simons, B.D., and Jones, P.H. (2007). A single type of progenitor cell maintains normal epidermis. Nature *446*, 185–189.

Cleveland, M.H., Sawyer, J.M., Afelik, S., Jensen, J., and Leach, S.D. (2012). Exocrine ontogenies: On the development of pancreatic acinar, ductal and centroacinar cells. Semin. Cell Dev. Biol. *23*, 711–719.

Clevers, H. (2015). What is an adult stem cell? Science *350*, 1319–1320.

Cotsarelis, G., Sun, T.-T., and Lavker, R.M. (1990). Label-retaining cells reside in the bulge area of pilosebaceous unit: Implications for follicular stem cells, hair cycle, and skin carcinogenesis. Cell *61*, 1329–1337.

D S Longnecker, H.S.E.F. (1968). Molecular pathology of in-vivo inhibition of protein synthesis. Electron microscopy of rat pancreatic acinar cells in puromycin-induced necrosis. The American Journal of Pathology *52*, 891–61.

Davoli, T., and de Lange, T. (2011). The causes and consequences of polyploidy in normal development and cancer. Annu. Rev. Cell Dev. Biol. *27*, 585–610.

Davoli, T., and de Lange, T. (2012). Telomere-driven tetraploidization occurs in human cells undergoing crisis and promotes transformation of mouse cells. Cancer Cell *21*, 765–776.

Dennis, G., Sherman, B.T., Hosack, D.A., Yang, J., Gao, W., Lane, H.C., and Lempicki, R.A. (2003). Genome Biology | Full text | DAVID: Database for Annotation, Visualization, and Integrated Discovery. Genome Biol. *4*, P3.

Desai, B.M., Oliver-Krasinski, J., De Leon, D.D., Farzad, C., Hong, N., Leach, S.D., and Stoffers, D.A. (2007). Preexisting pancreatic acinar cells contribute to acinar cell, but not islet β cell, regeneration. J. Clin. Invest. *117*, 971–977.

Dor, Y., Brown, J., Martinez, O.I., and Melton, D.A. (2004). Adult pancreatic beta-cells are formed by self-duplication rather than stem-cell differentiation. Nature *429*, 41–46.

Doupé, D.P., Alcolea, M.P., Roshan, A., Zhang, G., Klein, A.M., Simons, B.D., and Jones, P.H. (2012). A single progenitor population switches behavior to maintain and repair esophageal epithelium. Science *337*, 1091–1093.

Doupé, D.P., Klein, A.M., Simons, B.D., and Jones, P.H. (2010). The Ordered Architecture of Murine Ear Epidermis Is Maintained by Progenitor Cells with Random Fate. Developmental Cell *18*, 317–323.

Eiraku, M., Takata, N., Ishibashi, H., Kawada, M., Sakakura, E., Okuda, S., Sekiguchi, K., Adachi, T., and Sasai, Y. (2011). Self-organizing optic-cup morphogenesis in three-dimensional culture. Nature *472*, 51–56.

Essers, M.A.G., Offner, S., Blanco-Bose, W.E., Waibler, Z., Kalinke, U., Duchosal, M.A., and Trumpp, A. (2009). IFNα activates dormant haematopoietic stem cells in vivo. Nature *458*, 904–908.

Farin, H.F., Jordens, I., Mosa, M.H., Basak, O., Korving, J., Tauriello, D.V.F., de Punder, K., Angers, S., Peters, P.J., Maurice, M.M., et al. (2016). Visualization of a short-range Wnt gradient in the intestinal stem-cell niche. Nature *530*, 340–343.

Findlay, D., Mathias, A.P., and Rabin, B.R. (1962). The active site and mechanism of action of bovine pancreatic ribonuclease. 5. The charge types at the active centre. Biochem. J. *85*, 139–144.

Frey, B.J., and Dueck, D. (2007). Clustering by Passing Messages Between Data Points. Science *315*, 972–976.

Fuchs, E., Tumbar, T., and Guasch, G. (2004). Socializing with the Neighbors. Cell *116*, 769–778.

Fuentealba, L.C., Rompani, S.B., Parraguez, J.I., Obernier, K., Romero, R., Cepko, C.L., and Alvarez-Buylla, A. (2015). Embryonic Origin of Postnatal Neural Stem Cells. Cell *161*, 1644–1655.

Fujiwara, T., Bandi, M., Nitta, M., Ivanova, E.V., Bronson, R.T., and Pellman, D. (2005). Cytokinesis failure generating tetraploids promotes tumorigenesis in p53-null cells. Nature *437*, 1043–1047.

Fukuda, A., Wang, S.C., Morris, J.P., IV, Folias, A.E., Liou, A., Kim, G.E., Akira, S., Boucher, K.M., Firpo, M.A., Mulvihill, S.J., et al. (2011). Stat3 and MMP7 Contribute to Pancreatic Ductal Adenocarcinoma Initiation and Progression. Cancer Cell *19*, 441–455.

Furutachi, S., Miya, H., Watanabe, T., Kawai, H., Yamasaki, N., Harada, Y., Imayoshi, I., Nelson, M., Nakayama, K.I., Hirabayashi, Y., et al. (2015). Slowly dividing neural progenitors are an embryonic origin of adult neural stem cells. Nat Neurosci *18*, 657–665.

Furuyama, K., Kawaguchi, Y., Akiyama, H., Horiguchi, M., Kodama, S., Kuhara, T., Hosokawa, S., Elbahrawy, A., Soeda, T., Koizumi, M., et al. (2011). Continuous cell supply from a Sox9-expressing progenitor zone in adult liver, exocrine pancreas and intestine. Nature Genetics *43*, 34–41.

Gage, F.H. (2000). Mammalian Neural Stem Cells. Science *287*, 1433–1438.

Ganem, N.J., Cornils, H., Chiu, S.-Y., O'Rourke, K.P., Arnaud, J., Yimlamai, D., Théry, M., Camargo, F.D., and Pellman, D. (2014). Cytokinesis Failure Triggers Hippo Tumor Suppressor Pathway Activation. Cell *158*, 833–848.

Ganem, N.J., Storchova, Z., and Pellman, D. (2007). Tetraploidy, aneuploidy and cancer. Curr. Opin. Genet. Dev. *17*, 157–162.

Gillespie, D.T. (1976). A general method for numerically simulating the stochastic time evolution of coupled chemical reactions. Journal of Computational Physics *22*, 403–434.

Grieninger, G., and Granick, S. (1978). Synthesis and secretion of plasma proteins by embryonic chick hepatocytes: changing patterns during the first three days of culture. J Exp Med *147*, 1806–1823.

Gu, G., Dubauskaite, J., and Melton, D.A. (2002). Direct evidence for the pancreatic lineage: NGN3+ cells are islet progenitors and are distinct from duct progenitors. Development *129*, 2447–2457.

Guerra, C., Collado, M., Navas, C., Schuhmacher, A.J., Hernández-Porras, I., Cañamero, M., Rodriguez-Justo, M., Serrano, M., and Barbacid, M. (2011). Pancreatitis-Induced

Inflammation Contributes to Pancreatic Cancer by Inhibiting Oncogene-Induced Senescence. Cancer Cell *19*, 728–739.

Guerra, C., Schuhmacher, A.J., Cañamero, M., Grippo, P.J., Verdaguer, L., Pérez-Gallego, L., Dubus, P., Sandgren, E.P., and Barbacid, M. (2007). Chronic pancreatitis is essential for induction of pancreatic ductal adenocarcinoma by K-Ras oncogenes in adult mice. Cancer Cell *11*, 291–302.

Guo, L., Sans, M.D., Hou, Y., Ernst, S.A., and Williams, J.A. (2012). c-Jun/AP-1 is required for CCK-induced pancreatic acinar cell dedifferentiation and DNA synthesis in vitro. AJP: Gastrointestinal and Liver Physiology *302*, G1381–G1396.

Gupta, V., and Poss, K.D. (2012). Clonally dominant cardiomyocytes direct heart morphogenesis. Nature *484*, 479–484.

Haas, B.J., Papanicolaou, A., Yassour, M., Grabherr, M., Blood, P.D., Bowden, J., Couger, M.B., Eccles, D., Li, B., Lieber, M., et al. (2013). De novo transcript sequence reconstruction from RNA-seq using the Trinity platform for reference generation and analysis. Nat Protoc *8*, 1494–1512.

Habbe, N., Shi, G., Meguid, R.A., Fendrich, V., Esni, F., Chen, H., Feldmann, G., Stoffers, D.A., Konieczny, S.F., Leach, S.D., et al. (2008). Spontaneous induction of murine pancreatic intraepithelial neoplasia (mPanIN) by acinar cell targeting of oncogenic Kras in adult mice. Proc. Natl. Acad. Sci. U.S.a. *105*, 18913–18918.

Hanahan, D., and Weinberg, R.A. (2011). Hallmarks of cancer: the next generation. Cell *144*, 646–674.

Hanash, S.M., Strahler, J.R., Kuick, R., Chu, E.H., and Nichols, D. (1988). Identification of a polypeptide associated with the malignant phenotype in acute leukemia. J. Biol. Chem. *263*, 12813–12815.

Hawkins, T.L., O'Connor-Morin, T., Roy, A., and Santillan, C. (1994). DNA purification and isolation using a solid-phase. Nucleic Acids Research *22*, 4543–4544.

Hidalgo, M. (2010). Pancreatic Cancer. N Engl J Med *362*, 1605–1617.

Hingorani, S.R., Petricoin, E.F., III, Maitra, A., Rajapakse, V., King, C., Jacobetz, M.A., Ross, S., Conrads, T.P., Veenstra, T.D., Hitt, B.A., et al. (2003). Preinvasive and invasive ductal pancreatic cancer and its early detection in the mouse. Cancer Cell *4*, 437–450.

Hisha, H., Tanaka, T., Kanno, S., Tokuyama, Y., Komai, Y., Ohe, S., Yanai, H., Omachi, T., and Ueno, H. (2013). Establishment of a novel lingual organoid culture system: generation of organoids having mature keratinized epithelium from adult epithelial stem cells. Sci. Rep. *3*, 3224.

Horsley, V. (2012). Split decisions: oesophageal progenitor cell behaviour. Embo J *31*, 3653–3654.

Huang, L., Holtzinger, A., Jagan, I., BeGora, M., Lohse, I., Ngai, N., Nostro, C., Wang, R., Muthuswamy, L.B., Crawford, H.C., et al. (2015). Ductal pancreatic cancer modeling and drug screening using human pluripotent stem cell- and patient-derived tumor organoids. Nature Medicine *21*, 1364–1371.

Huch, M., and Koo, B.-K. (2015). Modeling mouse and human development using organoid cultures. Development *142*, 3113–3125.

Huch, M., Bonfanti, P., Boj, S.F., Sato, T., Loomans, C.J.M., van de Wetering, M., Sojoodi, M., Li, V.S.W., Schuijers, J., Gracanin, A., et al. (2013a). Unlimited in vitro expansion of adult bi-potent pancreas progenitors through the Lgr5/R-spondin axis. Embo J *32*, 2708–2721.

Huch, M., Dorrell, C., Boj, S.F., van Es, J.H., Li, V.S.W., van de Wetering, M., Sato, T., Hamer, K., Sasaki, N., Finegold, M.J., et al. (2013b). In vitro expansion of single Lgr5+ liver stem cells induced by Wnt-driven regeneration. Nature –.

Hughes, C.S., Postovit, L.M., and Lajoie, G.A. Matrigel: A complex protein mixture required for optimal growth of cell culture. Proteomics *10*, 1886–1890.

Hughes, C.S., Foehr, S., Garfield, D.A., Furlong, E.E., Steinmetz, L.M., and Krijgsveld, J. (2014). Ultrasensitive proteome analysis using paramagnetic bead technology. Mol. Syst. Biol. *10*, 757.

Hwang, C.-I., Boj, S.F., Clevers, H., and Tuveson, D.A. (2015). Preclinical models of pancreatic ductal adenocarcinoma. J. Pathol. *238*, 197–204.

Ishida, S., Huang, E., Zuzan, H., Spang, R., Leone, G., West, M., and Nevins, J.R. (2001). Role for E2F in control of both DNA replication and mitotic functions as revealed from DNA microarray analysis. Mol. Cell. Biol. *21*, 4684–4699.

Jaks, V., Kasper, M., and Toftgård, R. (2010). The hair follicle—a stem cell zoo. Experimental Cell Research *316*, 1422–1428.

Jensen, J.N., Cameron, E., Garay, M.V.R., Starkey, T.W., Gianani, R., and Jensen, J. (2005). Recapitulation of elements of embryonic development in adult mouse pancreatic regeneration. Ygast *128*, 728–741.

Jin, L., Feng, T., Shih, H.P., Zerda, R., Luo, A., Hsu, J., Mahdavi, A., Sander, M., Tirrell, D.A., Riggs, A.D., et al. (2013). Colony-forming cells in the adult mouse pancreas are expandable in Matrigel and form endocrine/acinar colonies in laminin hydrogel. Proceedings of the National Academy of Sciences.

Johnsen, J.I., Aurelio, O.N., and Kwaja, Z. (2000). p53-mediated negative regulation of stathmin/Op18 expression is associated with G2/M cell-cycle arrest. … Journal of Cancer.

Jones, P.H., and Watt, F.M. (1993). Separation of human epidermal stem cells from transit amplifying cells on the basis of differences in integrin function and expression. Cell *73*, 713–724.

Katsnelson, A. (2006). Kicking off adaptive immunity: the discovery of dendritic cells. J Exp Med *203*, 1622–1622.

Kaufmann, A., Rössler, O.G., and Thiel, G. (2014). Expression of the Transcription Factor Egr-1 in Pancreatic Acinar Cells Following Stimulation of Cholecystokinin or Gαq-Coupled Designer Receptors. Cell Physiol Biochem *33*, 1411–1425.

King, N. (2004). The Unicellular Ancestry of Animal Development. Developmental Cell *7*, 313–325.

Klein, A.M., and Simons, B.D. (2011a). Universal patterns of stem cell fate in cycling adult tissues. Development *138*, 3103–3111.

Klein, A.M., and Simons, B.D. (2011b). Universal patterns of stem cell fate in cycling adult tissues. Development *138*, 3103–3111.

Klein, A.M., Nakagawa, T., Ichikawa, R., Yoshida, S., and Simons, B.D. (2010). Mouse Germ Line Stem Cells Undergo Rapid and Stochastic Turnover. Cell Stem Cell *7*, 214–224.

Klink, T.A., Woycechowsky, K.J., Taylor, K.M., and Raines, R.T. Contribution of disulfide bonds to the conformational stability and catalytic activity of ribonuclease A. The FEBS Journal *267*, 566–572.

Knoll, A.H. (2011). The Multiple Origins of Complex Multicellularity. Annu. Rev. Earth Planet. Sci. *39*, 217–239.

Kong, B., Michalski, C.W., Erkan, M., Friess, H., and Kleeff, J. (2011). From tissue turnover to the cell of origin for pancreatic cancer. Nature Publishing Group *8*, 467–472.

Kong, Y. (2011). Btrim: a fast, lightweight adapter and quality trimming program for next-generation sequencing technologies. Genomics *98*, 152–153.

Kopinke, D., Brailsford, M., Shea, J.E., Leavitt, R., Scaife, C.L., and Murtaugh, L.C. (2011). Lineage tracing reveals the dynamic contribution of Hes1+ cells to the developing and adult pancreas. Development *138*, 431–441.

Kopp, J.L., Dubois, C.L., Hao, E., Thorel, F., Herrera, P.L., and Sander, M. (2014). Progenitor cell domains in the developing and adult pancreas. Cell Cycle *10*, 1921–1927.

Kopp, J.L., Dubois, C.L., Schaffer, A.E., Hao, E., Shih, H.P., Seymour, P.A., Ma, J., and Sander, M. (2011). Sox9+ ductal cells are multipotent progenitors throughout development but do not produce new endocrine cells in the normal or injured adult pancreas. Development *138*, 653–665.

Kopp, J.L., Figura, von, G., Mayes, E., Liu, F.-F., Dubois, C.L., Morris, J.P., IV, Pan, F.C., Akiyama, H., Wright, C.V.E., Jensen, K., et al. (2012). Identification of Sox9-Dependent Acinar-to-Ductal Reprogramming as the Principal Mechanism for Initiation of Pancreatic Ductal Adenocarcinoma. Cancer Cell.

Kopp, J.L., Grompe, M., and Sander, M. (2016). Stem cells versus plasticity in liver and pancreas regeneration. Nat. Cell Biol. *18*, 238–245.

Koppel, J., Loyer, P., Maucuer, A., Rehák, P., Manceau, V., Guguen-Guillouzo, C., and Sobel, A. Induction of stathmin expression during liver regeneration. FEBS Letters *331*, 65–70.

Korinek, V., Barker, N., Moerer, P., and van Donselaar, E. (1998). Depletion of epithelial stem-cell compartments in the small intestine of mice lacking Tcf-4. Nature Genetics.

Kotewicz, M.L. (1988). Isolation of cloned Moloney murine leukemia virus reverse transcriptase lacking ribonuclease H activity. Nucleic Acids ….

Kretzschmar, K., and Watt, F.M. (2012). Lineage tracing. Cell *148*, 33–45.

Kriegstein, A., and Alvarez-Buylla, A. (2009). The glial nature of embryonic and adult neural stem cells. Annu. Rev. Neurosci. *32*, 149–184.

Kuffer, C., Kuznetsova, A.Y., and Storchova, Z. (2013). Abnormal mitosis triggers p53-dependent cell cycle arrest in human tetraploid cells. Chromosoma *122*, 305–318.

La O, De, J.-P., Emerson, L.L., Goodman, J.L., Froebe, S.C., Illum, B.E., Curtis, A.B., and Murtaugh, L.C. (2008). Notch and Kras reprogram pancreatic acinar cells to ductal intraepithelial neoplasia. Proc. Natl. Acad. Sci. U.S.a. *105*, 18907–18912.

Lalitha S Y Nanduri, M.B.H.F.C.R.E.Z.G. de H.R.V.O.R.P.C. (2014). Purification and Ex Vivo Expansion of Fully Functional Salivary Gland Stem Cells. Stem Cell Reports *3*, 957.

Lancaster, M.A., Renner, M., Martin, C.-A., Wenzel, D., Bicknell, L.S., Hurles, M.E., Homfray, T., Penninger, J.M., Jackson, A.P., and Knoblich, J.A. (2013). Cerebral organoids model human brain development and microcephaly. Nature –.

Landsman, L., Parent, A., and Hebrok, M. (2011). Elevated Hedgehog/Gli signaling causes beta-cell dedifferentiation in mice. Proceedings of the National Academy of Sciences *108*, 17010–17015.

Langerhans P (1869). "Beitrage zur mikroskopischen Anatomie der Bauchspeichel Drüse". Inaugural-dissertation. Berlin: Gustav Lange

Lapidot, T., Sirard, C., Vormoor, J., Murdoch, B., Hoang, T., Caceres-Cortes, J., Minden, M., Paterson, B., Caligiuri, M.A., and Dick, J.E. (1994). A cell initiating human acute myeloid leukaemia after transplantation into SCID mice. Nature *367*, 645–648.

Larsson, N., Marklund, U., Gradin, H.M., Brattsand, G., and Gullberg, M. (1997). Control of microtubule dynamics by oncoprotein 18: dissection of the regulatory role of multisite phosphorylation during mitosis. Mol. Cell. Biol. *17*, 5530–5539.

Lee, J.-H., Bhang, D.H., Beede, A., Huang, T.L., Stripp, B.R., Bloch, K.D., Wagers, A.J., Tseng, Y.-H., Ryeom, S., and Kim, C.F. (2014). Lung Stem Cell Differentiation in Mice Directed by Endothelial Cells via a BMP4-NFATc1-Thrombospondin-1 Axis. Cell *156*, 440–455.

Lerch, M.M., and Gorelick, F.S. (2013). Models of acute and chronic pancreatitis. Gastroenterology *144*, 1180–1193.

Lescroart, F., Chabab, S., Lin, X., Rulands, S., Paulissen, C., Rodolosse, A., Auer, H., Achouri, Y., Dubois, C., Bondue, A., et al. (2014). Early lineage restriction in temporally distinct populations of Mesp1 progenitors during mammalian heart development. Nat. Cell Biol. *16*, 829–840.

Li, B., and Dewey, C.N. (2011). RSEM: accurate transcript quantification from RNA-Seq data with or without a reference genome. BMC Bioinformatics *12*, 323.

Li, D., Xie, K., Wolff, R., and Abbruzzese, J.L. (2004). Pancreatic cancer. The Lancet *363*, 1049–1057.

Li, J., Hu, G., Kong, F., Wu, K., Song, K., He, J., and Sun, W. (2015). Elevated STMN1 Expression Correlates with Poor Prognosis in Patients with Pancreatic Ductal

Adenocarcinoma. Pathol. Oncol. Res. *21*, 1013–1020.

Li, W., Nakanishi, M., Zumsteg, A., Shear, M., Wright, C., Melton, D.A., and Zhou, Q. (2014). In vivo reprogramming of pancreatic acinar cells to three islet endocrine subtypes. Elife *3*, e01846.

Lis, J.T. (1980). [42] Fractionation of DNA fragments by polyethylene glycol induced precipitation. Methods in Enzymology *65*, 347–353.

Livet, J., Weissman, T.A., Kang, H., Draft, R.W., Lu, J., Bennis, R.A., Sanes, J.R., and Lichtman, J.W. (2007). Transgenic strategies for combinatorial expression of fluorescent proteins in the nervous system. Nature *450*, 56–62.

Llinás, R.R. (2003). The contribution of Santiago Ramon y Cajal to functional neuroscience. Nat Rev Neurosci *4*, 77–80.

Llorens-Bobadilla, E., Zhao, S., Baser, A., Saiz-Castro, G., Zwadlo, K., and Martin-Villalba, A. (2015). Single-Cell Transcriptomics Reveals a Population of Dormant Neural Stem Cells that Become Activated upon Brain Injury. Cell Stem Cell.

Logsdon, C.D., and Ji, B. (2013). The role of protein synthesis and digestive enzymes in acinar cell injury. Nature Publishing Group *10*, 362–370.

Low, J.T., Shukla, A., and Thorn, P. (2010). Pancreatic acinar cell: New insights into the control of secretion. The International Journal of Biochemistry & Cell Biology *42*, 1586–1589.

Lu, C.P., Polak, L., Rocha, A.S., Pasolli, H.A., Chen, S.-C., Sharma, N., Blanpain, C., and Fuchs, E. (2012). Identification of Stem Cell Populations in Sweat Glands and Ducts Reveals Roles in Homeostasis and Wound Repair. Cell *150*, 136–150.

Luo, X.N., Mookerjee, B., Ferrari, A., Mistry, S., and Atweh, G.F. (1994). Regulation of phosphoprotein p18 in leukemic cells. Cell cycle regulated phosphorylation by p34cdc2 kinase. J. Biol. Chem. *269*, 10312–10318.

Lynn, F.C., Smith, S.B., Wilson, M.E., Yang, K.Y., Nekrep, N., and German, M.S. (2007). Sox9 coordinates a transcriptional network in pancreatic progenitor cells. Proc. Natl. Acad. Sci. U.S.a. *104*, 10500–10505.

Magami, Y., Azuma, T., Inokuchi, H., Kawai, K., and Hattori, T. (1990). Turnover of acinar cells in mouse pancreas. J Gastroenterol *25*, 514–514.

Manning, G., Young, S.L., and Miller, W.T. (2008). The protist, Monosiga brevicollis, has a tyrosine kinase signaling network more elaborate and diverse than found in any known metazoan.

McCulloch, E.A., and Till, J.E. (2005). Perspectives on the properties of stem cells. Nat Med *11*, 1026–1028.

Melhem, R.F., Zhu, X.X., Hailat, N., Strahler, J.R., and Hanash, S.M. (1991). Characterization of the gene for a proliferation-related phosphoprotein (oncoprotein 18) expressed in high amounts in acute leukemia. J. Biol. Chem. *266*, 17747–17753.

Meyer, G., Goffinet, A.M., and Fairén, A. (1999). What is a Cajal–Retzius cell? A reassessment of a classical cell type based on recent observations in the developing neocortex. Cerebral Cortex.

Mintz, B., and Illmensee, K. (1975). Normal genetically mosaic mice produced from malignant teratocarcinoma cells. Proc. Natl. Acad. Sci. U.S.a. *72*, 3585–3589.

Mirzadeh, Z., Merkle, F.T., Soriano-Navarro, M., Garcia-Verdugo, J.-M., and Alvarez-Buylla, A. (2008). Neural Stem Cells Confer Unique Pinwheel Architecture to the Ventricular Surface in Neurogenic Regions of the Adult Brain. Cell Stem Cell *3*, 265–278.

Mistry, S.J., and Atweh, G.F. (2001). Stathmin inhibition enhances okadaic acid-induced mitotic arrest: a potential role for stathmin in mitotic exit. J. Biol. Chem. *276*, 31209–31215.

Miyaoka, Y., Ebato, K., Kato, H., Arakawa, S., Shimizu, S., and Miyajima, A. (2012). Hypertrophy and Unconventional Cell Division of Hepatocytes Underlie Liver Regeneration. Current Biology *22*, 1166–1175.

Morris, J.P., Cano, D.A., Sekine, S., Wang, S.C., and Hebrok, M. (2010). Beta-catenin blocks Kras-dependent reprogramming of acini into pancreatic cancer precursor lesions in mice. J. Clin. Invest. *120*, 508–520.

Morris, R.J., Liu, Y., Marles, L., Yang, Z., Trempus, C., Li, S., Lin, J.S., Sawicki, J.A., and Cotsarelis, G. (2004). Capturing and profiling adult hair follicle stem cells. Nat Biotechnol *22*, 411–417.

Morrison, S.J., and Weissman, I.L. (1994). The long-term repopulating subset of hematopoietic stem cells is deterministic and isolatable by phenotype. Immunity *1*, 661–673.

Murphy, M., Ahn, J., Walker, K.K., Hoffman, W.H., Evans, R.M., Levine, A.J., and George, D.L. (1999). Transcriptional repression by wild-type p53 utilizes histone deacetylases, mediated by interaction with mSin3a. Genes & Development *13*, 2490–2501.

Nagashio, Y., Ueno, H., Imamura, M., Asaumi, H., Watanabe, S., Yamaguchi, T., Taguchi, M., Tashiro, M., and Otsuki, M. (2004). Inhibition of transforming growth factor β decreases pancreatic fibrosis and protects the pancreas against chronic injury in mice. Lab Invest *84*, 1610–1618.

Naqvi, N., Li, M., Calvert, J.W., Tejada, T., Lambert, J.P., Wu, J., Kesteven, S.H., Holman, S.R., Matsuda, T., Lovelock, J.D., et al. (2014). A Proliferative Burst during Preadolescence Establishes the Final Cardiomyocyte Number. Cell *157*, 795–807.

Oates, P.S., and Morgan, R.G. (1986). Changes in pancreatic acinar cell nuclear number and DNA content during aging in the rat. Am. J. Anat. *177*, 547–554.

Olive, K.P., Jacobetz, M.A., Davidson, C.J., Gopinathan, A., McIntyre, D., Honess, D., Madhu, B., Goldgraben, M.A., Caldwell, M.E., Allard, D., et al. (2009). Inhibition of Hedgehog signaling enhances delivery of chemotherapy in a mouse model of pancreatic cancer. Science *324*, 1457–1461.

Ousset, M., Van Keymeulen, A., Bouvencourt, G., Sharma, N., Achouri, Y., Simons, B.D., and Blanpain, C. (2012). Multipotent and unipotent progenitors contribute to prostate postnatal development. Nat. Cell Biol. *14*, 1131–1138.

P S Oates, R.G.M. (1989). Cell proliferation in the exocrine pancreas during development. Journal of Anatomy *167*, 235.

Pan, F.C., Bankaitis, E.D., Boyer, D., Xu, X., Van de Casteele, M., Magnuson, M.A., Heimberg, H., and Wright, C.V.E. (2013). Spatiotemporal patterns of multipotentiality in Ptf1a-expressing cells during pancreas organogenesis and injury-induced facultative restoration. Development *140*, 751–764.

Park, J., Brureau, A., Kernan, K., Starks, A., Gulati, S., Ogunnaike, B., Schwaber, J., and Vadigepalli, R. (2014). Inputs drive cell phenotype variability. Genome Research *24*, 930–941.

Perez-Mancera, P.A., Guerra, C., Barbacid, M., and Tuveson, D.A. (2012). What We Have Learned About Pancreatic Cancer From Mouse Models. Gastroenterology *142*, 1079–1092.

Petersen, O.H. (1992). Stimulus-secretion coupling: cytoplasmic calcium signals and the control of ion channels in exocrine acinar cells. The Journal of Physiology.

Picelli, S., Faridani, O.R., Björklund, Å.K., Winberg, G., Sagasser, S., and Sandberg, R. (2014). Full-length RNA-seq from single cells using Smart-seq2. Nat Protoc *9*, 171–181.

Polager, S., and Ginsberg, D. (2003). E2F mediates sustained G2 arrest and down-regulation of Stathmin and AIM-1 expression in response to genotoxic stress. J. Biol. Chem. *278*, 1443–1449.

Polzin, R.G., Benlhabib, H., Trepel, J., and Herrera, J.E. (2004). E2F sites in the Op18 promoter are required for high level of expression in the human prostate carcinoma cell line PC-3-M. Gene *341*, 209–218.

Porrello, E.R., Mahmoud, A.I., Simpson, E., Hill, J.A., Richardson, J.A., Olson, E.N., and Sadek, H.A. (2011). Transient regenerative potential of the neonatal mouse heart. Science *331*, 1078–1080.

Poss, K.D. (2007). Getting to the heart of regeneration in zebrafish. Semin. Cell Dev. Biol. *18*, 36–45.

Prud'homme, B., Gompel, N., Rokas, A., Kassner, V.A., Williams, T.M., Yeh, S.-D., True, J.R., and Carroll, S.B. (2006). Repeated morphological evolution through cis-regulatory changes in a pleiotropic gene. Nature *440*, 1050–1053.

Przyborski, S.A. (2005). Differentiation of human embryonic stem cells after transplantation in immune-deficient mice. Stem Cells *23*, 1242–1250.

Puri, S., and Hebrok, M. (2010). Cellular Plasticity within the Pancreas- Lessons Learned from Development. Developmental Cell *18*, 342–356.

Puri, S., Folias, A.E., and Hebrok, M. (2015). Plasticity and Dedifferentiation within the Pancreas: Development, Homeostasis, and Disease. Cell Stem Cell *16*, 18–31.

Rios, A.C., Fu, N.Y., Jamieson, P.R., Pal, B., Whitehead, L., Nicholas, K.R., Lindeman, G.J., and Visvader, J.E. (2016). Essential role for a novel population of binucleated mammary epithelial cells in lactation. Nat Comms *7*, 11400.

Robinson, M.D., and Oshlack, A. (2010). A scaling normalization method for differential expression analysis of RNA-seq data. Genome Biol. *11*, R25.

Rovira, M., Scott, S.G., Liss, A.S., Jensen, J., Thayer, S.P., and Leach, S.D. (2010). Isolation and characterization of centroacinar/terminal ductal progenitor cells in adult mouse pancreas. Proc. Natl. Acad. Sci. U.S.a. *107*, 75–80.

Rowlands, A, W., NA, J., SS, G., GM, R., PC, B., and G, B. (1995). Stathmin expression is a feature of proliferating cells of most, if not all, cell lineages. Lab Invest *72*, 100–113.

Roy, N., and Hebrok, M. (2015). Regulation of Cellular Identity in Cancer. Developmental Cell *35*, 674–684.

Saliba, A.-E., Westermann, A.J., Gorski, S.A., and Vogel, J. (2014). Single-cell RNA-seq: advances and future challenges. Nucleic Acids Research *42*, 8845–8860.

Sancho, R., Gruber, R., Gu, G., and Behrens, A. (2014). Loss of Fbw7 Reprograms Adult Pancreatic Ductal Cells into α, δ, and β Cells. Cell Stem Cell *15*, 139–153.

Sasai, Y. (2013). Next-Generation Regenerative Medicine: Organogenesis from Stem Cells in 3D Culture. Cell Stem Cell *12*, 520–530.

Sato, T., and Clevers, H. (2013). Growing Self-Organizing Mini-Guts from a Single Intestinal Stem Cell: Mechanism and Applications. Science *340*, 1190–1194.

Sato, T., van Es, J.H., Snippert, H.J., Stange, D.E., Vries, R.G., van den Born, M., Barker, N., Shroyer, N.F., van de Wetering, M., and Clevers, H. (2010). Paneth cells constitute the niche for Lgr5 stem cells in intestinal crypts. Nature *469*, 415–418.

Sato, T., Vries, R.G., Snippert, H.J., van de Wetering, M., Barker, N., Stange, D.E., van Es, J.H., Abo, A., Kujala, P., Peters, P.J., et al. (2009). Single Lgr5 stem cells build crypt villus structures in vitro without a mesenchymal niche. Nature *459*, 262–265.

Sauer, B., and Henderson, N. (1988). Site-specific DNA recombination in mammalian cells by the Cre recombinase of bacteriophage P1. Proc. Natl. Acad. Sci. U.S.a. *85*, 5166–5170.

Schmidt, W.M., and Mueller, M.W. (1999). CapSelect: a highly sensitive method for 5′ CAP-dependent enrichment of full-length cDNA in PCR-mediated analysis of mRNAs. Nucleic Acids Research *27*, e31–i–e31–iv.

Seaberg, R.M., Smukler, S.R., Kieffer, T.J., Enikolopov, G., Asghar, Z., Wheeler, M.B., Korbutt, G., and van der Kooy, D. (2004). Clonal identification of multipotent precursors from adult mouse pancreas that generate neural and pancreatic lineages. Nat Biotechnol *22*, 1115–1124.

Senyo, S.E., Steinhauser, M.L., Pizzimenti, C.L., Yang, V.K., Cai, L., Wang, M., Wu, T.-D., Guerquin-Kern, J.-L., Lechene, C.P., and Lee, R.T. (2012). Mammalian heart renewal by pre-existing cardiomyocytes. Nature *493*, 433–436.

Seymour, P.A., Freude, K.K., Tran, M.N., Mayes, E.E., Jensen, J., Kist, R., Scherer, G., and Sander, M. (2007). SOX9 is required for maintenance of the pancreatic progenitor cell pool. Proceedings of the National Academy of Sciences *104*, 1865–1870.

Shackleton, M., Vaillant, F., Simpson, K.J., Stingl, J., Smyth, G.K., Asselin-Labat, M.-L., Wu, L., Lindeman, G.J., and Visvader, J.E. (2006). Generation of a functional mammary gland from a single stem cell. Nature *439*, 84–88.

Shalchian-Tabrizi, K., Minge, M.A., Espelund, M., Orr, R., Ruden, T., Jakobsen, K.S., and Cavalier-Smith, T. (2008). Multigene Phylogeny of Choanozoa and the Origin of Animals. PLoS ONE *3*, e2098.

Shalek, A.K., Satija, R., Adiconis, X., Gertner, R.S., Gaublomme, J.T., Raychowdhury, R., Schwartz, S., Yosef, N., Malboeuf, C., Lu, D., et al. (2013). Single-cell transcriptomics reveals bimodality in expression and splicing in immune cells. Nature *498*, 236–240.

Shalek, A.K., Satija, R., Shuga, J., Trombetta, J.J., Gennert, D., Lu, D., Chen, P., Gertner, R.S., Gaublomme, J.T., Yosef, N., et al. (2014). Single-cell RNA-seq reveals dynamic paracrine control of cellular variation. Nature *510*, 363–369.

Shanks, N., Greek, R., and Greek, J. (2009). Are animal models predictive for humans? Philosophy, Ethics, and Humanities in Medicine 2009 4:1 *4*, 1.

Shin, J., Berg, D.A., Zhu, Y., Shin, J.Y., Song, J., Bonaguidi, M.A., Enikolopov, G., Nauen, D.W., Christian, K.M., Ming, G.-L., et al. (2015). Single-Cell RNA-Seq with Waterfall Reveals Molecular Cascades underlying Adult Neurogenesis. Cell Stem Cell *17*, 360–372.

Siminovitch, L., and McCULLOCH, E.A. (1963). The distribution of colony-forming cells among spleen colonies. Journal of Cellular and ….

Singer, S., Ehemann, V., Brauckhoff, A., Keith, M., Vreden, S., Schirmacher, P., and Breuhahn, K. (2007). Protumorigenic overexpression of stathmin/Op18 by gain-of-function mutation in p53 in human hepatocarcinogenesis. Hepatology *46*, 759–768.

Smukler, S.R., Arntfield, M.E., Razavi, R., Bikopoulos, G., Karpowicz, P., Seaberg, R., Dai, F., Lee, S., Ahrens, R., Fraser, P.E., et al. (2011). The adult mouse and human pancreas contain rare multipotent stem cells that express insulin. Cell Stem Cell *8*, 281–293.

Snippert, H.J., and Clevers, H. (2011). Tracking adult stem cells. Nature Publishing Group *12*, 113–122.

Snippert, H.J., Schepers, A.G., van Es, J.H., Simons, B.D., and Clevers, H. (2013). Biased competition between Lgr5 intestinal stem cells driven by oncogenic mutation induces clonal expansion. EMBO Reports *15*, 62–69.

Snippert, H.J., van der Flier, L.G., Sato, T., van Es, J.H., van den Born, M., Kroon-Veenboer, C., Barker, N., Klein, A.M., van Rheenen, J., Simons, B.D., et al. (2010). Intestinal Crypt Homeostasis Results from Neutral Competition between Symmetrically Dividing Lgr5 Stem Cells. Cell *143*, 134–144.

Solar, M., Cardalda, C., Houbracken, I., Martín, M., Maestro, M.A., De Medts, N., Xu, X., Grau, V., Heimberg, H., Bouwens, L., et al. (2009). Pancreatic Exocrine Duct Cells Give Rise to Insulin-Producing β Cells during Embryogenesis but Not after Birth. Developmental Cell *17*, 849–860.

Spangrude, G.J., Heimfeld, S., and Weissman, I.L. (1988). Purification and characterization of mouse hematopoietic stem cells. Science.

Stanger, B.Z., and Hebrok, M. (2013). Control of Cell Identity in Pancreas Development and Regeneration. Gastroenterology *144*, 1170–1179.

Steinman, R.M., and Cohn, Z.A. (1974). Identification of a novel cell type in peripheral lymphoid organs of mice. II. Functional properties in vitro. J Exp Med *139*, 380–397.

Steinman, R.M., Adams, J.C., and Cohn, Z.A. (1975). Identification of a novel cell type in peripheral lymphoid organs of mice. IV. Identification and distribution in mouse spleen. J Exp Med *141*, 804–820.

Steinman, R.M., Kaplan, G., Witmer, M.D., and Cohn, Z.A. (1979). Identification of a novel cell type in peripheral lymphoid organs of mice. V. Purification of spleen dendritic cells, new surface markers, and maintenance in vitro. J Exp Med *149*, 1–16.

Steinman, R.M., Lustig, D.S., and Cohn, Z.A. (1974). Identification of a novel cell type in peripheral lymphoid organs of mice III. Functional properties in vivo. The Journal of Experimental ….

Steinman, R.M., and Cohn, Z.A. (1973). Identification of a novel cell type in peripheral lymphoid organs of mice I. Morphology, quantitation, tissue distribution. J Exp Med *137*, 1142–1162.

Stingl, J., Eirew, P., Ricketson, I., Shackleton, M., Vaillant, F., Choi, D., Li, H.I., and Eaves, C.J. (2006). Purification and unique properties of mammary epithelial stem cells. Nature *439*, 993–997.

Swenson, E.S., Xanthopoulos, J., Nottoli, T., McGrath, J., Theise, N.D., and Krause, D.S. (2009). Chimeric mice reveal clonal development of pancreatic acini, but not islets. Biochem. Biophys. Res. Commun. *379*, 526–531.

Tabansky, I., Lenarcic, A., Draft, R.W., Loulier, K., Keskin, D.B., Rosains, J., Rivera-Feliciano, J., Lichtman, J.W., Livet, J., Stern, J.N.H., et al. (2013). Developmental Bias in Cleavage-Stage Mouse Blastomeres. Current Biology *23*, 21–31.

Takahashi, K., and Yamanaka, S. (2006). Induction of Pluripotent Stem Cells from Mouse Embryonic and Adult Fibroblast Cultures by Defined Factors. Cell *126*, 663–676.

Talchai, C., Xuan, S., Lin, H.V., Sussel, L., and Accili, D. (2012). Pancreatic β Cell Dedifferentiation as a Mechanism of Diabetic β Cell Failure. Cell *150*, 1223–1234.

Tanaka, Y., Hamano, S., Gotoh, K., Murata, Y., Kunisaki, Y., Nishikimi, A., Takii, R., Kawaguchi, M., Inayoshi, A., Masuko, S., et al. (2007). T helper type 2 differentiation and intracellular trafficking of the interleukin 4 receptor-α subunit controlled by the Rac activator Dock2. Nat. Immunol. *8*, 1067–1075.

Thorel, F., Nepote, V., Avril, I., Kohno, K., Desgraz, R., Chera, S., and Herrera, P.L. (2010). Conversion of adult pancreatic α-cells to β-cells after extreme β-cell loss. Nature *464*, 1149–1154.

Till, J.E., and McCulloch, E.A. (1961). A direct measurement of the radiation sensitivity of normal mouse bone marrow cells. Radiat. Res. *14*, 213–222.

Trapnell, C. (2015). Defining cell types and states with single-cell genomics. Genome

Research *25*, 1491–1498.

Treutlein, B., Brownfield, D.G., Wu, A.R., Neff, N.F., Mantalas, G.L., Espinoza, F.H., Desai, T.J., Krasnow, M.A., and Quake, S.R. (2014). Reconstructing lineage hierarchies of the distal lung epithelium using single-cell RNA-seq. Nature *509*, 371–375.

Tumbar, T., Guasch, G., Greco, V., Blanpain, C., Lowry, W.E., Rendl, M., and Fuchs, E. (2004). Defining the epithelial stem cell niche in skin. Science *303*, 359–363.

Turner, D.J., Cowles, R.A., and Segura, B.J. (2001). Cholinergic stimulation of rat acinar cells increases c-fos and c-jun expression via a mitogen-activated protein kinase-dependent pathway. Journal of Gastrointestinal ….

Uhlen, M., Fagerberg, L., Hallstrom, B.M., Lindskog, C., Oksvold, P., Mardinoglu, A., Sivertsson, A., Kampf, C., Sjostedt, E., Asplund, A., et al. (2015). Tissue-based map of the human proteome. Science *347*, 1260419–1260419.

van Es, J.H., Sato, T., van de Wetering, M., Lyubimova, A., Yee Nee, A.N., Gregorieff, A., Sasaki, N., Zeinstra, L., van den Born, M., Korving, J., et al. (2012). Dll1+ secretory progenitor cells revert to stem cells upon crypt damage. Nat. Cell Biol. *14*, 1099–1104.

Van Keymeulen, A., Rocha, A.S., Ousset, M., Beck, B., Bouvencourt, G., Rock, J., Sharma, N., Dekoninck, S., and Blanpain, C. (2011). Distinct stem cells contribute to mammary gland development and maintenance. Nature *479*, 189–193.

Vidal, V.P.I., Chaboissier, M.-C., Lützkendorf, S., Cotsarelis, G., Mill, P., Hui, C.-C., Ortonne, N., Ortonne, J.-P., and Schedl, A. (2005). Sox9 Is Essential for Outer Root Sheath Differentiation and the Formation of the Hair Stem Cell Compartment. Current Biology *15*, 1340–1351.

Visvader, J.E. (2011). Cells of origin in cancer. Nature *469*, 314–322.

Wagers, A.J., and Weissman, I.L. (2004). Plasticity of Adult Stem Cells. Cell *116*, 639–648.

Walsh, S., Ponten, A., Fleischmann, B.K., and Jovinge, S. (2010). Cardiomyocyte cell cycle control and growth estimation in vivo--an analysis based on cardiomyocyte nuclei. Cardiovascular Research *86*, 365–373.

Wang, B., Zhao, L., Fish, M., Logan, C.Y., and Nusse, R. (2015). Self-renewing diploid Axin2+ cells fuel homeostatic renewal of the liver. Nature *524*, 180–185.

Wang, J.C.Y., and Dick, J.E. (2005). Cancer stem cells: lessons from leukemia. Trends in Cell Biology *15*, 494–501.

Watabe-Uchida, M., John, K.A., Janas, J.A., Newey, S.E., and Van Aelst, L. (2006). The Rac activator DOCK7 regulates neuronal polarity through local phosphorylation of stathmin/Op18. Neuron *51*, 727–739.

Weissman, I.L. (2000). Stem cells: units of development, units of regeneration, and units in evolution. Cell *100*, 157–168.

Weissman, I.L. (2014). Clonal origins of the hematopoietic system: the single most elegant experiment. J. Immunol. *192*, 4943–4944.

Wen, L., and Tang, F. (2015). Computational biology: How to catch rare cell types. Nature *525*, 197–198.

Westphalen, C.B., Takemoto, Y., Tanaka, T., Macchini, M., Jiang, Z., Renz, B.W., Chen, X., Ormanns, S., Nagar, K., Tailor, Y., et al. (2016). Dclk1 Defines Quiescent Pancreatic Progenitors that Promote Injury-Induced Regeneration and Tumorigenesis. Cell Stem Cell *18*, 441–455.

Wiktor-Brown, D.M., Hendricks, C.A., Olipitz, W., and Engelward, B.P. (2006). Age-dependent accumulation of recombinant cells in the mouse pancreas revealed by in situ fluorescence imaging. Proceedings of the National Academy of Sciences *103*, 11862–11867.

Wilson, A., Laurenti, E., and Trumpp, A. (2009). Balancing dormant and self-renewing hematopoietic stem cells. Curr. Opin. Genet. Dev. *19*, 461–468.

Wilson, A., Laurenti, E., Oser, G., van der Wath, R.C., Blanco-Bose, W., Jaworski, M., Offner, S., Dunant, C.F., Eshkind, L., Bockamp, E., et al. (2008). Hematopoietic stem cells reversibly switch from dormancy to self-renewal during homeostasis and repair. Cell *135*, 1118–1129.

Xu, Y., Zhang, M., Li, W., Zhu, X., Bao, X., Qin, B., Hutchins, A.P., and Esteban, M.A. (2016). Transcriptional Control of Somatic Cell Reprogramming. Trends in Cell Biology *26*, 272–288.

Yamamoto, R., Morita, Y., Ooehara, J., Hamanaka, S., Onodera, M., Rudolph, K.L., Ema, H., and Nakauchi, H. (2013). Clonal Analysis Unveils Self-Renewing Lineage-Restricted Progenitors Generated Directly from Hematopoietic Stem Cells. Cell *154*, 1112–1126.

Yanger, K., and Stanger, B.Z. (2011). Facultative stem cells in liver and pancreas: Fact and fancy. Dev. Dyn. *240*, 521–529.

Yanger, K., Knigin, D., Zong, Y., Maggs, L., Gu, G., Akiyama, H., Pikarsky, E., and Stanger, B.Z. (2014). Adult hepatocytes are generated by self-duplication rather than stem cell differentiation. Cell Stem Cell *15*, 340–349.

Yule, D.I. (2010). Pancreatic acinar cells: Molecular insight from studies of signal-transduction using transgenic animals. The International Journal of Biochemistry & Cell Biology *42*, 1757–1761.

Zaret, K.S., and Grompe, M. (2008). Generation and regeneration of cells of the liver and pancreas. Science *322*, 1490–1494.

Zhou, Q., Brown, J., Kanarek, A., Rajagopal, J., and Melton, D.A. (2008). In vivo reprogramming of adult pancreatic exocrine cells to β-cells. Nature *455*, 627–632.

Zhou, Q., Law, A.C., Rajagopal, J., Anderson, W.J., Gray, P.A., and Melton, D.A. (2007). A multipotent progenitor domain guides pancreatic organogenesis. Developmental Cell *13*, 103–114.

Ziv, O., Glaser, B., and Dor, Y. (2013). The Plastic Pancreas. Developmental Cell *26*, 3–7.

Zulewski, H., Abraham, E.J., Gerlach, M.J., Daniel, P.B., Moritz, W., Muller, B., Vallejo, M., Thomas, M.K., and Habener, J.F. (2001). Multipotential Nestin-Positive Stem Cells Isolated

From Adult Pancreatic Islets Differentiate Ex Vivo Into Pancreatic Endocrine, Exocrine, and Hepatic Phenotypes. Diabetes *50*, 521–533.

Appendix

List of Figures

List of Tables

Abbreviations

2ME	β-mercaptoethanol
ALDH1	Aldehyde dehydrogenase family 1
AP	Affinity propagation
Atf3	Activating transcription factor 3
BAC	Bacterial artificial chromosome
Bhlha15	Basic helix-loop-helix family, member a15
BSA	Bovine serum albumin
CAG	CMV early enhancer/chicken β actin
CCK	Cholecystokinin
cDNA	Complementary deoxyribonucleic acid
CK19	Cytokeratin 19
CNS	Central nervous system
CNTF	Ciliary neurotrophic factor
Dclk1	Doublecortin-like kinase 1
dNTP	Deoxynucleoside triphosphates
DPBS	Dulbecco's phosphate-buffered saline
DPI	Day(s) post injection
DTT	Dithiothreitol
EGF	Epidermal growth factor
Egr1	Early growth response 1
ERCC	External RNA Controls Consortium
FACS	Fluorescence-activated cell sorting
Fbw7	F-box and WD-40 domain protein 7
FGF	Fibroblast growth factor
FISH	Fluorescence *in situ* hybridization
Fos	FBJ osteosarcoma oncogene
Fosb	FBJ osteosarcoma oncogene B
Gli2	GLI-Kruppel family member GLI2
GO	Gene ontology
GuaHCl	Guanidine hydrochloride
H2afz	H2A histone family, member Z

HBSS	Hank's balanced salt solution
Hmgn2	High mobility group nucleosomal binding domain 2
HSC	Hematopoietic stem cell
HSV	Hue, Saturation, Value
IFNα	Interferon-α
Ins	Insulin
iPS	Induced pluripotent stems
Jun	Jun proto-oncogene
kb	Kilobase
Klf6	Kruppel-like factor 6
Lgr5	Leucine rich repeat containing G protein coupled receptor 5
M	Molar
M-MLV	Moloney murine leukemia virus
mRNA	Messenger ribonucleic acid
MTOC	Microtubule organizing centre
NSC	Neural stem cell
Op18	Oncoprotein 18
PanIN	Pancreatic intraepithelial neoplasia
PBS	Phosphate-buffered saline
PCA	Principle component analysis
PDAC	Pancreatic ductal adenocarcinoma
Pdx-1	Pancreatic and duodenal homeobox 1
PEG	Polyethylene glycol
PFA	Paraformaldehyde
pH3	Phospho-Histone H3
PMT	Photomultiplier tube
Ptf1a	Pancreas specific transcription factor, 1a
RGB	Red, green, blue
RNA	Ribonucleic acid
SD	Standard deviation
SEM	Standard error of the mean
Sox9	SRY (sex determining region Y)-box 9

SPRI	Solid-phase reversible immobilization
Stmn1	Stathmin 1
TGF-β	Transforming growth factor, beta 2
TMM	Trimmed mean of M-values
TPM	Transcript per million
TSO	Template switching oligo
Tuba1b	Tubulin, alpha 1B
TUNEL	Terminal deoxynucleotidyl transferase dUTP nick end labeling
Xbp-1	X-box binding protein 1
YFP	Yellow fluorescent protein

Acknowledgements

Writing these closing words for my thesis feels a lot like closing a chapter of my life. It has been a long journey and there are a number of people that travelled along my side whom I want to thank.

First of all, I would like to thank my advisor, Ana.
For opening the doors to a place that very much felt like home. I truly enjoyed working in your lab. You provided me with a challenging environment where I was able to meet extraordinary people and do experiments that really excited me. I sincerely appreciate the freedom, trust and support that you gave me over the last years. Furthermore, I would like to thank you for contacting Prof. Auffarth, which had a profound impact on my health.

I also would like to thank my thesis advisory committee members: Prof. Jan Lohmann and Prof. Peter Angel. For your time, effort and honest interest in helping me to push this project forward.

Thanks to all the people in the lab, particularly the past and present fellow inmates of our office: Avni, Enric, Georgios, Liang, Robert, Si and Wilson:
For making me feel like I´m stuck in an episode of *Friends*. Working in science can be rough at times, but working with you guys was nothing but fun! During the last years I spend more time with you than with anyone else and it never got boring. If I could chose I´d work with you for the rest of my life. I will miss you all!

I also would like to thank the rest of the lab and everybody that worked with me over the years: Alex, Alvaro, Ceci, Desiree, Frederik, Gonzalo, Gülce, Irmgard, Jan, Katrin, Klara, Marcin, Maxim, Melanie, Moritz, Nadine, Sabrina, Sascha, Sheng, Steffi and Suse. In particular, I want to thank my students, Isabelle and Xiaokang: For your hard work and for making me realize that I still have a lot to learn.

Further, my sincere gratitude goes to the team of the Department of Ophthalmology at the University of Heidelberg: Prof. Gerd Auffarth, Prof. Michael Koss, Tawfic Swaid, Dr. Sun-Hye Lee and all nurses:
For saving my eye

Last, but most of all, I want to thank my family and my friends:
For staying by my side and supporting me unconditionally. You provide me with a perspective on life that is irrespective of success or failure. You are what keeps me sane when the days get dark.
Thank you.